Aus der Klinik für Allgemein-, Viszeral- und Transplantationschirurgie
Klinikum der Ludwig-Maximilians-Universität München
Leitung: Univ.-Prof. Dr. med. Jens Werner

Quantification of the Tumor immune Stroma (QTiS) and the Metabolic Checkpoint Molecules in Pancreatic Cancer: Comparison between Primary and Metastatic Tumor

Dissertation
zum Erwerb des Doktorgrades der Medizin
an der Medizinischen Fakultät der
Ludwig-Maximilians-Universität zu München

vorgelegt von

Tao Zhang
aus
Henan, China

2022

Mit Genehmigung der Medizinischen Fakultät

der Universität München

Erster Gutachter:	Univ.-Prof. Dr. med. Jens Werner
Zweiter Gutachter:	Prof. Dr. Jens Neumann
Dritter Gutachter:	Priv. Doz. Dr. Michael Haas
Dekan:	Prof. Dr. med. Thomas Gudermann
Tag der mündlichen Prüfung:	28.01.2022

Table of contents

Zusammenfassung

Das Pankreaskarzinom gehört zu den tödlichsten Tumorerkrankungen der Welt. Bis heute gelingt die erfolgreiche Heilung nur durch die operative Entfernung des Tumors und dies nur für wenige Patienten, die sich in frühen Tumorstadien befinden. Obwohl viele Anstrengungen unternommen wurden das Pankreaskarzinom zu heilen, ist das Überleben auch nach durchgeführter Operation limitiert. Diverse Vorarbeiten haben gezeigt, dass das Immunsystem als Teil des Tumormikromilieus eine sehr wichtige Rolle sowohl in Bezug auf Tumorwachstum als auch den Effekt der neo- und adjuvanten Therapie beim Pankreaskarzinom. Der Glukosemetabolismus dient als wichtige Energiequelle für das Tumorwachstum und für die Metastasierung. Die Bedeutung von Tumor-infiltrierenden Leukozyten und des Metabolismus auf das Überleben beim Pankreaskarzinom sind bekannt. Wohingegen, der Stellenwert der Tumor-infiltrierenden Leukozyten und des Metabolismus beim metastasierten Pankreaskarzinom weiterhin unklar ist.

In dieser Arbeit können wir uns glücklich schätzen insgesamt 26 Fälle eines metastasierten Pankreaskarzinoms zu präsentieren. Uns liegen Paraffinschnitte des Primarius und der korrespondierenden Metastasen (Leber, Lunge und Peritoneum) vor. Immunhistochemische Färbungen wurden durchgeführt. Der Algorithmus zur Quantifizierung des Tumorimmunostromas (QTiS) wurde angewandt, um die Infiltration mit $CD3^+$, $CD8^+$, $CD20^+$ und $CD66b^+$ Leukozyten sowie die Expression von metabolischen Checkpoint-Molekülen (HIF-1α, GLUT1 und PDHK1) zu analysieren. In einem nächsten Schritt erfolgte der Vergleich der Infiltration von Leukozyten und die Expression von metabolischen Checkpoint-Molekülen im Tumormikromilieu des Primarius und der korrespondierenden Metastasen. Diese immunhistochemischen Ergebnisse wurden ebenfalls mit den demographischen und klinischen Daten

der Patienten, dem Gesamtüberleben und dem Erkrankungsfreien-Überleben verglichen.

Die Infiltration of $CD3^+$, $CD8^+$, and $CD20^+$ Leukozyten im Tumormikromilieu war im Pankreaskarzinomprimarius höher als in der korrespondierenden Metastase. Eine hohe Infiltration von $CD20^+$ Leukozyten im Primarius korrelierte signifikant mit einem besseren Gesamtüberleben (p=0.013). Eine hohe Infiltration von $CD8^+$ Leukozyten im Metastasengewebe des Pankreaskarzinoms korrelierte mit einem besseren Gesamtüberleben (p=0.023). Niedrige Werte von Thrombozyten im peripheren Blut waren mit einem besseren Gesamtüberleben assoziiert. Die Expression von HIF-1α und PDHK1 waren mehr intratumoral als im peritumoralen Tumormikromilieu vorhanden, sowohl beim Primarius als auch der Metastase. Eine niedrige Dichte von GLUT1 im Tumorstroma des Primarius korrelierte mit einem besseren Gesamtüberleben (p=0.009). Ein signifikant besseres Gesamtüberleben zeigte sich auch für GLUT1 im Metastasengeweben (p=0.01). Mittels der multivariaten Analyse konnte nachgewiesen werden, dass eine erhöhte Infiltration mit $CD8^+$ Leukozyten im Tumorimmunstroma des Metastasengewebes ein unabhängiger Prognosefaktor ist (p=0.032). Eine sehr dichte Expression von GLUT1 sowohl im Tumorstroma des Primarius (p=0.049) als auch der Metastase (p=0.022) ist ebenfalls ein unabhängiger Prognosefaktor.

Zusammengefasst zeigt diese Arbeit, dass der beim primären Pankreaskarzinom bereits etablierte QTiS Algorithmus zur Analyse des Tumormikromilieus beim Primarius inklusive der korrespondieren Metastasen angewendet werden kann und die gewonnen Daten konsistent sind. Diese Arbeit ist nach bestem Wissen die erste Veröffentlichung von einem Vergleich der Tumor-infiltrierenden Leukozyten und metabolischen Checkpoint-Molekülen zwischen Primarius und korrespondierender Metastase des Pankreaskarzinoms. Unsere Arbeit ermöglicht ein besseres Verständnis der

Immunsubtypen und des Metabolismus beim metastasierten Pankreaskarzinom. Diese Daten sind in Bezug auf eine zukünftig bessere Diagnostik, Prognose und Therapie sehr hilfreich.

Abstract

Pancreatic cancer (PC) remains one of the most lethal cancers in the world. Currently, surgical resection is still the most effective treatment for PC, yet it only works for a few early-stage patients. Although multiple efforts have been ongoing to treat metastatic pancreatic cancer, the outcome remains unsatisfactory. Previous studies have shown that immune imbalance within the tumor microenvironment (TME) promotes tumor progression. Furthermore, glucose metabolism is essential to providing energy for tumor growth, progression, and distant metastasis. There have been studies on tumor-infiltrating leukocytes (TILs) and energy metabolism in the TME of pancreatic cancer, while research on metastatic PC is unavailable because of the surgical treatment of metastatic pancreatic cancer.

We were fortunate to have this opportunity to study 26 cases of metastatic PC in our institution. Quantification of the tumor immune stroma (QTiS) algorithm was used to quantify seven markers after immunohistochemical staining, including four markers of leukocytes ($CD3^+$, $CD8^+$, $CD20^+$, and $CD66b^+$) and three markers of metabolic checkpoint molecules (HIF-1α, GLUT1, PDHK1). Afterward, differences in tumor-infiltrating leukocytes (TILs) and metabolic checkpoint molecules (MCMs) between primary and metastatic lesions of metastatic pancreatic cancer were analyzed. Furthermore, the correlation between seven staining markers and clinical data, including overall survival (OS) and disease-free survival (DFS), was also analyzed.

The results showed that the infiltration of $CD3^+$, $CD8^+$, and $CD20^+$ in PC primary tumors was higher than that in metastatic tumors. High infiltration of $CD20^+$ TILs ($p=0.013$) in primary tumors of PC correlates with improved overall survival, and high infiltration of $CD8^+$ ($p=0.023$) in metastatic tumors of PC correlates with improved overall survival. Low level of platelets in blood circulation system

associated with improved OS. The density of HIF-1α and PDHK1 in tumor cell area was higher than that in tumor stroma areas of primary and metastatic tumors. Low-density GLUT1 in tumor stroma areas of primary tumors (p=0.009) and metastatic tumors (p=0.01) of PC correlates with improved OS. Notably, in multivariate analysis, CD8+TILs (HR 0.196, 95% CI 0.044-0.872, p=0.032) in metastatic tumors of PC is an independent prognostic factor; and GLUT1 in tumor stromal areas of primary (HR 5.816, 95% CI 1.006-33.624, p=0.049) and metastatic (HR 5.056, 95% CI 1.258-20.324, p=0.022) tumors is independent prognostic factor to metastatic pancreatic cancer.

Overall, the present study used the QTiS algorithm to quantify stroma tumor-infiltrating leukocytes in metastatic PC. We extended this method to quantify metabolic checkpoint molecules in tumor cell and stromal areas, efficiently analyzing IHC staining images. Furthermore, we depicted the characters and differences of TILs and MCMs between primary and metastatic lesions of metastatic PC and the correlation between TILs and MCMs with OS and DFS. Our work can contribute to a better understanding of the immune subtypes and energy metabolism in metastatic PC, which could be vital in improving the diagnosis, prognosis, and treatment of advanced PC.

List of figures

List of tables

List of Abbreviations

%	Percentage
°C	Degree Celsius
µg	Microgram
µl	Microliter
µm	Micrometer
ABC-AP	VECTASTAIN® ABC-AP Kit
APCs	Antigen-presenting cells
ATP	Adenosine triphosphate
B-cell	B-lymphocyte
BCR	B-cell receptor
bHLH–PAS	Basic helix–loop–helix/Per-ARNT-SIM
Breg	Regulatory B cell
BSA	Bovine serum albumin
CD3	A cluster of differentiation 3
CI	Confidence interval
CRP	C-reactive protein
CTL	Cytotoxic T lymphocytes
CTLA-4	Cytotoxic T-lymphocyte-associated protein 4
DC	Dendritic cells
DDR	Deoxyribonucleic acid damage repair
DFS	Disease-free survival
ECM	Extracellular matrix
EDTA	Ethylenediaminetetraacetic acid
FOLFIRINOX	5-fluorouracil, leucovorin, irinotecan, and oxaliplatin
GB	Gigabyte
GLUT1	Glucose transporter
GPS	Glasgow prognostic score

HIF-1α	Hypoxia-inducible factor-1α
HR	Hazard ratio
HTCR	Human tissue and cell research foundation
IFN	Interferon
IgG	Immunoglobulin G
IHC	Immunohistochemistry
IL - 4	Interleukin- 4
IST	ImageJ software with subjective threshold
KRAS	Kirsten rat sarcoma viral oncogene homolog
MB	Megabyte
mCRC	Metastatic colorectal cancer
MCT	Mast cell tryptase
mFOLFIRINOX	Modified FOLFIRINOX: 5-fluorouracil, leucovorin, irinotecan, and oxaliplatin
MHC	Major histocompatibility complex
min	Minutes
ml	Milliliter
mm	Millimeter
MPV	Mean platelet volume
MMP-9	Matrix metalloproteinase 9
MS4A	Transmembrane 4-domain family A protein
N	Sample size, the number
NaCl	Sodium chloride
NK cells	Natural killer cells
NLR	Neutrophil-to-lymphocyte ratio
OS	Overall survival
OvCa	Ovarian cancer
PanIN	Pancreatic intraepithelial neoplasia
PBS	Phosphate buffer saline

PC	Pancreatic cancer
PCR	Polymerase chain reaction
PD-1	Programmed death 1
PDAC	Pancreatic ductal adenocarcinoma
PDH	Pyruvate dehydrogenase
PDHK1	Pyruvate dehydrogenase kinase 1
PDL-1	Programmed death ligands
PLT	Platelet
PrPD	Pancreaticoduodenectomies
PPPD	Pylorus-preserving pancreaticoduodenectomies
QTiS	Quantification of the tumor immune stroma
ROC	Receiver operating characteristic
RNA	Ribonucleic acid
SD	Standard deviation
SHH	Sonic hedgehog pathway
SPSS	Statistical Product and Service Solutions
TBS	Tris-buffered saline
TBS-T	Tris-buffered saline with Tween 20
T-cell	T-lymphocyte
TCA	Tricarboxylic acid cycle
T eff	Effector T cells
Treg	T-regulatory cell
TILs	Tumor-infiltrating leukocytes
TINs	Tumor-infiltrating neutrophils
TLR4	Toll-like receptor 4
TME	Tumor microenvironment
TNM	TNM Classification of Malignant Tumors
VEGF	Vascular endothelial growth factor
ZEN	ZEISS Efficient Navigation software

1. Introduction

Pancreatic cancer (PC) remains one of the most lethal cancers in the world [1]. In recent years, research on tumor-infiltrating leukocytes (TILs) and metabolic checkpoint molecules (MCMs) of PC has become a hot issue[2, 3]. This dissertation aimed to elucidate the characters and differences in TILs and MCMs between primary and metastatic lesions of metastatic PC and the correlation of TILs and MCMs with overall survival (OS) and disease-free survival (DFS). This work was an experimental investigation of a retrospective cohort study of metastatic pancreatic cancer conducted at our institution.

1.1 Epidemiological features of pancreatic cancer

PC is a malignant tumor that develops from pancreatic tissues. Among them, pancreatic ductal adenocarcinoma (PDAC) is an important type of primary pancreatic cancer, accounting for about 85-90% of all pancreatic neoplasms[4]. Based on the report of the World Health Organization, the occurrence of pancreatic cancer has a precise geographical distribution; the incidence of pancreatic cancer in men and women is high in developed territories and countries (such as Central and Eastern- Europe, USA, and Japan). In contrast, it is lower in developing territories (such as Eastern Africa and South-Eastern Asia) [5]. In addition, the global incidence of pancreatic cancer is associated with age and is more prevalent in men than in women [5].

The Global Burden of Disease Study in 2017 showed that the number of new cases and deaths of pancreatic cancer rose by 2-3 times compared with 1990–2017 in global 195 countries and territories, and the incidence of PC has increased three times in countries with a high socio-demographic index calculated by birth rate, level of education and income [6, 7]. During 2018, an

estimated 460,000 new PC cases and 433,000 deaths occurred worldwide, ranking 11th among the most common cancer in the world. Although progress has been made in understanding the risk factors that cause PC and new early detection approaches, its incidence was predicted to increase, and the world might have 355,317 new cases by 2040 [8]. In the European Union, mortality from the disease was predicted to increase by almost 50% by 2025, compared with 2010 levels [9].

1.2 Risk factors and tumor biology

There are multiple and complex risk factors for PC. Many studies have indicated that age, gender, ethnicity, blood type, diabetes mellitus, family history, and genetic factors are the non-modifiable factors for pancreatic cancer, obesity, smoking, alcohol, dietary factors, and infection are considered as modifiable factors [8, 10, 11].

The progression model for pancreatic cancer, characterized by transforming from normal pancreatic ducts to preinvasive lesions called pancreatic intraepithelial neoplasia (PanIN), is critically essential and can eventually evolve into invasive PC [12, 13].

1.3 Stage and prognosis

Pancreatic cancer is typically diagnosed late due to its silence, rapid growth, aggressive development, and tendency to distant metastases [14]. Distant metastases are present in approximately 50% of patients at the first diagnosis [6]. According to the 8th edition staging system, PC is classified as stages I-IV [15]. PC with a maximum diameter of ≤4 cm is considered stage I; cancer with metastases up to 3 regional lymph nodes is considered stage II; cancer invaded

major blood vessels or metastasized to 4 or more regional lymph nodes is defined as stage III; cancer with distant metastases is defined as stage IV (also known as metastatic pancreatic cancer). Usually, advanced-stage pancreatic cancer includes stages III and IV [16].

Regarding the prognosis of pancreatic cancer, the 5-year survival rate after diagnosis is about 10% [17]. To make matters worse, the 5-year survival rate for metastatic PC is only about 3% [18]. In 2018, PC mortality in men and women was higher in significantly developed territories and countries (Entire Europe, North America, and Japan) than that in some developing territories and countries (such as south and north Africa, South-Eastern Asia) [5].

1.4 Treatments of PC

1.4.1 Surgery, chemotherapy, and radiotherapy

The first purpose of treatment is to extract the cancerous tissue by procedure before it starts to spread. Unfortunately, only about 10-20% of patients have the opportunity to undergo surgical resection [19]. To date, the surgical procedure remains the only way to obtain a cure for fit patients at stage I and II [20, 21]. Different surgical procedures are available on the I tumor's location, such as pancreaticoduodenectomy (known as Whipple procedure), distal pancreatectomy, and total pancreatectomy.

Furthermore, adjuvant therapy (mFOLFIRINOX = modified FOLFIRINOX: 5-fluorouracil, leucovorin, irinotecan, and oxaliplatin) could improve OS in fit patients with PC after the surgical procedure [22-24]. The treatment of patients with locally advanced PC primarily involves systemic chemotherapy [25, 26], and this treatment may have the potential to convert locally advanced PC to

surgically resectable PC [27]. Systemic chemotherapy is still the primary approach for metastatic PC patients to relieve cancer-related symptoms and prolong life [28, 29]，and FOLFIRINOX may benefit younger and healthier patients even more [30, 31].

Radiotherapy may help in palliating the pain by shrinking the tumor [32]. Moreover, supportive care and palliative care are necessary for the treatment of metastatic pancreatic cancer [6, 28].

In view of the unfavorable clinical outcome of radiotherapy and chemotherapy on PC, especially advanced PC, many treatment methods have emerged.

1.4.2 Targeted therapies

According to previous research, the development of aberrant ducts in PC is accompanied by approximately 60 mutations in 12 different signaling pathways [33]. Targeting the Kirsten rat sarcoma viral oncogene homolog (KRAS) pathway [34] and the phosphatidylinositol-3-kinase (PI3K)/Akt and the mammalian target of rapamycin (PI3K/AKT/mTOR) signaling pathway [35, 36] did not bring the expected results, so further studies are underway. In preliminary studies, both targeted growth factor receptors erlotinib and nimotuzumab combined with gemcitabine showed improved overall survival in metastatic PC with wild-type KRAS [37, 38]. Targeting vascular endothelial growth factor (VEGF) signaling did not present expected positive results and increased the incidence of side effects [39]. A preliminary study targeting the deoxyribonucleic acid (DNA) damage repair (DDR) pathway showed that Progression-free survival (PFS) has improved in patients with metastatic pancreatic cancer, but no data were available on overall survival (OS) [40]. The combination of targeting tumor metabolism devimistat and mFOLFIRINOX is

underway to evaluate the effectiveness against PC (NCT03504423). The first preliminary results from a small trial showed promising results [41]. The PC stroma is distinctive and plays a crucial role in tumor development, thus boosting remote metastases and increasing medication resistance [34]. Therefore, targeting tumor stroma and extracellular matrix may be a potential option for treating metastatic PC. Although a novel recombinant polyethylene human hyaluronidase enzyme (PEGPH20) in combination with mFOLFIRINOX for advanced pancreatic cancer cannot be continued due to the increased adverse effects [42], and the sonic hedgehog signaling pathway (SHH) inhibitor vismodegib did not show an expected activity in the treatment of metastatic PC [43].

Early studies described anti-cytotoxic T-lymphocyte-associated protein 4 antibody (anti-CTLA-4 antibody) Ipilimumab, a targeted immune checkpoint inhibitor, alone or with gemcitabine, did not show a significant positive response to advanced PC [44]. A clinical trial of avelumab (anti-PDL1 antibody) combined with binimetinib for pancreatic cancer is ongoing [45]. Cytotoxic $CD8^+$T cells (CTLs), the front-line defense cell type against cancer [46], become dysfunctional and exhausted as tumors develop due to tolerance and immunosuppression in the TME [47]. Therefore, to generate an effective anti-tumor response, $CD8^+$ T cells need to be initiated and activated as effector CTL in TME [48]. Several studies are being conducted to treat pancreatic cancer through rational immunotherapeutic strategies that either reinitiate and reactivate $CD8^+$ T cells or slow its exhaustion [49-52]. The activation of CD40, a tumor necrosis factor of the family member, reverses immunosuppression and induces anti-tumor T cell responses [53, 54].

At present, radiotherapy, chemotherapy, targeted therapy, and immunotherapy are not adequate for advanced or metastatic PC, and more combinations of

those treatment modalities are still being tried continuously [45, 55, 56]. With the advent of new technologies and a better understanding of PC, it is believed that there will be more effective ways to treat metastatic pancreatic cancer [6]. An enhanced understanding of the dense, hypoxic, and immunosuppressive stroma of the PC microenvironment, which inhibits penetration of immune cells and therapeutic agents, will help discover new targeted treatment strategies [57]. Although pancreatic cancer has been resistant to current therapeutic measures, immunotherapy will remain a promising treatment modality [58]. To sum up, there is still a long way to go for pancreatic cancer treatment.

1.5 Immunology of PC

The immune system, a complex biological system, is composed of innate and adaptive immunity that protects the host from foreign pathogens, including cancer cells [59]. Innate immunity is composed of various cells that are always present in the first line against pathogens or tumor cells [60]. The adaptive immune system is regulated and consists mainly of B and T cells, typically triggered by secreting cytokines and presenting antigens [61]. Therefore, the self-recognition of the immune system is beneficial for maintaining the immune balance of the body [62]. For example, regulatory T cells play an essential role in the regulation and prevention of immune responses [63]. Besides, the programmed death-1 (PD-1), an immunoinhibitory receptor, is also a critical regulator of T-cells, collaborating with suppressor cells to dampen immune activities [64]. PD-1 was activated by engaging its programmed death ligands (PDL-1) or PDL-2 to inhibit the anti-tumor effects of T cells [64].

T cells commonly expressed as a marker of the cluster of differentiation 3 (CD3), are the primary type of adaptive immune cells. CD3 is a marker for detecting T cells because of the specificity of its antigen for T cells and its appearance at

various stages of T cell development [65]. $CD3^+$ and $CD8^+$ T cells are mainly involved in recognizing immune cells and killing cancer cells [48, 66]. Many studies have shown that high infiltration of $CD3^+$ T-cells is associated with improved OS in PC [3, 67-70]. The CD8 molecule is a marker of the cytotoxic T cell population and was identified as an essential antitumor component in PC [71, 72]. Previous studies have shown that high-level infiltration of $CD8^+$ lymphocytes is a characteristic of immunogenic tumors and responds well to immunotherapy [73, 74]. Furthermore, high infiltration of CD8+ lymphocytes is related to improved overall survival [3].

B lymphocytes (usually expressing the marker CD20) are antibody-producing lymphocytes responsible for the humoral immune component of adaptive immunity [75]. Under some circumstances, B lymphocytes may serve as antigen-presenting cells [76]. Several studies showed that high infiltration of CD20+ lymphocyte in PC is associated with improved OS and PFS [3, 77].

Neutrophils (commonly expressing marker CD66b), a component of innate immunity, are present in the first line against invading pathogens [78]. Tumor-infiltrating neutrophils (TINs) are one of the central invasive immune cell populations in tumors [79] and act as a prognostic marker in cancers [80-83]. In PC, TINs are a possible tool for classifying other immune subtypes [3, 84]. In peripheral blood, the relationship between systemic inflammation and immunity is reflected by the neutrophil-to-lymphocyte ratio (NLR). Moreover, NLR is used as a prognostic biomarker for many cancers, such as gastric cancer [85]，rectal cancer [86], breast cancer [87], oral cancer, and pancreatic cancer [88, 89]. Recently, the NLR in pathological tissues, such as pancreatic cancer [90] in esophageal squamous cell carcinomas [91, 92], has also proved its prognostic value.

The immune system is widely known for its role in the battle against cancer [93]. Therefore, understanding the immune components in PC can guide the use of immunotherapy and other immunomodulatory therapies.

1.6 Glucose metabolism in tumor cells and immune cells

Glucose is a vital energy substance necessary for the activation, proliferation, and function of the immune cells and the most absorbent and consumed of the tumor cells [94, 95]. In the tumor microenvironment (TME), tumor cells compete to consume more glucose, so as to reduce glucose uptake by T cells, leading to T cell dysfunction and immune escape [47]. Therefore, a promising strategy to eliminate the effects of metabolic competition between tumor and immune system could be targeted [96].

1.6.1 Glucose metabolism in tumor cells

Regardless of the oxygen status, many cancer cells rely on high-rate glycolysis for energy instead of mitochondrial oxidative phosphorylation, and this phenomenon is called the Warburg effect [97]. Especially under hypoxia, tumor cells produce pyruvate by glycolysis, which is then converted into lactate to produce adenosine triphosphate (ATP) [98]. This process of lactate accumulation acidifies the TME, making the tumor cells equipped with environmental conditions for proliferation, invasion, and migration [99].

1.6.2 Glucose metabolism in immune cells

Complex and diverse glucose metabolism is present in tumor cells and immune cells [59]. In the adaptive immune system, T cells are the most numerous lymphocyte group [100]. A study showed that naive T cells require

only a minimal rate of glycolysis to maintain nutrient uptake and biosynthesis [101]. Once becoming effector T cells (Teff), they exhibit an increased rate of glycolysis and an activated state of metabolism for protein synthesis, which ultimately allows T cells capable of growing and proliferating and producing posterity cells to perform killing function [101, 102]. For neutrophils, glycolysis not only produces most of the ATP required for neutrophil functions but also regulates many of its functions [102, 103]. For B cells, stimulation of B cell receptors promotes increased expression of glucose transporters on the surface of B cells and enhances glycolysis [104, 105].

1.7 Energy metabolism in PC cells

Aerobic oxidation of glucose and glycolysis provides energy for the development and differentiation of tissues and cells. Glycolysis is a set of biochemical reactions that metabolize glucose to pyruvate and then to lactate, producing adenosine triphosphate (ATP) and other substrates [95, 106]. Lactate and glucose are also nutrients for cancer cells [107-109]. Although glycolysis is less energy efficient than the tricarboxylic acid (TCA) cycle, cancer cells prefer producing ATP by it [106, 110]; this is the so-called Warburg effect [111, 112]. Glycolysis contributes to the increased production of lactate, which alters the microenvironment and increases the invasiveness of PC [113].

The energy produced by glycolysis is the primary energy source to maintain the proliferation, invasion, migration, and metastasis of pancreatic cancer cells, even under normal aerobic conditions [114]. PC cells are rich in the dense stroma which consists of cellular and acellular components, including fibrin, collagen, fibronectin, hyaluronan, endothelial cells, cancer-associated fibroblasts, and pancreatic cells, stellate cells, and immune cells [115]. Hypoxia and nutritional deficiencies within PC result from its impermeable stroma and inadequate blood supply, forcing PC cells to fail to produce energy by aerobic

metabolism [114, 116]. Increased glycolysis in PC cells promotes the expression and migration of the glucose transporter 1 (GLUT1) to cancer cell membranes [116, 117].

Hypoxia-inducible factor-1 is a transcription factor comprising alpha and beta subunits and plays a major role in regulating O_2 homeostasis physiological responses to O_2 deprivation [118, 119]. Of which HIF-1α is the only subunit regulated by O_2 that determines the activity of HIF-1 [120, 121]. In the process of tumor cells adapting to hypoxia, HIF-1α is a vital transcription factor that mediates the hypoxia response of the cell，and correlates with the tumor proliferation, invasion, metastasis, and prognosis [122-124]. In PC, the expression of HIF-1α relates with energy consumption [125], tumor angiogenesis [126], cell proliferation [127, 128], tumor size [127], advanced TNM stage [127], anti-apoptotic capacity [125], and metastasis [129], and is a prognostic factor of PC [127].

Pyruvate dehydrogenase kinase 1 (PDHK1) is a crucial regulator of glycolysis by phosphorylating the E1α subunit of pyruvate dehydrogenase (PDH)，and promotes the conversion of pyruvate to lactate to meet the energy consumption of cells in an anoxic environment [130]. Under hypoxia conditions, HIF-1 activates glycolysis and inhibits mitochondrial function and oxygen consumption by inducing PDHK1 [131, 132]. In PC, HIF-1α regulates the expressions of PDHK1, which then inhibits the aerobic oxidation of glucose [125].

PC has abundant dense stroma, leading to low blood vessels in pancreatic cancer tissue [133], according to a prominent feature of PC in imaging diagnosis [134]. Furthermore, under hypoxia conditions, the presence of HIF-1α promotes the expression of GLUT1 and PDHK1 to undergo anaerobic

glycolysis [116, 117, 132]. Glycolysis is the first step of the metabolic pathway that converts one glucose molecule into two pyruvate molecules, producing energy in ATP. In normal cells, pyruvate enters the TCA cycle to produce ATP. As for tumor cells and stromal cells, they prefer to obtain energy by glycolysis, converting pyruvate to lactate [111, 135]. Glucose transporter 1, a plasma membrane protein responsible for the uptake of glucose into cells [136], and the expression of the GLUT1 is associated with the survival of PC [137-139]. Pyruvate dehydrogenase kinase 1 (PDHK1) has shown to have increased activity in hypoxia due to the presence of HIF-1α, and PDHK1 prevents pyruvate from entering the TCA cycle by phosphorylating pyruvate dehydrogenase and promotes the conversion of pyruvate to lactate [131, 132, 140] (**Figure 1**). Therefore, this project introduced HIF-1α, GLUT1, and PDHK1 as the energy metabolism checkpoint molecules of PC, compared them in the primary and metastatic lesions, and analyzed their impact on survival.

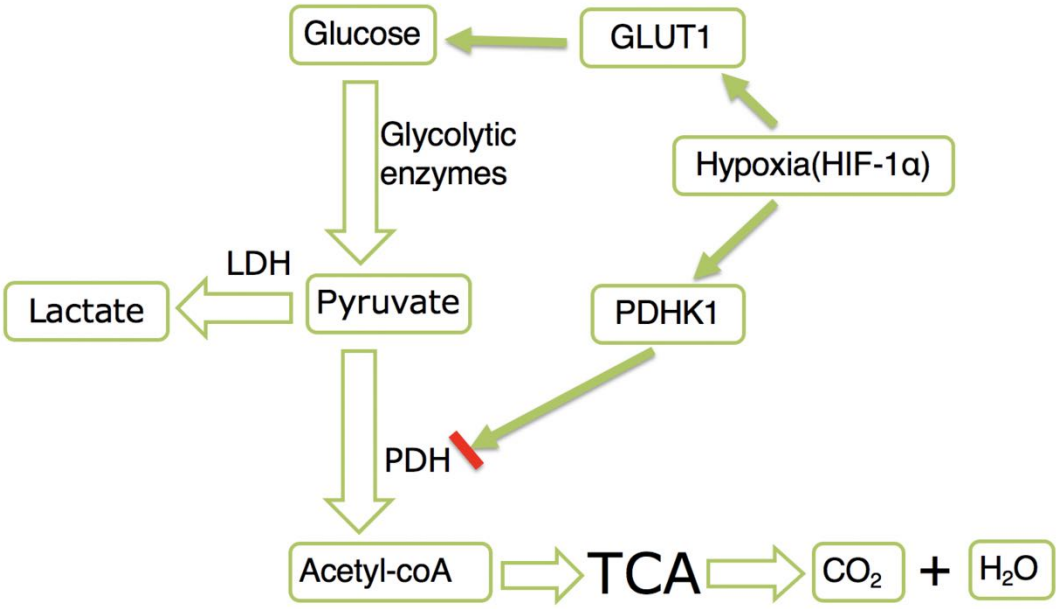

Figure 1. Hypoxia increases the expression of HIF-1α and GLUT1 and induces the activity of PDHK1 [125].

1.8 Aim of this study

The aim of the present study is to investigate the differences in primary and metastatic lesions of TILs and MCMs in metastatic PC and the correlation of TILs and MCMs with clinical data, including OS and DFS. Understanding these differences in immune subtypes and metabolic checkpoint molecules could be vital to improving PC diagnosis, prognosis, and exploring a new therapy for advanced PC.

2. Material and Methods

2.1. Materials

2.1.1. Consumables

Aqueous mounting agent	1.08562.0050, Merck Chemicals, Germany
Coverslips	Menzel, Thermo Fisher, USA
Centrifuge tube	TPP, Switzerland
Gloves	Eco SHIELD, USA
Hydrophobic pen	S2002, Dako Pen, Agilent Technologies, USA
Microscope slides	Super frost Plus, Thermo Fisher, USA
Parafilm	Pechiney, USA
Pipettes reload	Eppendorf, Germany
Serological pipettes	SIGMA-ALORICH, USA
Safe-Lock tubes	Eppendorf, Germany

2.1.2. Immunohistochemistry equipment

-20°C fridge	Bosch, Germany
Four °C fridge	Liebherr, Germany
37°C incubator	Binder, Germany
54°C incubator	Memmert, Germany
Electronic pH meter	Knick, Germany
Electronic balance	Chyo, Japan
Micro-Centrifuge	NeoLab, Germany
Microtome	Thermo Scientific, USA

Microscope	Olympus, Japan
Pipettes	Eppendorf, Germany
Shaker	Edmund Bühler, Germany
Magnetic mixer	GLW, Germany
Ventana Benchmark Ultra autostainer	Ventana Medical Systems, Oro Valley, AZ, USA
Water bath	Julaba, Germany

2.1.3. Chemicals

Albumin fraction V, biotinfrei	0163.4, CARL ROTH, Germany
Cell conditioning solution 1	CC1, pH 8.4, Ventana
Citric acid	X863.2, CARL ROTH, Germany
99% Ethanol	603-002-00-5, SAV LIQUID PRODUTALION, Germany
96% Ethanol	1000463926011, CLN GmbH Chemikalien Laborbedarf, Germany
70% Ethanol	1004051526001, CLN GmbH Chemikalien Laborbedarf, Germany
Ethylenediaminetetraacetic acid (EDTA) disodium salt dihydrate	E5513, SIGMA-ALORICH, USA
Epitope retrieval solution	pH 8, Novocastra, Newcastle upon Tyne, UK
Horse Serum	H1270, SIGMA-ALORICH, USA
PBS buffer (10X Dulbecco's)	Power BC, PanReac AppliChem, Germany
Sodium chloride	71380, SIGMA-ALORICH, USA
Mayer's hemalum solution	109249, Merck Chemicals, Germany
Trisodium citrate dehydrate	3580.3 CARL ROTH, Germany
Tris	1610716, BIO-RAD, USA
Tween 20	37470.01, SERVA, Germany

Xylene	9713.2 CARL ROTH, Germany

2.1.4. Buffers and Solutions

5% BSA (bovine serum albumin) /PBS solution	
	2g Albumin fraction V, biotin-free
	40ml 1x PBS buffer
10x TBS buffer	
	24.2g Tris
	80g Sodium chloride
	1L Distilled water
1x TBS buffer	
	100ml 10x TBS buffer
	900ml Distilled water
1x TBS-T buffer	
	1L 1x TBS buffer
	1ml Tween 20
Citrate Buffer	
	18ml Solution A
	82ml Solution B
	pH 6.0
Citrate Buffer Solution A	
	10.5g Citric acid
	500ml Distilled water
Citrate Buffer Solution B	
	14.7g Trisodium citrate dehydrate
	500ml Distilled water
10x PBS buffer	

	95.5g PBS buffer (10X Dulbecco's)
	1L Distilled water
1x PBS buffer	
	100ml l 10x PBS buffer
	900m Distilled water
	pH 7.4
EDTA solution	
	0.372g EDTA disodium salt dihydrate
	1L Distilled water
	pH 8.0

2.1.5. Antibodies

Anti-CD66b	Ab197678, Abcam, UK
Anti-CD20	Clone L26, Dako
Anti-CD8	Clone C8/144B, Dako, Glostrup, Denmark
Anti-CD3	Clone SP7, SpringBio, Pleasanton, CA, USA
Anti- HIF-1α	Clone 54, BD Biosciences, San Jose CA, USA
Anti-GLUT1	Clone SPM498, Abcam, Cambridge, UK
Anti-PDHK1	Ab110025, Abcam, UK
Biotinylated Horse Anti-Mouse IgG	BA-2000, VECTOR Laboratories, USA
Biotinylated Horse Anti-Rabbit IgG	BA-1100, VECTOR Laboratories, USA

2.1.6. Staining, Blocking, and Substrate kits

Alkaline phosphatase (AP) polymer detection system	MACH 3 Biocare Medical, Pacheco, CA, USA

Avidin/Biotin Blocking Kit	SP-2001, VECTOR Laboratories, USA
Levamisole Solution	SP-5000, VECTOR Laboratories, USA
ImmPACT Red Substrate Kit, Alkaline Phosphatase	SK-5105, VECTOR Laboratories, USA
Permanent red AP kit	Zytomed Systems, Bargteheide, Germany
UltraView diaminobenzidine kit	UltraView Universal DAB Detection Kit, Ventana, USA
VECTASTAIN ABC-AP Staining Kit (Alkaline Phosphatase)	AK-5000, VECTOR Laboratories, USA

2.1.7. Computer and Software

Ai	Adobe Illustrator CC 22.1 USA
Computer hardware	MacBook Pro, USA
Excel	Excel for Mac 16.43
ImageJ software	Version 2.0.0-RC-69/1.52p, National Institutes of Health, USA
Prism	Version 8.0.0(131), GraphPad Software, USA
SPSS Statistics	Health, USA Version 26.0, IBM, USA
R programming language and packages	R (version 3.6.3) (statistical analysis and visualization)
R programming language and packages	R (version 3.6.3) ggplot2 (for visualization)
ZEN software	Version 2.0, Carl Zeiss, Germany

2.2. Methods

2.2.1. Study objective and design

The purpose of this study is to illuminate the difference and connection between tumor-infiltrating leukocytes (TILs) and metabolic checkpoint molecules (MCMs) and their impact on the survival of patients with metastatic PC via the application of immunohistochemistry (IHC) staining of PC and its paired metastatic specimens. The QTiS method was applied to analyze the TILs of PC and its corresponding metastatic lesion. In a second, metabolic molecules will be stained and analyzed. There will be a comparison of seven staining markers between primary and metastatic tumors, and additionally, a correlation of seven staining markers with clinical data will be analyzed. Seven markers were stained in 26 metastatic PC specimens, including four leukocyte markers and three metabolic molecule markers **(Table 1**), and then TILs and MCMs were analyzed in terms of OS and DFS.

Table 1. Markers for IHC staining

IHC staining Marker	Type of Leukocytes	Type of Metabolic Molecules
CD3	T cells	
CD8	Cytotoxic T cells	
CD20	B cells	
CD66b	Neutrophils	
GLUT1		Glucose transporter 1
HIF-1α		Hypoxia-inducible factor-1a
PDHK1		Pyruvate dehydrogenase kinase 1

2.2.2. Patients and Clinical Data

In the present study, all tissue specimens to be stained were taken from the pathology department of Klinikum Großhadern, Ludwig-Maximilians University (LMU). The tumor samples were coded anonymously, as required by the HTCR Foundation and the Declaration of Helsinki. Before starting this study, we passed the application and got approval from the institutional ethics committee of LMU in Munich (Project No.19-257).

As noted above, tumor samples from 26 patients who underwent resection at our institution from November 2001 to October 2018 were included **(Figure 2)**. In addition, clinical characteristics, including gender, age, type of metastasis (metachronous, synchronous), were compared with the initial pancreatic tumor. The location of the metastatic lesions was liver, lung, and peritoneum. As well, lab values were collected in our database **(Table 2)**.

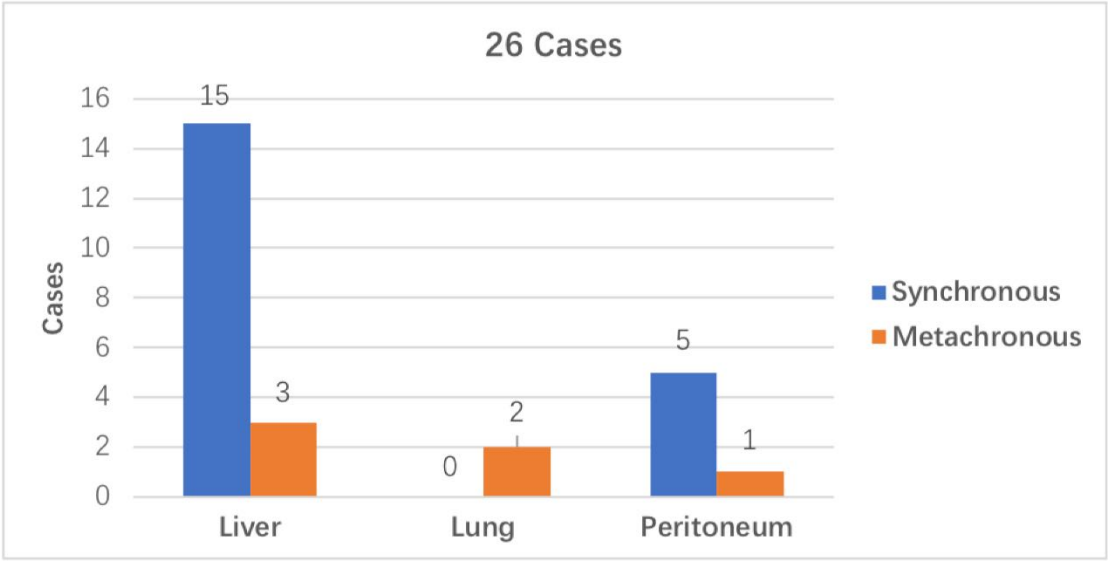

Figure 2. Characteristics of 26 cases: 20 synchronous metastases cases (15 cases in the liver and 5 cases in the peritoneum); 6 metachronous metastases cases (including 3 in the liver, 2 in the lungs, and 1 in the peritoneum).

2.2.3. Immunohistochemistry Staining

For staining CD66b (anti-CD66b, ab197678), and PDHK1(anti-PDHK1, Ab110025), all sections at the thickness of 4 μm to be stained were dewaxed and rehydrated gradually with xylene (5 mins, two times), 100% ethanol (10 mins, two times), 96% ethanol (10 mins, two times), 70% ethanol (10 mins, two times), and then washed with distilled water for 3 min. Antigen retrieval in citrate buffer was carried out in a 96°C water bath for 30 minutes (pH 6.0). The avidin/biotin block took place in humidified chambers for 20 minutes each, followed by protein block for more than 1 hour. For the dilution of both primary antibodies and the corresponding isotype controls, 5%BSA/PBS solution was used (working concentrations: anti-CD66b 1:250, anti-PDHK1 1:200). Gastric and breast cancer specimens were set as positive controls for CD66b and PDHK1, respectively. Incubation was carried out overnight at 4 °C.

On the second day, PBS solution was used to dilute the appropriate secondary antibodies after washed with TBS solution, and then incubated at room temperature for 30 min and washed again with TBS-T solution. The staining activity was monitored under the microscope after the addition of the ABC-AP reagent. As soon as a sufficient staining intensity was found, the staining procedure would be terminated. Counterstaining was conducted for 1 second in fresh hematoxylin. In the final step, a coverslip was placed on the slide with the agent.

The immunohistochemical staining of $CD3^+$, $CD8^+$, $CD20^+$, GLUT1, and HIF-1α were carried out by staining sections at the thickness of 4 μm according to the manufacturer's directions on an autostainer (Ventana Medical Systems, Oro Valley, AZ, USA). Heat mediated antigen retrieval was performed for CD3 (clone SP7, SpringBio, Pleasanton, CA, USA, dilution 1:150), CD8 (clone C8/144B, Dako, Glostrup, Denmark, dilution 1:50), CD20 (clone L26, Dako, Glostrup, Denmark, dilution 1:400), and GLUT-1 (clone SPM498, Abcam,

Cambridge, UK, dilution 1:200) using cell conditioning solution 1 (CC1, pH 8.4, Ventana). The ultraView diaminobenzidine kit (Ventana) was used to detect the signal. The detection of HIF1-α expression was performed using a monoclonal antibody (clone 54, BD Biosciences, San Jose CA, USA) at 1:30 dilution after heat mediated antigen retrieval (epitope retrieval solution, pH 8, Novocastra, Newcastle upon Tyne, UK). The signal was detected by alkaline phosphatase (AP) polymer detection system (MACH 3 Biocare Medical, Pacheco, CA, USA) and permanent red AP dye (Zytomed Systems, Bargteheide, Germany). Normal human tonsils served as a positive control for CD3, CD8, CD20 and ubiquitously present erythrocytes served as an internal positive control for GLUT-1 in each staining.

2.2.4. Digital Imaging

The hot spots were captured with the use of ZEN software after all staining slides were visualized with a microscope at 200x magnification. If possible, take three hot spots with the highest density of target marker on each slide (hotspots: high densities of IHC staining markers) [3]. Avoid the tumor cells when taking the stained marker in the stromal areas, and similarly, avoid the stromal cells when taking the stained marker in the tumor cell areas.

2.2.5. Counting Methods

Our department has developed a new reliable, accurate, and practical algorithm called QTiS to quantify the infiltration in malignant tumors[3, 141, 142] (**figure 3**). This study extended this algorithm to quantify MCMs (HIF-1α, GLUT1, PDHK1).

Firstly, the location with the maximum infiltration of the IHC staining cell ($CD3^+$, $CD8^+$, $CD20^+$, or $CD66b^+$) was characterized as the hotspot, representing the

aggregation of specific immune cells in the TME [3, 143]. In this study, we also extended this definition of the hot spot to MCMs. It is recommended to quantify the mean value of three hot spots; however, one hot spot is also desirable in the case of low infiltration density. A study from Miksch, R.C., et al. demonstrated that one observer is reasonable and reliable for the subjective selection of hotspots[141]. This selected approach was also used in quantifying Ki67 [144]. In this study, we processed the quantitation of tumor stroma (QTS) for leukocyte markers ($CD3^+$, $CD8^+$, $CD20^+$, and $CD66b^+$) and MCMs (HIF-1α, GLUT1, PDHK1). The correlation between seven staining markers and survival of metastatic pancreatic cancer was investigated by utilizing the quantitation of tumor immune stroma (QTiS).

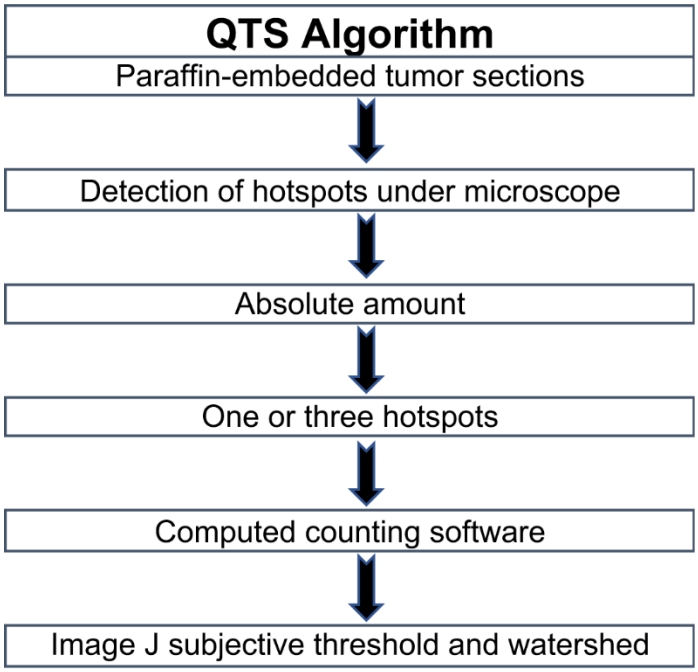

Figure 3. Schematic diagram of the QTiS algorithm: from staining paraffin sections to quantification of tumor stroma[3, 141].

The counting method was carried out in three steps with the use of ImageJ software. Firstly, the original images (jpeg format) were converted into 32-bit and the ImageJ Standard was used to set the subjective staining threshold to clearly and accurately visualize the target marker's contour. Then the large particles can be separated by the watershed function of ImageJ software. Finally, the

function of "analyze particles" was employed to automatically count these particles, so as to complete the quantification of the target marker (**Figure 4**).

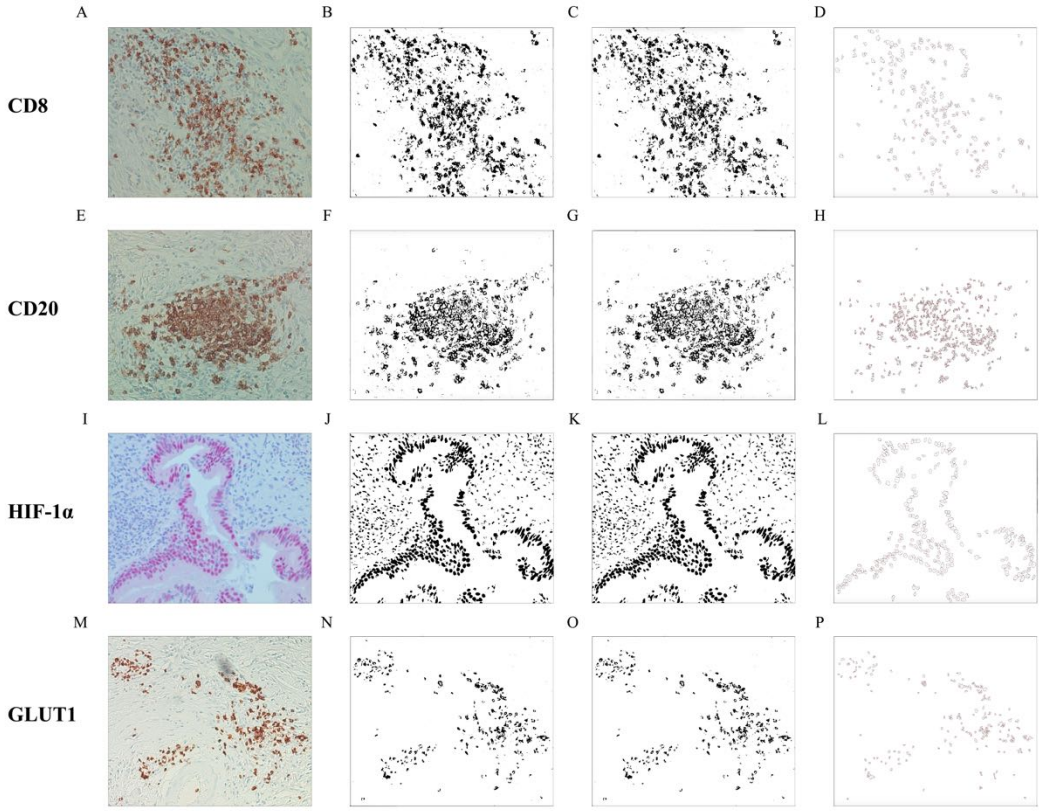

Figure 4. **Representative the process of quantifies IHC staining marker.** The original images (A, E, I M); images after the threshold (B, F, J, N); images after watershed (C, G, K, O); Quantitative images (D, H, L, P). HIF-1α represents the quantitative process of molecules in tumor cell areas. GLUT1 represents the quantitative process of molecules in tumor stroma areas.

2.2.6. Statistical analysis

Statistical analysis was conducted with the use of R packages (version 3.6.3), and SPSS (Version 26.0, IBM, USA). P-values <0.050 in univariate analysis were included in multivariate for analysis, and statistical significance was considered as a P-value of less than 0.050. Continuous variables were expressed as mean ± SD. Independent t-tests was performed to analyze data with a normal distribution, while the Wilcoxon rank-sum tests were employed to

analyze data with a non-normal distribution. Spearman correlations were used to calculate the correlation between IHC staining markers and clinical data in this study.

Statistical analysis was performed on the immunohistochemical results of seven markers (CD3, CD8, CD20, CD66b, GLUT1, HIF-1α, PDHK1). First, the mean value of each antibody and each patient (primary lesion and metastatic lesion were obtained separately) were calculated as a continuous variable for comparison between groups, and the ROC curve was drawn. Then the median value of 26 different mean values (obtained separately for the primary and metastatic lesion) was determined, the two groups with the median (High filtration group >medians or Low infiltration group ≤medians) were analyzed.
The combining of two high markers (greater than the median) was defined as a high infiltration group. It would be considered as a high infiltration group to combine three markers if at least two of them were high infiltration, a high infiltration group for the combination of four markers if at least three of them were high infiltration. High and low categorical variables were used to perform univariate survival analysis (Log-rank) and correlation analysis (Binary logistic regression). Time-dependent ROC curves (1 year) were drawn to predict OS and DFS. DFS is the period when the primary tumors or/and the metastatic tumors of PC have no evidence of recurrence after resection. After resection of the primary tumor or/and metastatic tumors of PC to death is referred to as OS.

3. Results

3.1 Characteristics of the pancreatic cancer study cohort

Twenty-six (26) PC patients were recruited in this study, 20 of whom had concomitant metastases to other organs, and 6 developed distant organ metastases at different times after PC resection. The patients aged from 44 to 78 years, with a median age of 63.8 years, and 57.7% of them were female. Sixteen patients underwent preoperative neoadjuvant chemotherapy, and 21 patients underwent postoperative chemotherapy. Seven pylorus resections pancreaticoduodenectomies (PrPD), six pylorus-preserving pancreaticoduodenectomies (PPPD), twelve left pancreatectomies, and one total pancreatectomy were performed (**Table 2 and 3**). One patient developed two pulmonary metastases after resection the primary pancreatic lesion and had both pulmonary metastases removed. In addition, three patients underwent resection of the colon and ovarian appendages and resection of the primary and metastatic pancreatic cancer tumors.

The mean DFS was 17.0 months (SD ± 25.262), while the mean OS was 27.5 months (SD ± 45.343). Twenty (20) patients underwent simultaneous resection of primary and metastatic tumors of metastatic pancreatic cancer. Six (6) patients developed distant tumor metastases during follow-up, including one case with two times pulmonary metastases, and all six (6) cases underwent resection of metastatic tumors after confirmation of metastases. Eighteen patients (69.2%) finished the adjuvant chemotherapy with gemcitabine, while the remaining eight patients (30.8%) did not due to intolerance or death. Two patients underwent gemcitabine chemotherapy combined with 45 and 60 GY doses of radiation therapy separately. No patient survived the follow-up period (median 11.0 months).

The laboratory values before PC resection and quantitative IHC staining markers are shown in **Tables 4 and 5.**

Table 2: Patient characteristics.

(Abbreviations: Perit: peritoneum; Metachron: metachronous; Synchron: synchronous; PrPD: pylorus resections pancreaticoduodenectomy; PPPD: pylorus-preserving pancreaticoduodenectomy; LP: left pancreatectomy PDAC: pancreatic ductal adenocarcinoma)

N	Gender	Age	Location of the primary tumor	Metastasis sites	Kind of metastasis	First surgery	Second surgery	Pathological type	Adjuvant therapy
1	w	60	Head	Liver	Metachron	PrPD	liver V	PDAC	Yes
2	m	59	Head	Liver	Synchron	PPPD+ liver II		PDAC	Yes
3	w	66	Tail	Liver	Synchron	LP + liver VII		PDAC	Yes
4	w	57	Corpus	Liver	Synchron	TP		PDAC	Yes
5	m	78	Corpus	Liver	Synchron	LP		PDAC	No
6	w	63	Head	Liver	Synchron	PrPD+ liver III		PDAC	Yes
7	w	44	Head	Liver	Synchron	PPPD + Liver Ivb -VI		PDAC	No
8	m	60	Head	Lung	Metachron	LP	Left lung segment	PDAC	Yes
9	m	69	Head	Lung	Metachron	PPPD	Left lung segment	PDAC	Yes
10	m	75	Tail	Liver	Metachron	LP	liver VII	PDAC	Yes
11	w	74	Tail	Perit	Synchron	LP+Perit		PDAC	No
12	w	73	Head	Liver	Synchron	PrPD +liver II		PDAC	Yes
13	w	66	Corpus	Liver	Synchron	LP +liver III / IVb		PDAC	Yes
14	w	73	Tail	Liver	Synchron	LP + liver VII		PDAC	No
15	m	52	Head	Liver	Metachron	PPPD	liver VII	PDAC	Yes

16	m	77	Head	Liver	Synchron	PrPD +liver II		PDAC	No
17	m	57	Corpus	Perit	Metachron	LP	Perit	PDAC	Yes
18	w	44	Corpus	Liver	Synchron	LP + liver Iv		PDAC	Yes
19	w	69	Head	Perit	Synchron	PrPD+ Perit	liver V	PDAC	Yes
20	m	59	Head	Liver	Synchron	PrPD +liver II		PDAC	No
21	m	67	Head	Perit	Synchron	PrPD+ Perit		PDAC	Yes
22	w	63	Head	Liver	Synchron	PPPD+ liver III		PDAC	Yes
23	w	54	Tail	Perit	Synchron	LP+ Perit		PDAC	No
24	w	64	Tail	Liver	Synchron	LP + liver II III		PDAC	Yes
25	m	62	Tail	Perit	Synchron	LP+ Perit		PDAC	Yes
26	w	74	Head	Liver	Synchron	PPPD+ liver II	Left lung segment	Mucinous AdenoCa.	No

Note：The second lung metastasectomy of case 8 was performed six months after the first left lung metastasectomy.

Table 3. Demographics of Study Population.

Variables	Results
Age (Year, Mean ± SD)	63.808 ± 9.261
Gender (Female/Male)	15 (57.7%)/11 (42.3%)
Operation	7 PrPD (26.9%)
	6 PPPD (23.1%)
	12 Distal pancreatic resections (46.2%)
	1 Total pancreatectomy (3.8%)
Location	13 Head (50%)
	5 Corpus (19.2%)
	8 Tail (30.8%)
TNM Classification Grading	7 G2 (26.9%)
	17 G3 (65.4%)
	2 G4 (7.7%)
TNM Classification Tumor	2 T2 (7.7%)
	23 T3 (88.5%)
	1 T4 (3.8%)
	11 N0 (42.3%)

TNM Classification Lymph Nodes	14 N1(53.8%)
	1 N2 (3.8%)
TNM Classification Metastasis	6 M0 (23.1%)
	20 M1 (76.9%)
TNM Classification Resection	12 R0 (46.2%)
	12 R1 (46.2%)
	2 R2 (7.7%)

Table 4. Laboratory values before PC resection.

(Abbreviations: SD: standard deviation; AFP: serum alpha-fetoprotein; CA19-9: Carbohydrate antigen 19-9; Hb: Hemoglobin; CRP: C-reactive protein; INR: international normalized ratio; ALP: alkaline phosphatase; GGT: Gamma-glutamyl transpeptidase.)

Variables	Results
CEA	6.052±11.459
CA19-9	1258.553±2178.596
Bilirubin (mg/dl) (Mean ± SD)	1.851±3.592
Albumin (g/L) (Mean ± SD)	42.785±5.766
Lipase (U/L) (Mean ± SD)	80.456±84.852
Amylase (U/L) (Mean ± SD)	72.861±38.791
INR (Mean ± SD)	11.45±25.198
Creatinine (mg/dl) (Mean ± SD)	0.872±0.154
CRP (mg/L) (Mean ± SD)	1.737±4.457
ALP (U/L) (Mean ± SD)	162.916±218.021
GGT (U/L) (Mean ± SD)	280.76±744.902
Leukocytes (/mm^3) (Mean ± SD)	7384.231±2793.957
Platelets (/mm^3) (Mean ± SD)	240.923±59.574
Hb (g/dl) (Mean ± SD)	12.684±2.757
Quick (Mean ± SD)	94.895±24.516

Table 5. The density of IHC staining markers in PC.

Variables	Results
Primary tumors of PC	
CD3 **P** (concentration)	157-698.667(median 442.667)/0.145 mm^2
CD8 **P** (concentration)	79.667-552.667 (median 362.833)/0.145 mm^2
CD20 **P** (concentration)	19-1227 (median 676.5)/0.145 mm^2
CD66 **P** (concentration)	0-238 (median 45.167)/0.145 mm^2
T GLUT1 **P** (concentration)	26-320.667(median 217.167)/0.145 mm^2
T HIF-1α **P** (concentration)	0-388(median 188)/0.145 mm^2
T PDHK1 **P** (concentration)	0-326(median 118.833)/0.145 mm^2
S GLUT1 **P** (concentration)	60.667-450(median 141.333)/0.145 mm^2
S HIF-1α **P** (concentration)	10-205.333(median 93.167)/0.145 mm^2
S PDHK1 **P** (concentration)	0-170.333(median 46.333)/0.145 mm^2
Metastatic tumors of PC	
CD3 **M** (concentration)	71–780.667 (median 362.833)/0.145 mm^2
CD8 **M** (concentration)	0–298 (median 101.833)/0.145 mm^2
CD20 **M** (concentration)	0–629.333 (median 155.665)/0.145 mm^2
CD66 **M** (concentration)	0–233.333 (median 71.665)/0.145 mm^2
T GLUT1 **M** (concentration)	13.667–466.333 (median 223.5)/0.145 mm^2
T HIF-1α **M** (concentration)	0–306.667 (median 199)/0.145 mm^2
T PDHK1 **M** (concentration)	0–251 (median 129)/0.145 mm^2
S GLUT1 **M** (concentration)	16.333-529.333(median 175.167)/0.145 mm^2
S HIF-1α **M** (concentration)	0-221(median 103.417)/0.145 mm^2
S PDHK1 **M** (concentration)	0-104.667(median 38.667)/0.145 mm^2

Note: P stands for Primary lesion of PC, **M** stands for metastatic tumors of PC, **S** stands for tumor stroma areas, **T** stands for tumor cell areas.

3.2 TILs infiltration in primary and metastatic tumor of PC

Immunohistochemistry revealed positive staining for $CD3^+$, $CD8^+$, $CD20^+$, and $CD66b^+$ in the stromal area of PC's primary and metastatic lesions (**Figure 5 and 6**).

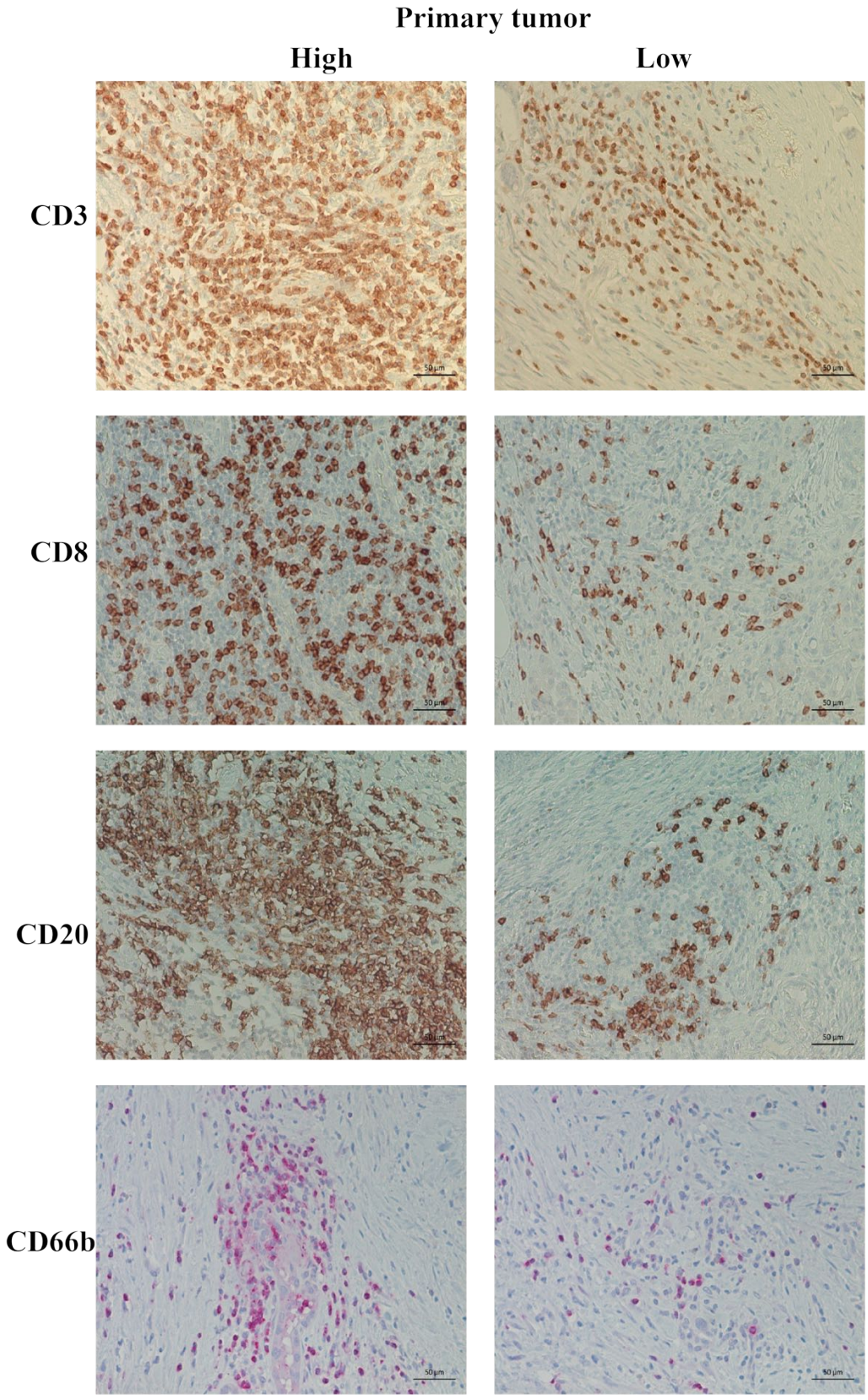

Figure 5. Representative pictures of high and low infiltration for $CD3^+$, $CD8^+$, $CD20^+$, $CD66b^+$ in PC primary lesions under 200x magnification(High and low infiltration were defined by median).

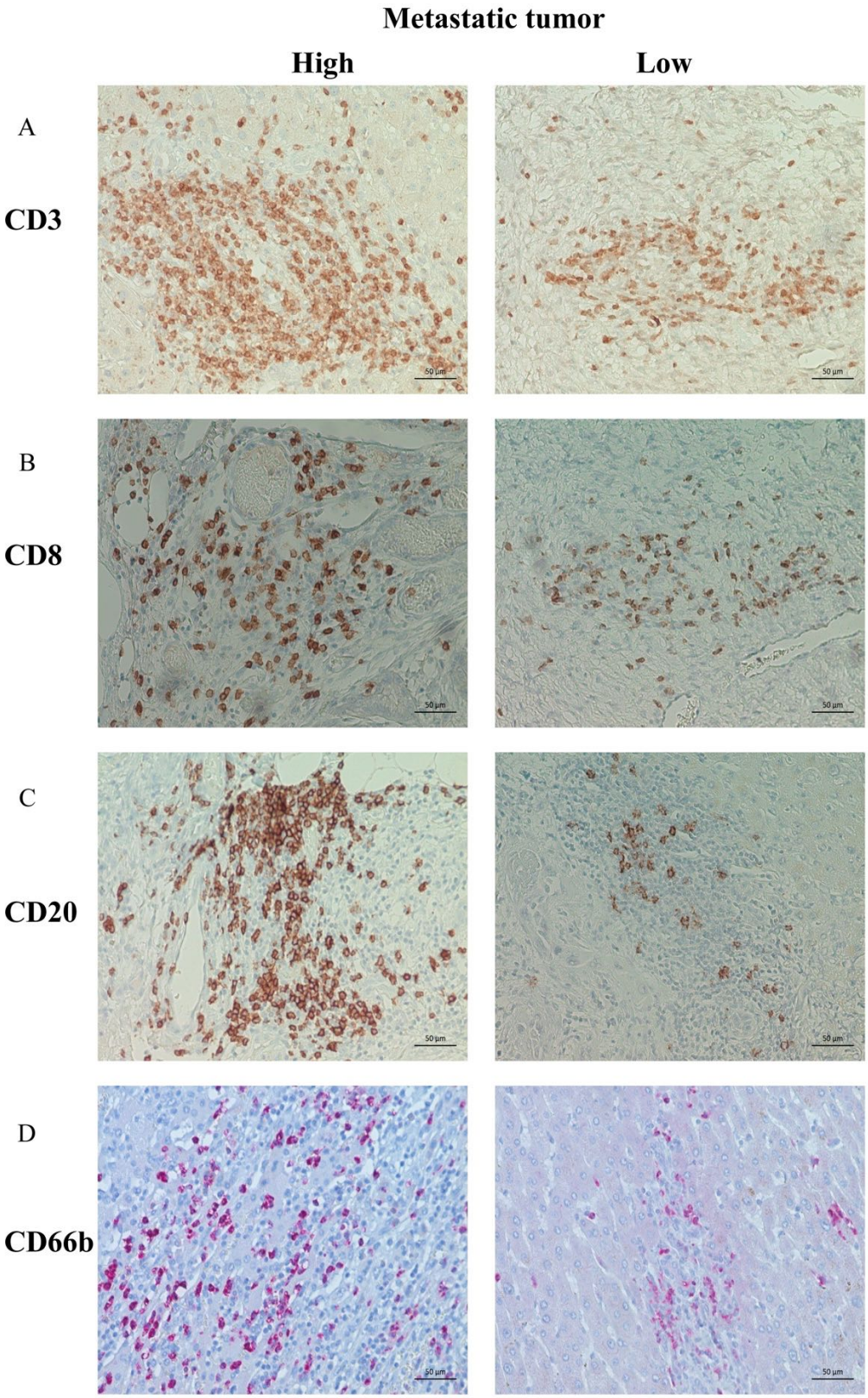

Figure 6. Representative pictures of high and low infiltration for $CD3^+$, $CD8^+$, $CD20^+$, $CD66b^+$ in PC metastatic lesions under 200x magnification(High and low infiltration were defined by median).

3.3 MCMs staining in primary and metastatic lesion of PC

Immunohistochemistry revealed the staining for GLUT1, HIF-1α, and PDHK1 in PC's primary and metastatic lesions (**Figure 7 and 8**).

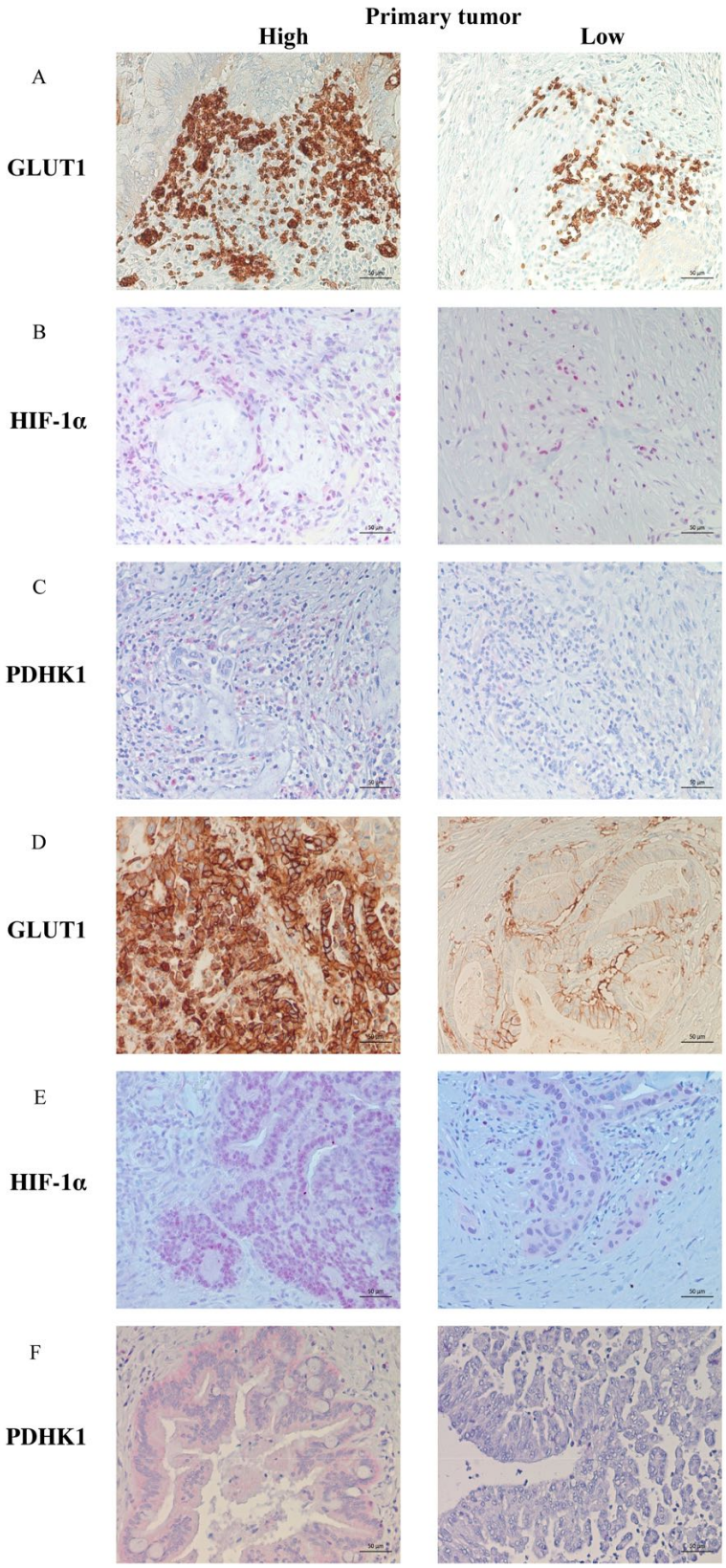

Figure 7. Representative pictures of high and low density for GLUT1, HIF-1α, and PDHK1 in PC primary lesions under 200x magnification. A, B, C show staining in tumor stromal areas; D, E, F show staining in tumor cell areas (High and low density were defined by median).

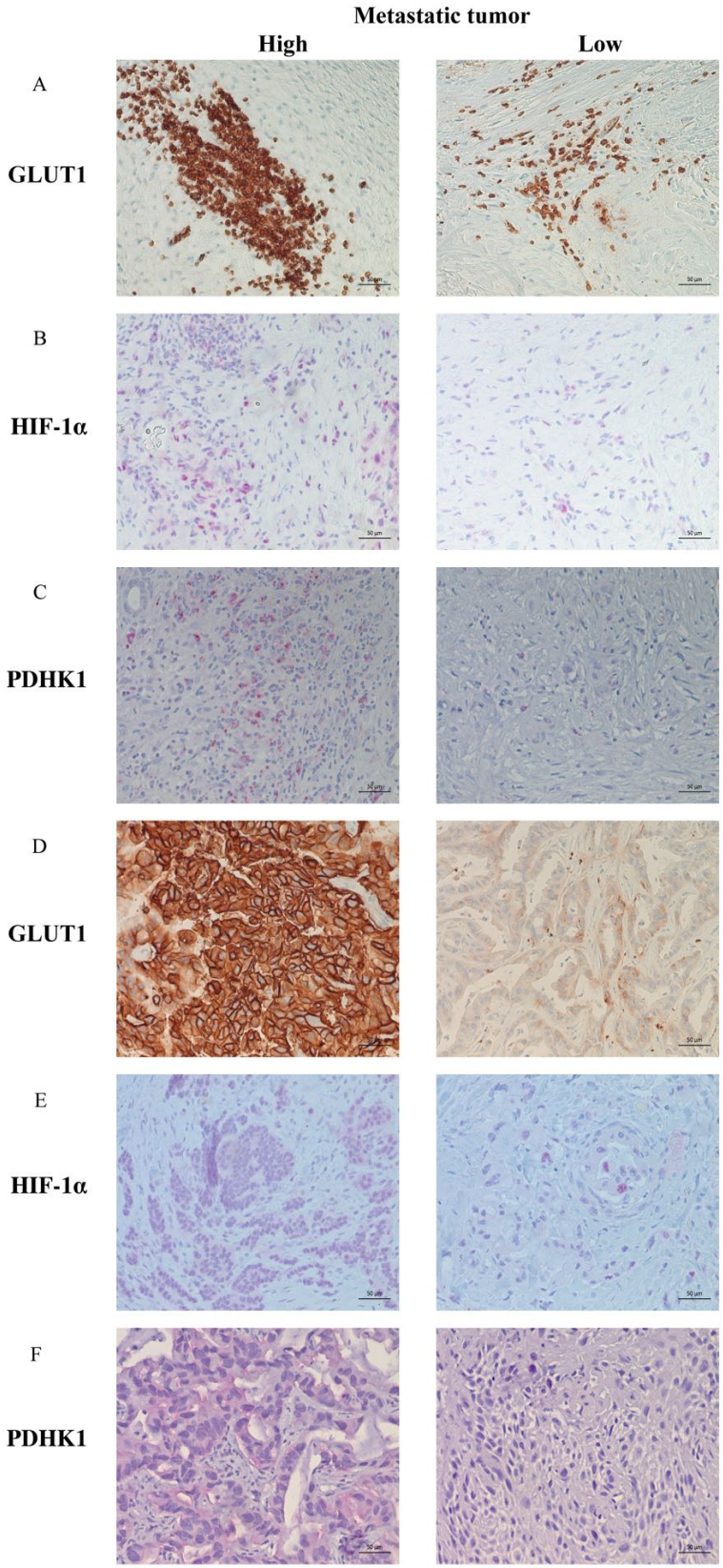

Figure 8. Representative pictures of high and low density for GLUT1, HIF-1α, and PDHK1 in PC metastatic lesions under 200x magnification. A, B, C show staining in tumor stromal areas; D, E, F show staining in tumor cell areas (High and low density were defined by median).

3.4 Differential analysis of leukocyte infiltration

The infiltration of $CD3^+$ T lymphocytes ($P<0.05$), $CD8^+$ T lymphocytes ($P<0.001$), $CD20^+$ B lymphocytes ($P<0.001$) in PC primary tumors was higher than in metastatic tumors. However, the difference infiltration of $CD66b^+$ ($p=0.65$) was not statistically significant. Furthermore, there was no statistically significant difference in TILs infiltration between liver and non-liver group ($CD3^+$ TILs $p=0.5$, $CD8^+$ TILs $p=0.58$, $CD20^+$ TILs $p=0.79$, $CD66b^+$ TINs $p=0.58$), synchronous and metachronous group ($CD3^+$ TILs $p=0.21$, $CD8^+$ TILs $p=0.15$, $CD20^+$ TILs $p=0.09$, $CD66b^+$ TINs $p=0.74$) (**Figure 9**).

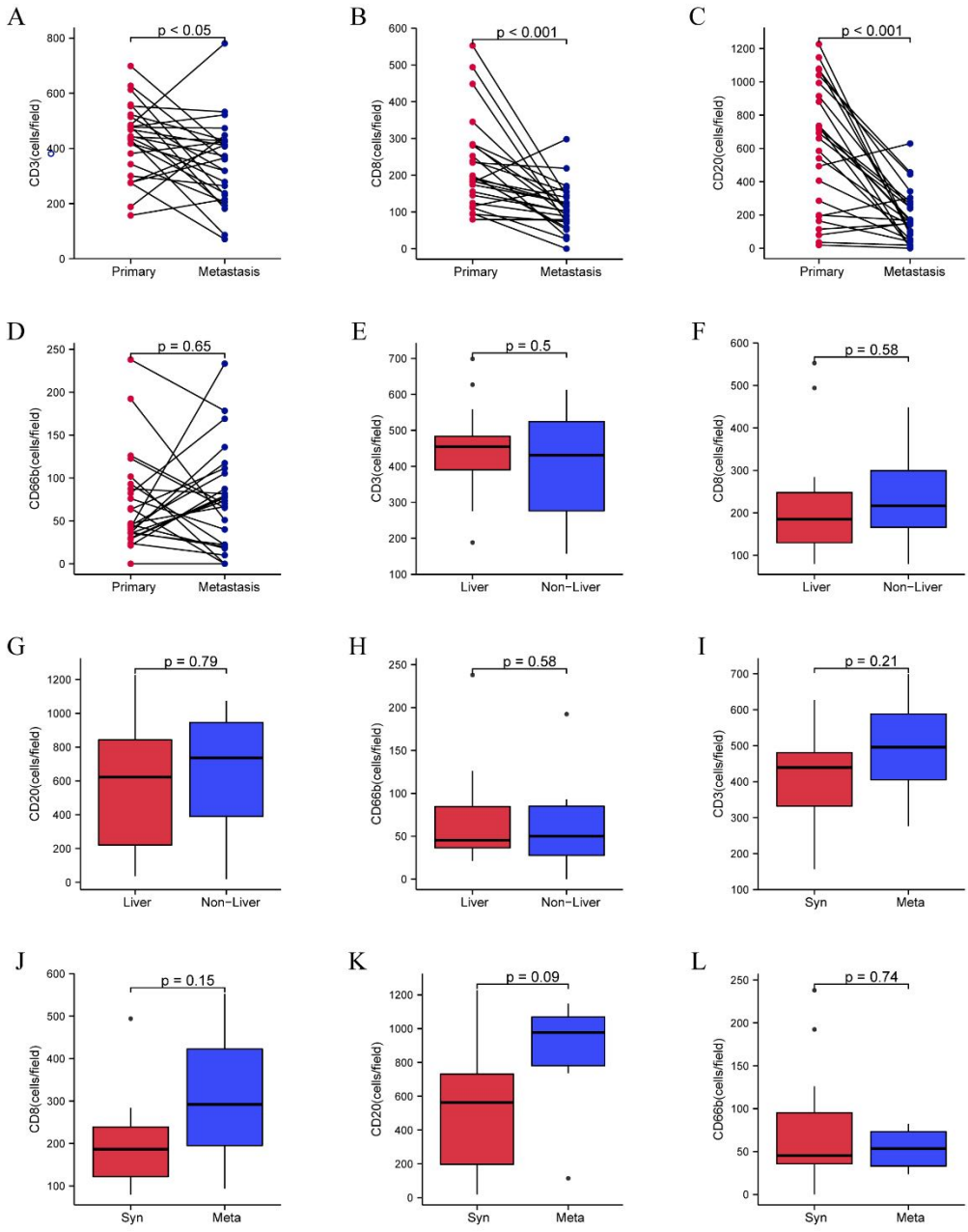

Figure 9. Differential analysis of leukocyte infiltration in primary and metastasis group (A, B, C, D), liver and non-liver group (E, F, G, H), synchronous and metachronous group (I, J, K, L). $CD3^+$, $CD8^+$, and $CD20^+$ are highly expressed in primary tumors than in metastatic tumors in metastatic pancreatic cancer. **Note**: Syn stands for synchronous metastasis, Meta stands for metachronous metastasis.

3.5 Prognostic value of TILs in pancreatic cancer on patient's survival

3.5.1 Prognostic value of TILs in primary tumor of PC on OS

Kaplan-Meier plots revealed high infiltration of $CD20^+$ (Log-rank P=0.013) correlated with improved OS in PC primary tumors. We analyzed all the leukocytes in different combinations and found that high group of $CD3^+$+$CD20^+$ (p=0.018), $CD8^+$+$CD20^+$ (p=0.03), $CD3^+$+$CD8^+$+$CD20^+$ (p=0.025), and $CD3^+$+$CD20^+$+$CD66b^+$ (p=0.02) correlated with better OS in PC primary tumors (**Figure 10**).

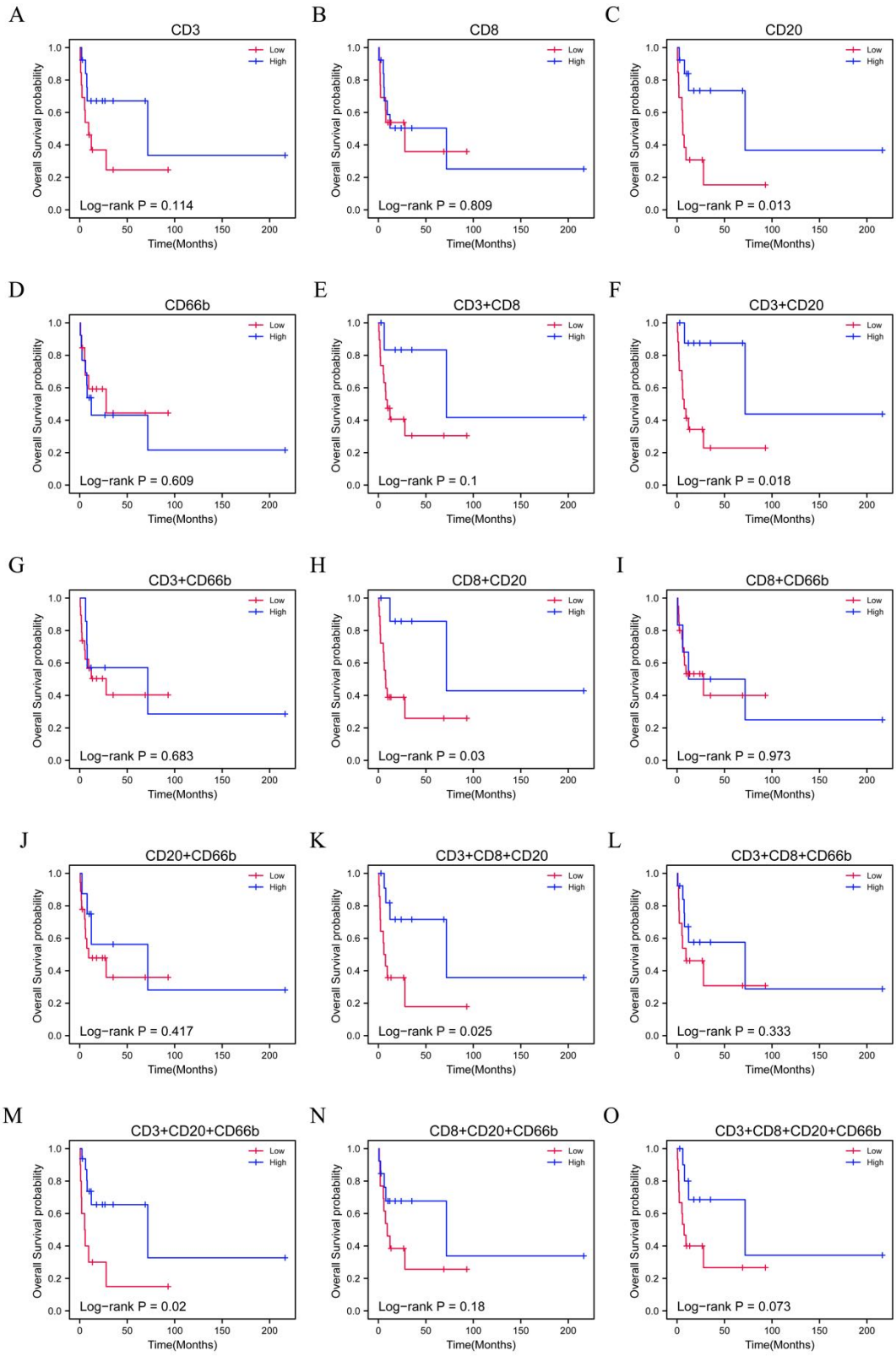

Figure 10. Kaplan-Meier plots of $CD3^+$, $CD8^+$, $CD20^+$, $CD66b^+$ and leukocytes combinations on OS.

3.5.2 Prognostic value of TILs in primary tumor of PC on DFS

Kaplan-Meier plots revealed high or low infiltration of $CD3^+$ (p=0.931), $CD8^+$ (p=0.528), $CD20^+$ (p=0.458), $CD66b^+$ (p=0. 312) didn't correlate with DFS, and all the leukocytes in different combinations showed the same results ($CD3^+$+$CD8^+$ P=0.842, $CD3^+$+$CD20^+$ P=0.548, $CD3^+$+$CD66b^+$ P=0.223, $CD8^+$+$CD20^+$ P=0.859, $CD8^+$+$CD66b^+$ P=0.061, $CD20^+$+$CD66b^+$ P=0.722, $CD3^+$+$CD8^+$+$CD20^+$ P=0.979, $CD3^+$+$CD8^+$+$CD66b^+$ P=0.866, $CD3^+$+$CD20^+$+$CD66b^+$ P=0.948, $CD8^+$+$CD20^+$+$CD66b^+$ P=0.22, $CD3^+$+$CD8^+$+$CD20^+$+$CD66b^+$ P=0.729) (**Figure 11**).

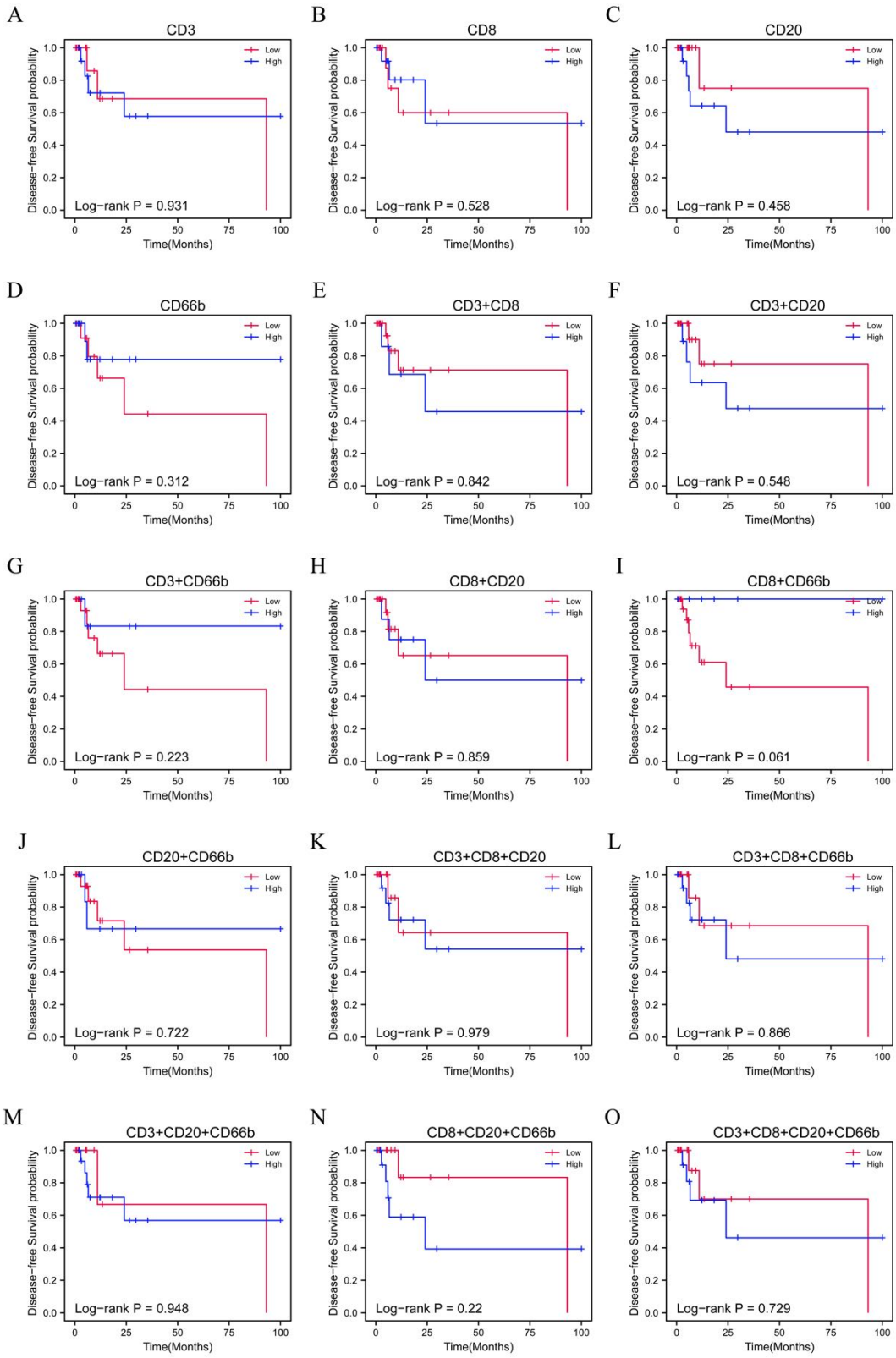

Figure 11. Kaplan-Meier plots of $CD3^+$, $CD8^+$, $CD20^+$, $CD66b^+$ and leukocytes combinations on DFS.

3.5.3 Time-dependent ROC curve of immune leukocytes infiltrating in primary tumor of PC on OS (1 year) and DFS (1 year)

Analysis of Time-dependent ROC curves (1 year) of immune leukocytes infiltrating in PC primary tumors was performed. None of leukocytes showed significant ability to predict the improved OS ($CD3^+$ AUC=0.339, $CD8^+$ AUC=0.405, $CD20^+$ AUC=0.274, $CD66b^+$ AUC=0.607) and DFS ($CD3^+$ AUC=0.466, $CD8^+$ AUC=0.369, $CD20^+$ AUC=0.422, $CD66b^+$ AUC=0.341) (**Figure 12**).

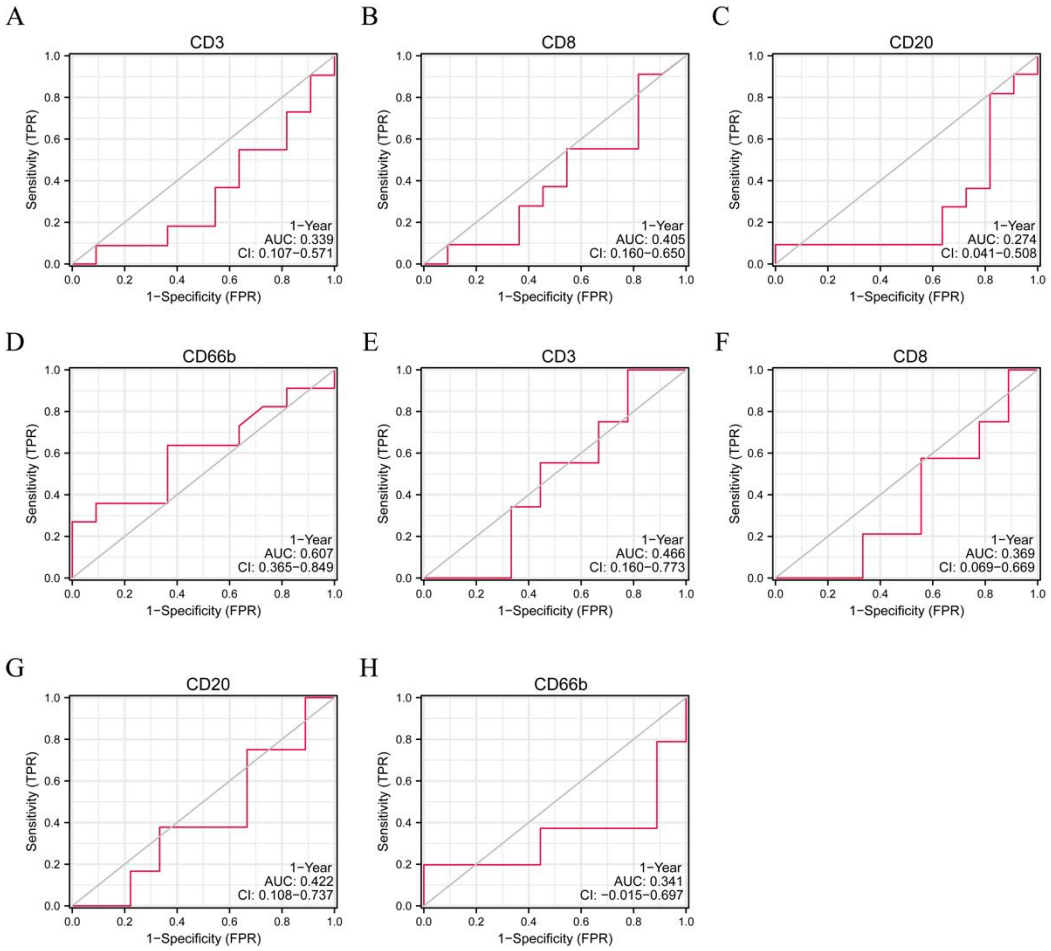

Figure 12. Time-dependent ROC curves were drawn to predict the OS (A, B, C, D) and DFS (E, F, G, H) in PC primary tumors.

3.5.4 Prognostic value of TILs in metastatic tumor of PC on OS

Kaplan-Meier plots revealed high infiltration of $CD8^+$ (Log-rank P=0.023) correlated with improved OS in PC metastatic tumors. However, none of the leukocytes in different combinations showed statistical significance ($CD3^+$+$CD8^+$ P=0.388, $CD3^+$+$CD20^+$ P=0.624, $CD3^+$+$CD66b^+$ P=0.639, $CD8^+$+$CD20^+$ P=0.429, $CD8^+$+$CD66b^+$ P=0.072, $CD20^+$+$CD66b^+$ P=0.243, $CD3^+$+$CD8^+$+$CD20^+$ P=0.451, $CD3^+$+$CD8^+$+$CD66b^+$ P=0.831, $CD3^+$+$CD20^+$+$CD66b^+$ P=0.699, $CD8^+$+$CD20^+$+$CD66b^+$ P=0.447, $CD3^+$+$CD8^+$+$CD20^+$+$CD66b^+$ P=0.734) (**Figure 13**).

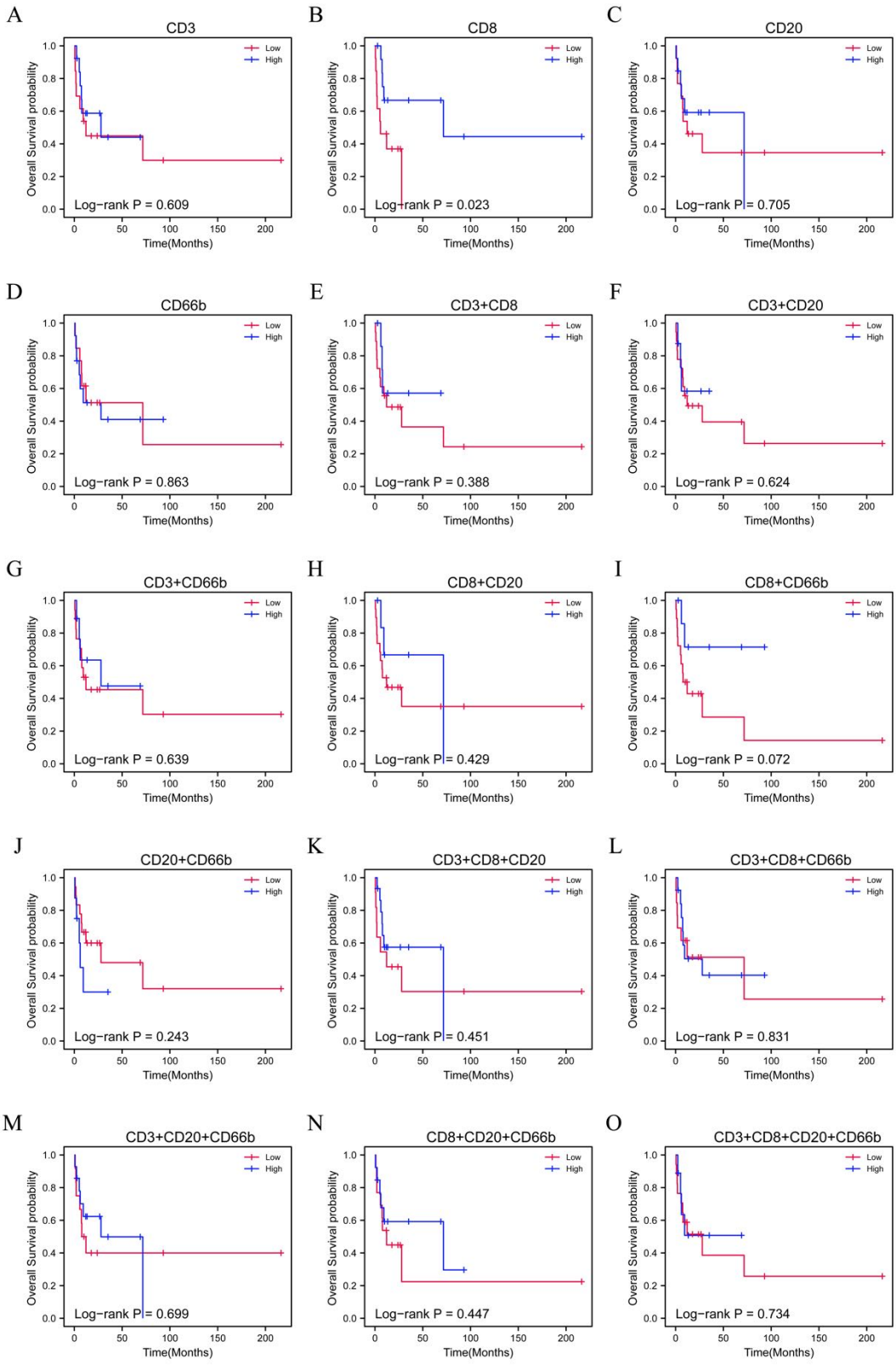

Figure 13. Kaplan-Meier plots of $CD3^+$, $CD8^+$, $CD20^+$, $CD66b^+$ and leukocytes combinations on OS.

3.5.5 Prognostic value of TILs in metastatic tumor of PC on DFS

Kaplan-Meier plots revealed high or low infiltration of $CD3^+$ (p=0.357), $CD8^+$ (p=0.531), $CD20^+$ (p=0.076), $CD66b^+$ (p=0. 562) didn't correlate with DFS, and all the leukocytes in different combinations showed the same results ($CD3^+$+$CD8^+$ P=0.906, $CD3^+$+$CD20^+$ P=0.139, $CD3^+$+$CD66b^+$ P=0.387, $CD8^+$+$CD20^+$ P=0.214, $CD8^+$+$CD66b^+$ P=0.884, $CD20^+$+$CD66b^+$ P=0.327, $CD3^+$+$CD8^+$+$CD20^+$ P=0.645, $CD3^+$+$CD8^+$+$CD66b^+$ P=0.713, $CD3^+$+$CD20^+$+$CD66b^+$ P=0.581, $CD8^+$+$CD20^+$+$CD66b^+$ P=0.743, $CD3^+$+$CD8^+$+$CD20^+$+$CD66b^+$ P=0.944) (**Figure 14**).

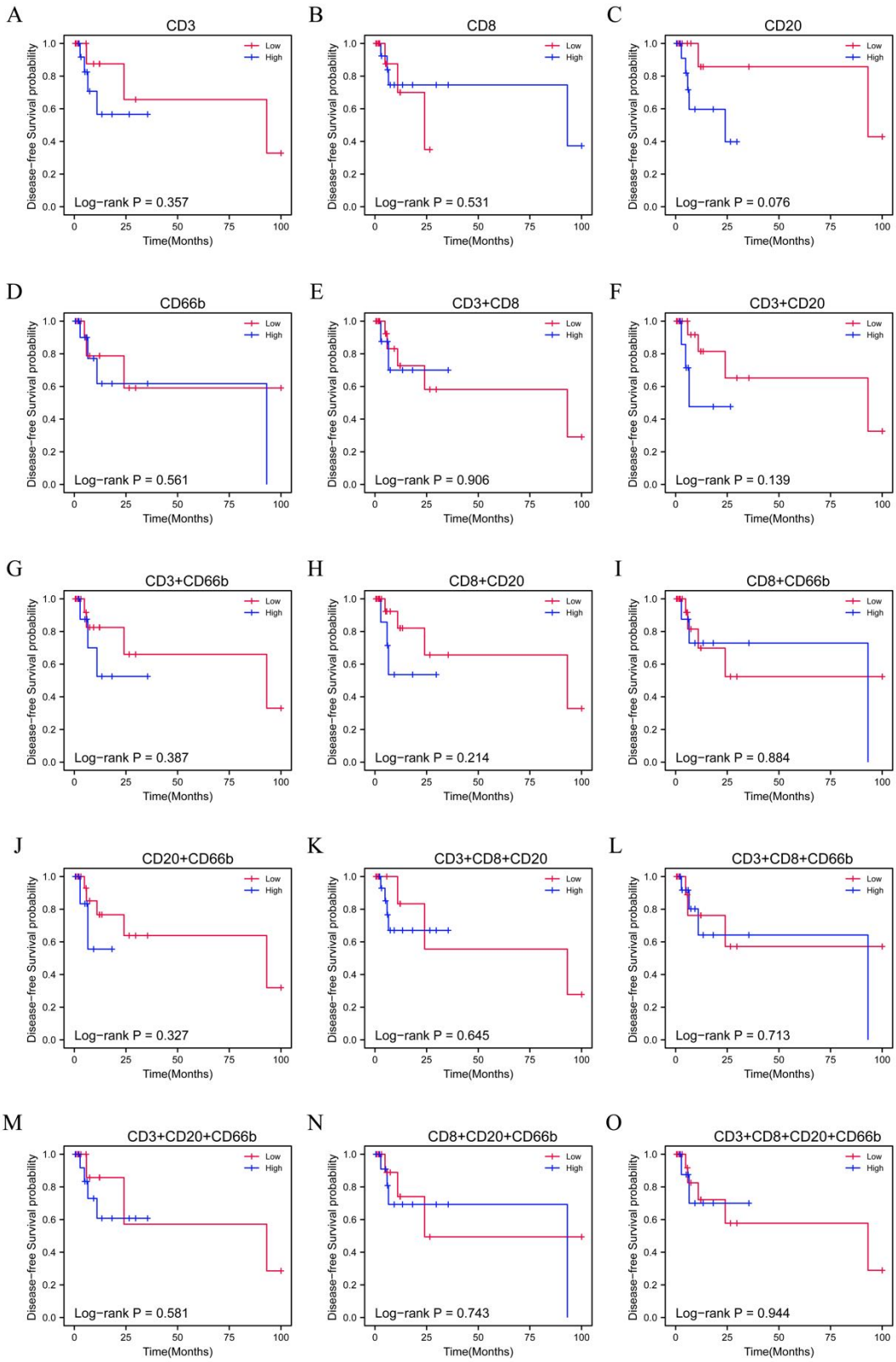

Figure 14. Kaplan-Meier plots of $CD3^+$, $CD8^+$, $CD20^+$, $CD66b^+$ and leukocytes combinations on DFS.

3.5.6 Time-dependent ROC curve of immune leukocytes infiltrating in metastatic tumor of PC on OS (1 year) and DFS (1 year)

Analysis of Time-dependent ROC curves (1 year) analysis of immune leukocytes infiltrating in PC primary tumors was performed. None of leukocytes showed significant ability to predict the improved OS ($CD3^+$ AUC=0.492, $CD8^+$ AUC=0.41, $CD20^+$ AUC=0.456, $CD66b^+$ AUC=0.533) and DFS ($CD3^+$ AUC=0.854, $CD8^+$ AUC=0.504, $CD20^+$ AUC=0.678, $CD66b^+$ AUC=0.625) (**Figure 15**).

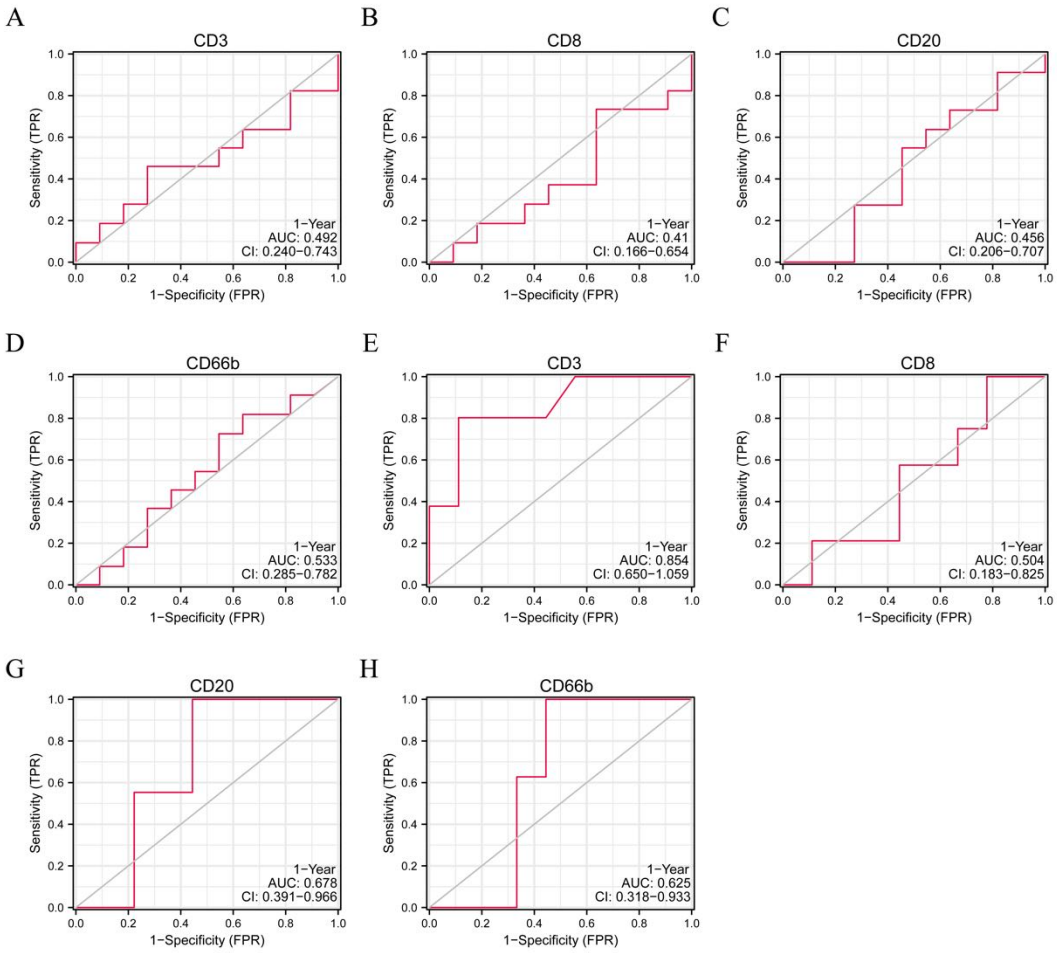

Figure 15. Time-dependent ROC curves were drawn to predict the OS (A, B, C, D) and DFS (E, F, G, H) in PC metastatic tumors.

3.6 The Neutrophil-to-lymphocyte ratio (NLR) in primary and metastatic tumor of PC

3.6.1 Prognostic value of NLR in the primary tumors of PC on OS and DFS

Neutrophil-to-lymphocyte ratio in PC primary tumors showed no correlation with OS ($CD66b^+/CD3^+$ p=0.597, $CD66b^+/CD8^+$ p=0.489) and DFS ($CD66b^+/CD3^+$ p=0.066, $CD66b^+/CD8^+$ p=0.524, $CD66b^+/CD20^+$ p=0.813), except for low $CD66b^+/CD20^+$ (p=0.009) ratio correlated with improved OS (**Figure 16**).

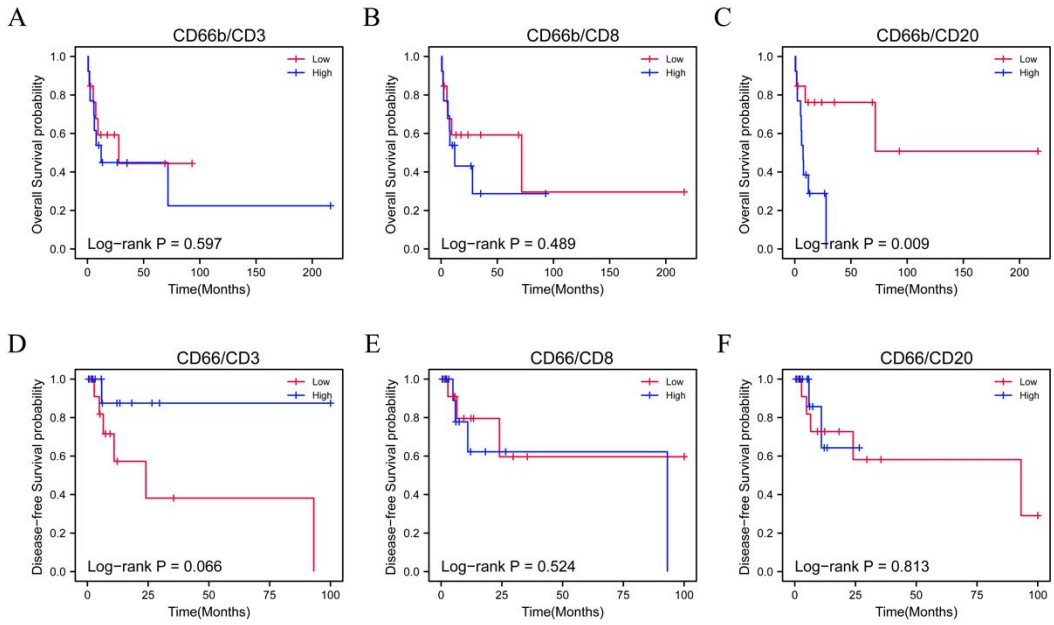

Figure 16. The prognostic value of the NLR in PC primary tumors on OS (A, B, C) and DFS (D, E, F).

3.6.2 Time-dependent ROC curve of NLR in primary tumors of PC on OS (1 year) and DFS (1 year)

None of NLR showed significant ability to predict the OS ($CD66b^+/CD3^+$ AUC=0.646, $CD66b^+/CD8^+$ AUC=0.646 $CD66b^+/CD20^+$ AUC=0.695) and DFS ($CD66b^+/CD3^+$ AUC=0.381, $CD66b^+/CD8^+$ AUC=0.566 $CD66b^+/CD20^+$ AUC=0.495) (**Figure 17**).

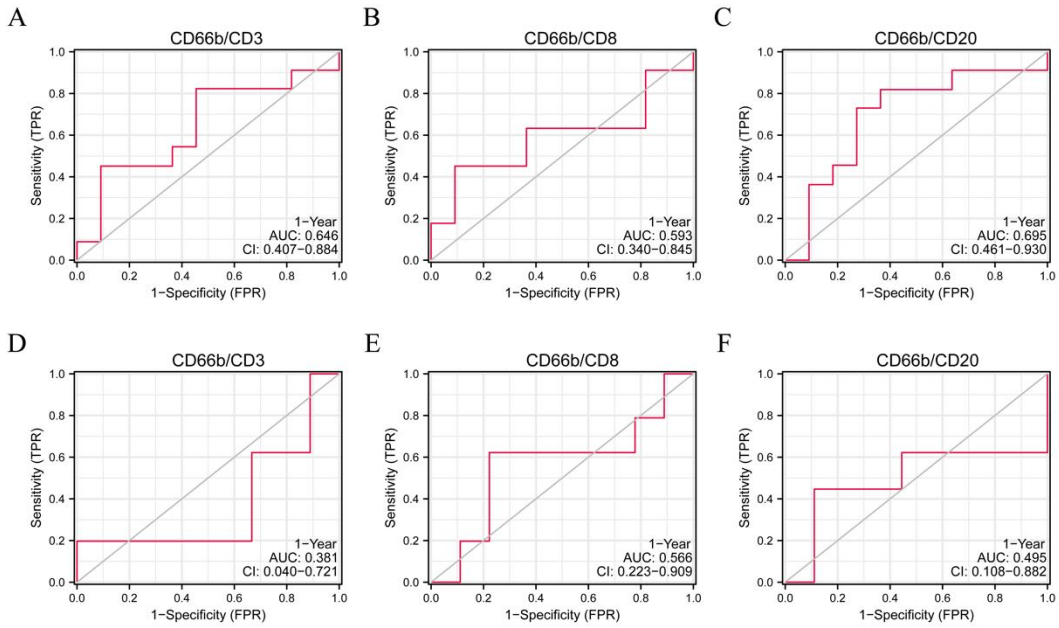

Figure 17. Time-dependent ROC curves of NLR were drawn to predict the OS (A, B, C) and DFS (D, E, F) in pancreatic cancer primary tumors.

3.6.3 Prognostic value of NLR in metastatic tumor of PC on OS and DFS

Neutrophil-to-lymphocyte ratio in PC primary tumors showed no correlation with OS ($CD66b^+/CD3^+$ p=0.852, $CD66b^+/CD8^+$ p=0.638, $CD66b^+/CD20^+$ p=0.595) and DFS ($CD66b^+/CD3^+$ p=0.403, $CD66b^+/CD8^+$ p=0.164, $CD66b^+/CD20^+$ p=0.12) (**Figure 18**).

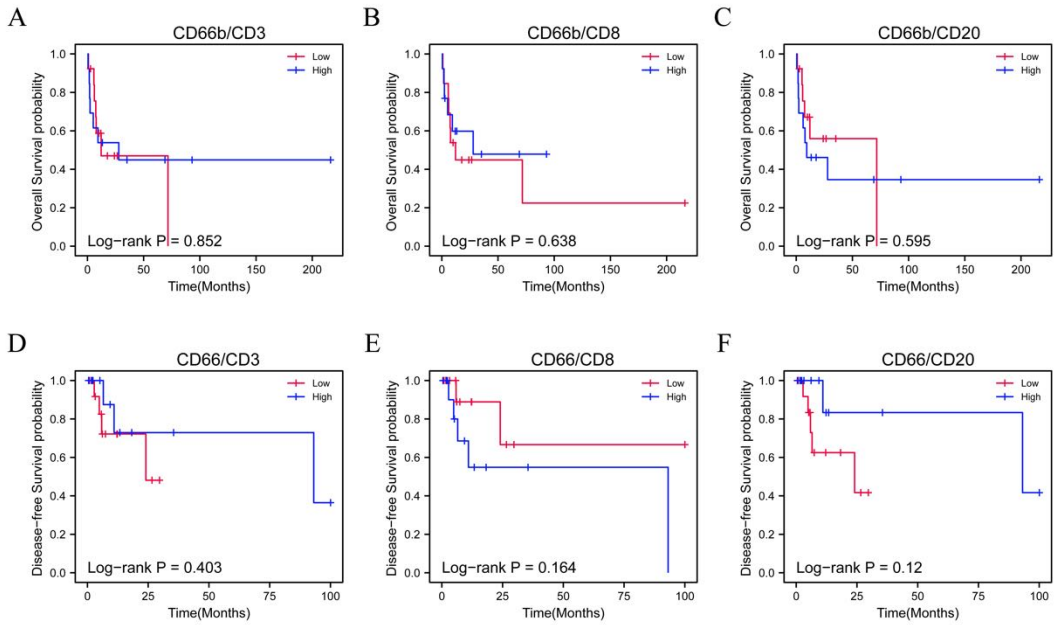

Figure 18. The prognostic value of NLR in PC metastatic tumors on OS (A, B, C) and DFS (D, E, F).

3.6.4 Time-dependent ROC curve of NLR in metastatic tumor of PC on OS (1 year) and DFS (1 year)

None of NLR showed significant ability to predict the OS ($CD66b^+/CD3^+$ AUC=0.556, $CD66b^+/CD8^+$ AUC=0.52, $CD66b^+/CD20^+$ AUC=0.492) and DFS ($CD66b^+/CD3^+$ AUC=0.496, $CD66b^+/CD8^+$ AUC=0.649 $CD66b^+/CD20^+$ AUC=0.389) (**Figure 19**).

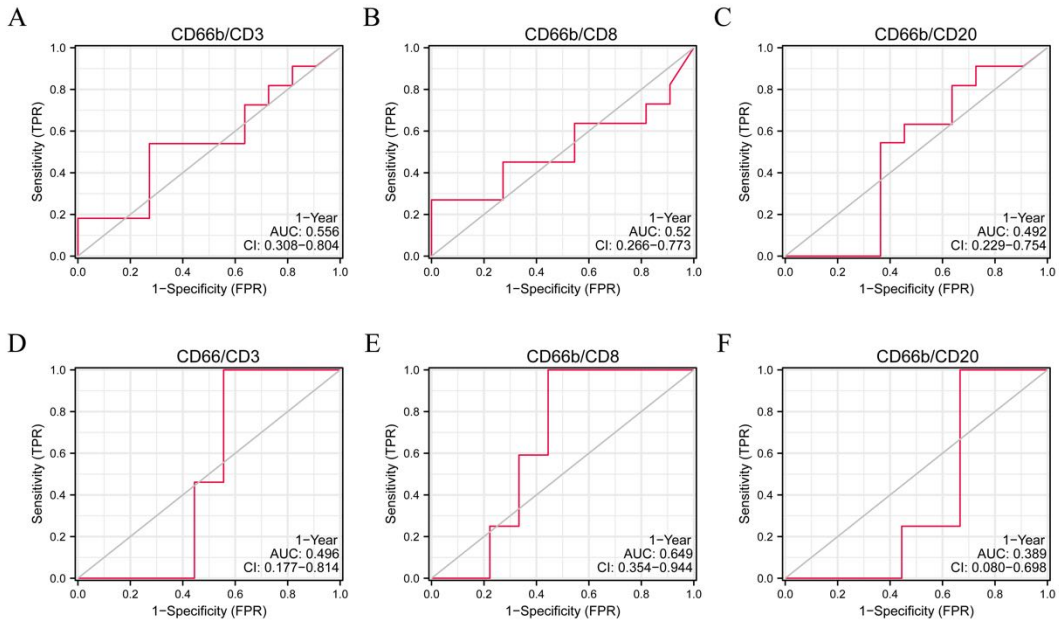

Figure 19. Time-dependent ROC curves of NLR were drawn to predict the OS (A, B, C) and DFS (D, E, F) in PC metastatic tumors.

3.7 Differential analysis of MCMs in tumor cell areas of PC

The density of each molecule was used as a continuous variable for analysis, and no significant difference was discovered between primary and metastasis group (HIF-1α p=0.88, GLUT1 p=0.76, PDHK1 p=0.6), liver and non-liver group (HIF-1α p=0.38, GLUT1 p=0.58, PDHK1 p=0.81), synchronous and metachronous group (HIF-1α p=0.33, GLUT1 p=0.61, PDHK1 p=0.08) (**Figure 20**).

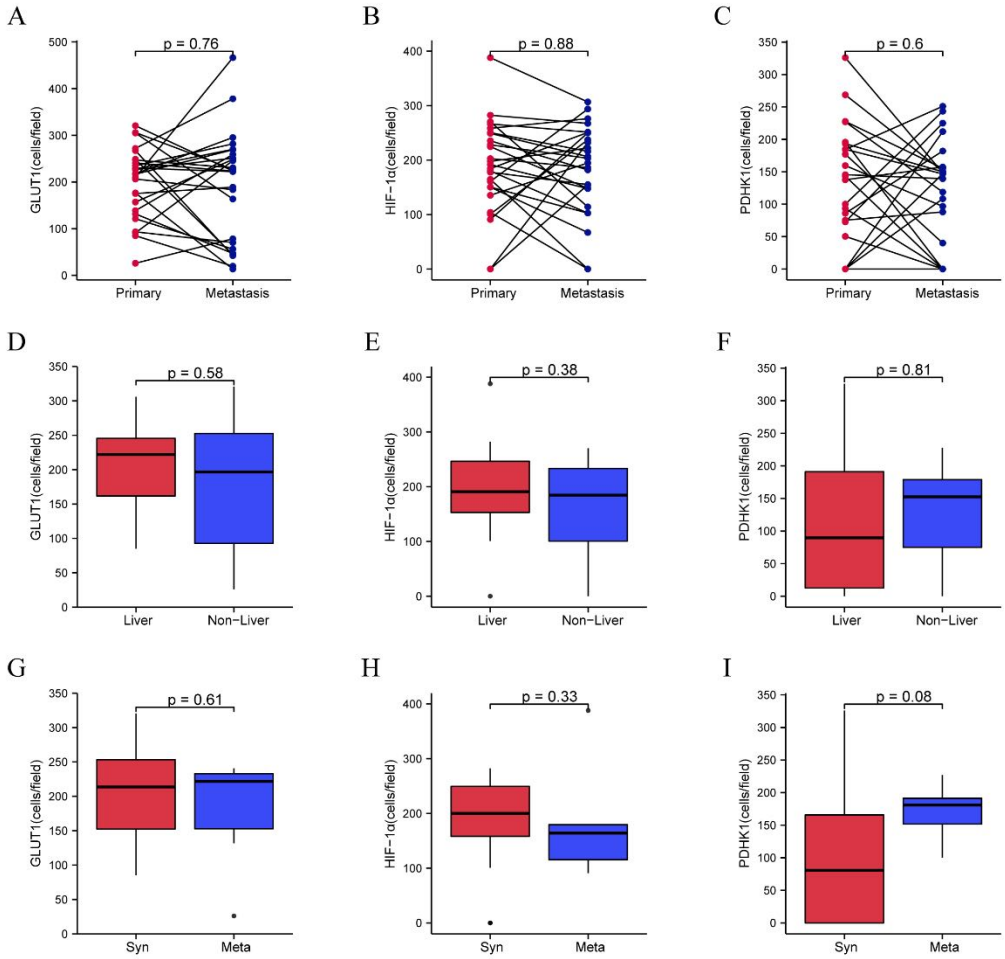

Figure 20. Differential analysis of MCMs in the tumor cell areas of primary and metastatic lesions of PC (A, B, C,), liver and non-liver group (D, E, F), synchronous and metachronous group (G, H, I). **Note:** Syn for synchronous metastasis, Meta for metachronous metastasis.

3.8 Prognostic value of MCMs in tumor cell areas of PC on patient's survival

3.8.1 Prognostic value of MCMs in tumor cell area of PC primary tumors on OS and DFS

There was no statistical significance for each metabolic molecule and their combinations in tumor cell area of PC primary tumor on OS (HIF-1α p=0.189, GLUT1 p=0.794, PDHK1 p=0.209, HIF-1α+GLUT1 p=0.674, GLUT1+PDHK1

p=0.594, HIF-1α+PDHK1 p=0.937, GLUT1+HIF-1α+PDHK1 p=0.545), and DFS (HIF-1α p=0.218, GLUT1 p=0.768, PDHK1 p=0.39, HIF-1α+GLUT1 p=0.617, GLUT1+PDHK1 p=0.415, HIF-1α+PDHK1 p=0.688, GLUT1+ HIF-1α+PDHK1 p=0.192) (**Figure 21**).

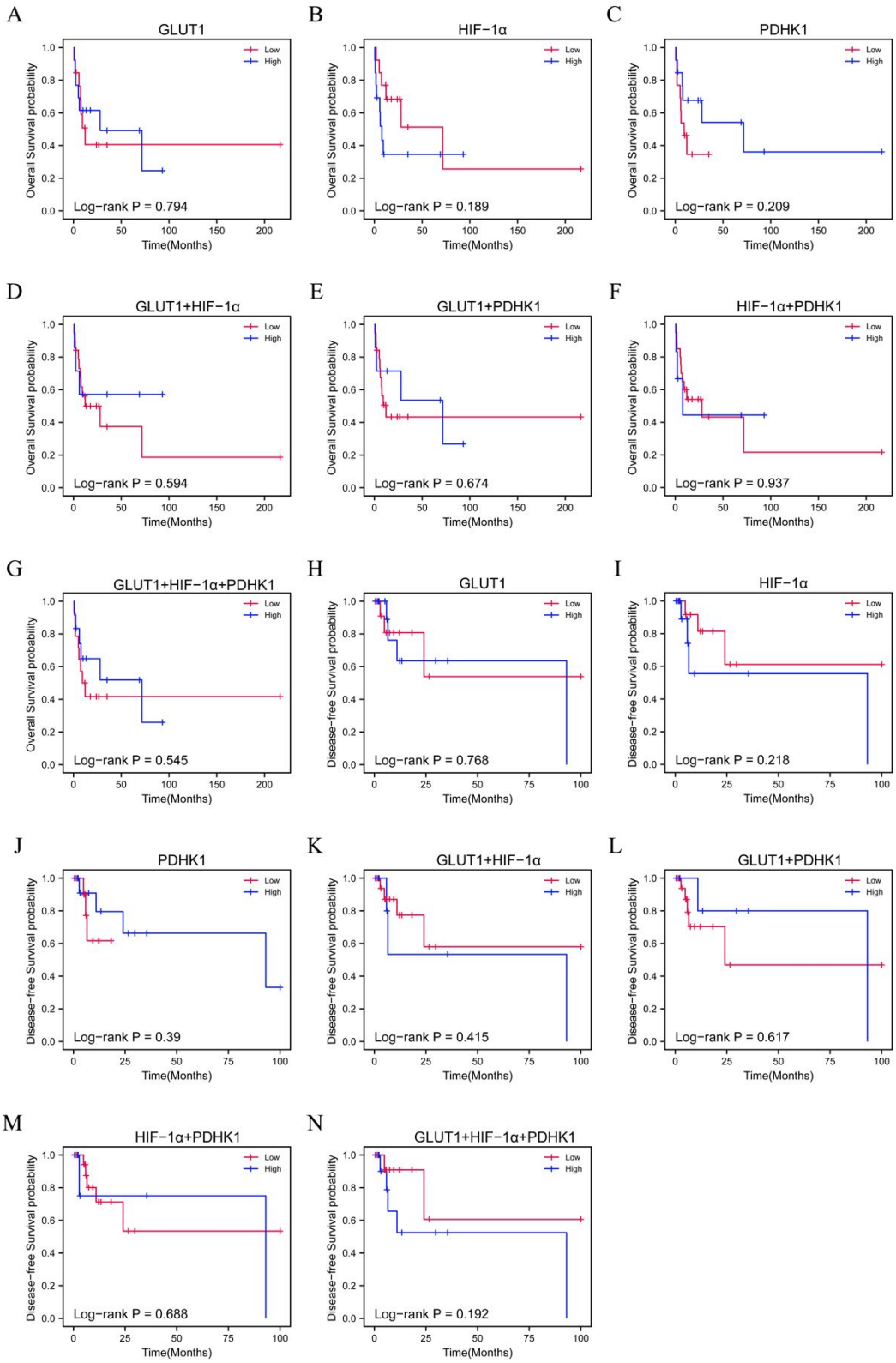

Figure 21. The prognostic value of MCMs in the tumor cell areas of PC primary tumors on OS (A, B, C, D, E, F, G) and DFS (H, I, J, K, L, M, N).

3.8.2 Time-dependent ROC curve of MCMs in tumor cell area of PC primary tumors on OS (1 year) and DFS (1 year)

None of the metabolic molecules in tumor cell area of PC primary tumors showed significant ability to predict the OS (GLUT1 AUC=0.453, HIF-1α AUC=0.707, PDHK1 AUC=0.317) and DFS (GLUT1 AUC=0.68, HIF-1α AUC=0.586, PDHK1 AUC=0.386) (**Figure 22**).

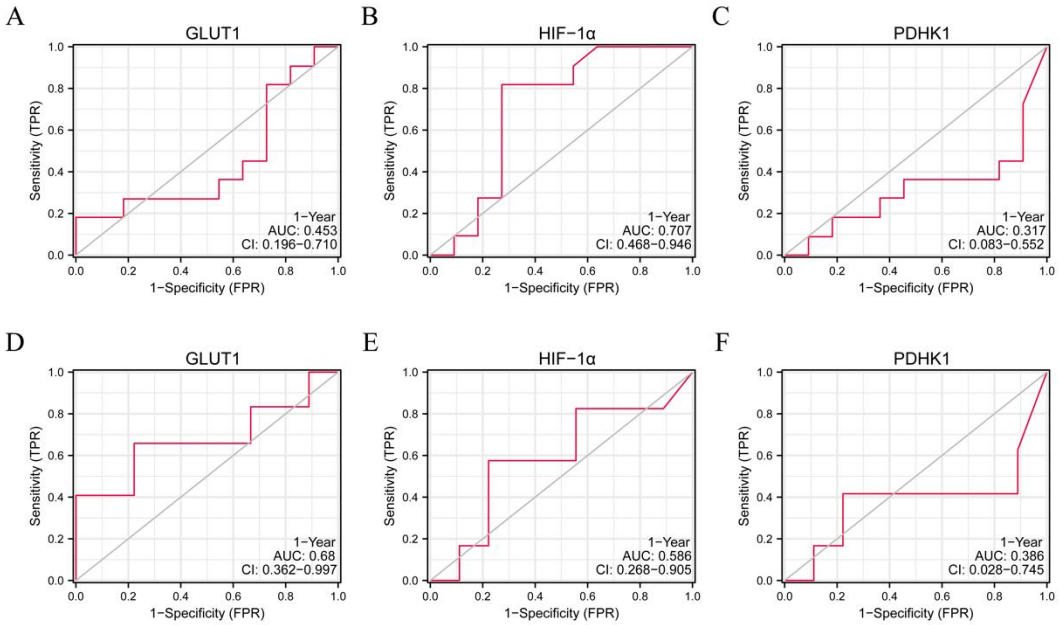

Figure 22. Time-dependent ROC curves were drawn to predict the OS (A, B, C) and DFS (D, E, F) in the tumor cell areas of PC primary tumors.

3.8.3 Prognostic value of MCMs in tumor cell area of metastatic tumor of PC on OS and DFS

There was no statistical significance for each metabolic molecule and their combinations in the tumor cell areas of PC metastatic tumor on OS (HIF-1α p=0.139, GLUT1 p=0.721, PDHK1 p=0.697, HIF-1α+GLUT1 p=0.066, GLUT1+PDHK1 p=0.424, HIF-1α+PDHK1 p=0.555, GLUT1+HIF-1α+PDHK1 p=0.783), and DFS (HIF-1α p=0.922, GLUT1 p=0.571, PDHK1 p=0.806, HIF-1α+GLUT1 p=0.699, GLUT1+PDHK1 p=0.735, HIF-1α+PDHK1 p=0.523, GLUT1+HIF-1α+PDHK1 p=0.605) (**Figure 23**).

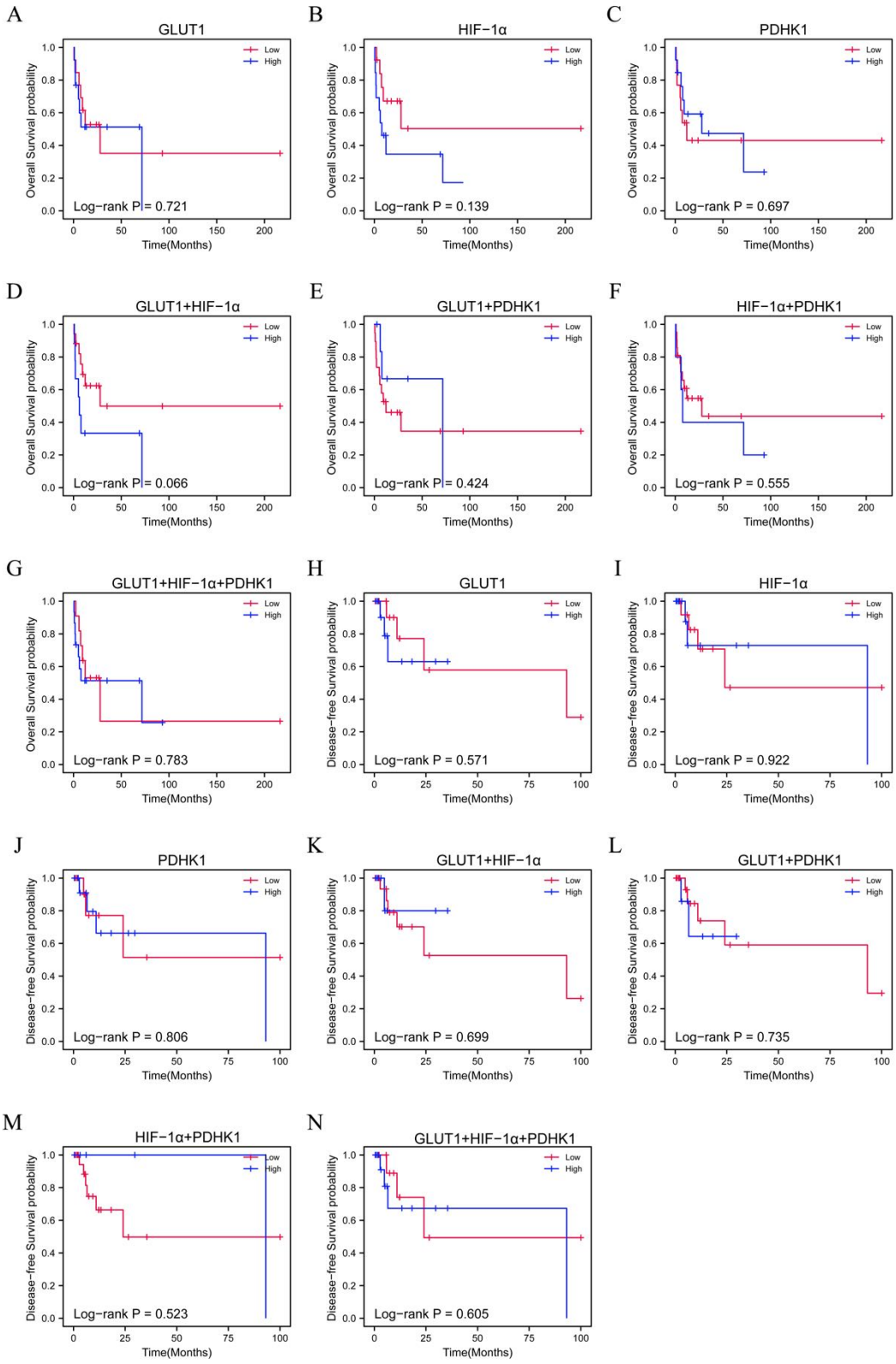

Figure 23. The prognostic value of MCMs in the tumor cell areas of PC metastatic tumors on OS (A, B, C, D, E, F, G) and DFS (H, I, J, K, L, M, N).

3.8.4 Time-dependent ROC curve of MCMs in tumor cell areas of metastatic tumor of PC on OS (1 year) and DFS (1 year)

None of the metabolic molecules in the tumor cell areas of PC metastatic tumors showed significant ability to predict the OS (HIF-1α AUC=0.672, GLUT1 AUC=0.469, PDHK1 AUC=0.471), and DFS (HIF-1α AUC=0.477, GLUT1 AUC=0.666, PDHK1 AUC=0.553) (**Figure 24**).

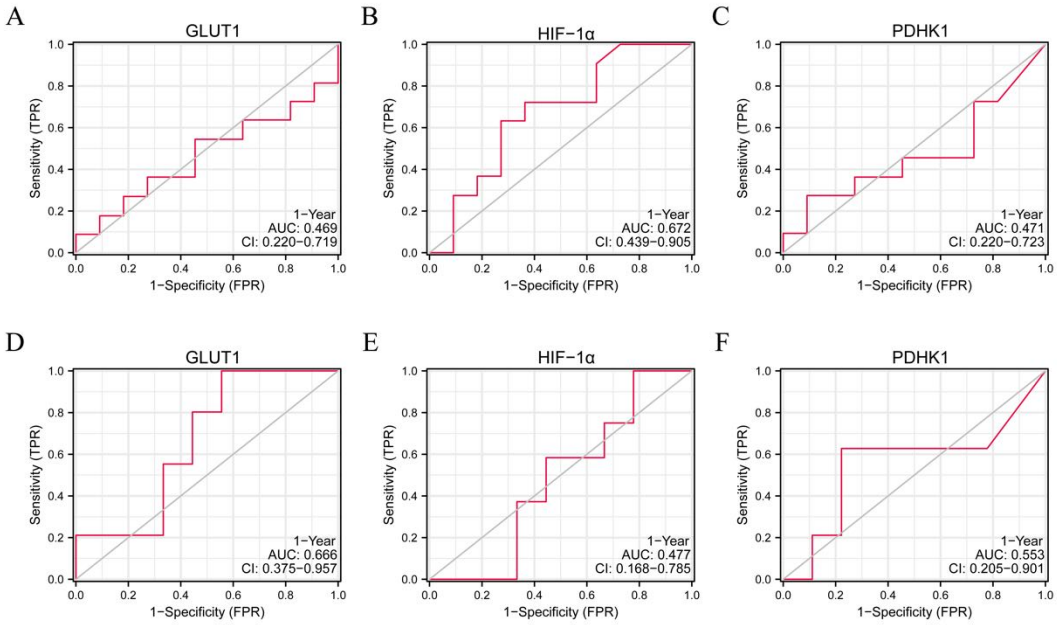

Figure 24. Time-dependent ROC curves were drawn to predict the OS (A, B, C) and DFS (D, E, F) in the tumor cell areas of PC metastatic tumors.

3.9 Differential analysis of MCMs in tumor stromal areas of PC

The density of each molecule was used as a continuous variable for analysis, and no significant was discovered among primary and metastasis group (HIF-1α p=0.72, GLUT1 p=0.44, PDHK1 p=0.46), liver and non-liver group (HIF-1α p=0.24, GLUT1 p=0.34, PDHK1 p=0.46), synchronous and metachronous group (HIF-1α p=0.46, GLUT1 p=0.11, PDHK1 p=0.17) (**Figure 25**).

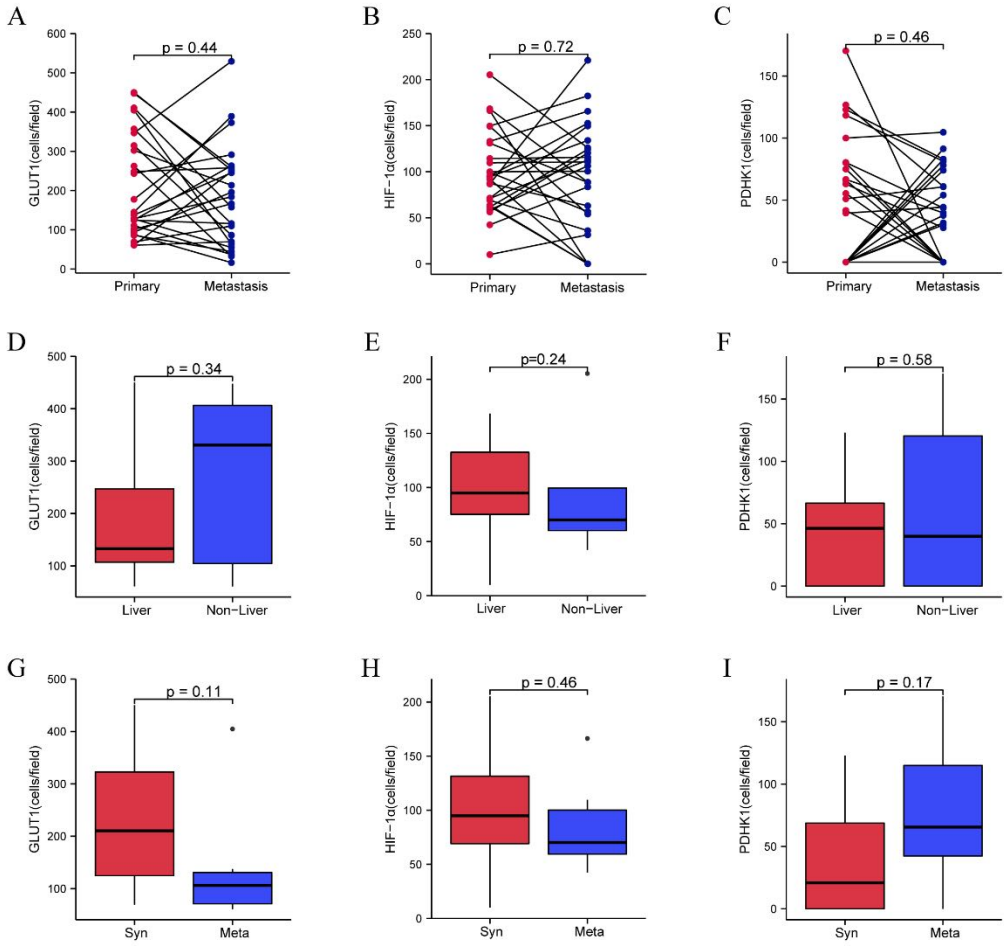

Figure 25. Differential analysis of MCMs in the tumor stromal areas of tumors in primary and metastatic lesions of PC (A, B, C), in the liver and non-liver group (D, E, F), and the synchronous and metachronous group (G, H, I).
Note: Syn for synchronous metastasis, Meta for metachronous metastasis.

3.10 Prognostic value of MCMs in tumor stromal areas of PC on patient's survival

3.10.1 Prognostic value of MCMs in tumor stromal area of PC primary tumors on OS and DFS

I found low-density of GLUT1 (p=0.009) was associated with improved OS in tumor stromal area of PC primary tumor; however, the combination of molecules didn't correlate with OS (GLUT1+HIF-1α p=0.111, HIF-1α+PDHK1

p=0.445, GLUT1+PDHK1 p=0.098, GLUT1+HIF-1α+PDHK1 p=0.274). Moreover, there was no statistical significance in each metabolic molecule and their combinations in tumor stromal area of PC primary tumor on DFS (GLUT1 p=0.085, HIF-1α p=0.148, PDHK1 p=0.069, GLUT1+HIF-1α p=0.981, HIF-1α+PDHK1 p=0.205, GLUT1+PDHK1 p=0.311, GLUT1+HIF-1α+PDHK1 p=0.502) (**Figure 26**).

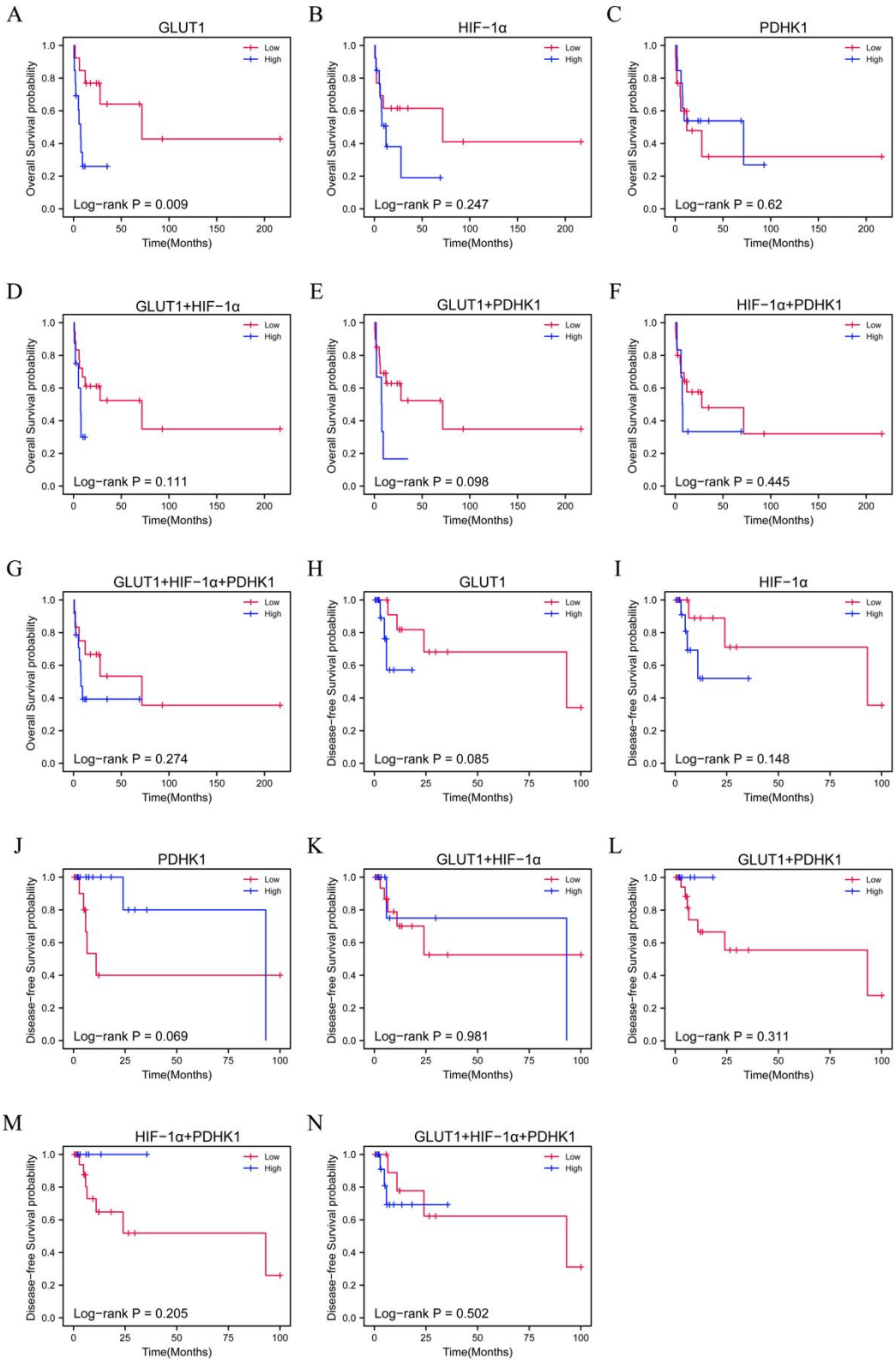

Figure 26. The prognostic value of MCMs in the tumor stromal areas of PC primary tumors on OS (A, B, C, D, E, F, G) and DFS (H, I, J, K, L, M, N).

3.10.2 Time-dependent ROC curve of MCMs in tumor stromal area of PC primary tumors on OS (1 year) and DFS (1 year)

GLUT1 (AUC=0.823) in tumor stromal area of PC primary tumor showed significant ability to predict the OS, while HIF-1α (AUC=0.613) and PDHK1 (AUC=0.377) did not. Furthermore, GLUT1 (AUC=0.813) and HIF-1α (AUC=0.854) in the tumor stromal areas of PC primary tumors showed significant ability to predict the DFS, while PDHK1 (AUC=0.139) did not. (**Figure 27**).

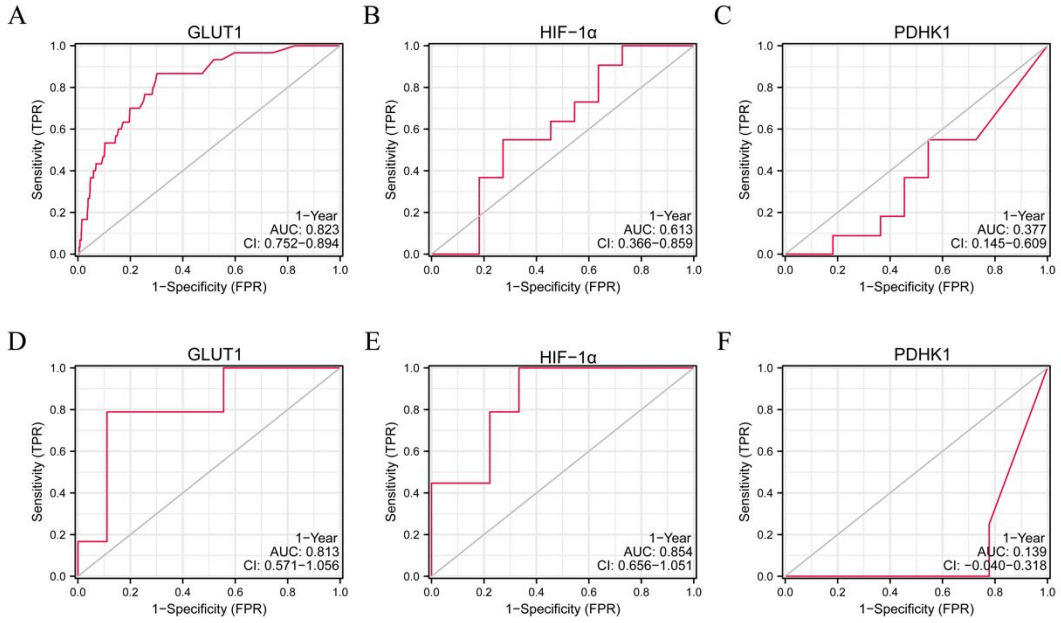

Figure 27. Time-dependent ROC curves were drawn to predict the OS (A, B, C) and DFS (D, E, F) in the tumor stromal areas of PC primary tumors.

3.10.3 Prognostic value of MCMs in tumor stromal area of metastatic tumor of PC on OS and DFS

I found low-density of GLUT1 (p=0.01) and GLUT1+PDHK1 (p=0.034) in tumor stromal area of PC metastatic tumors correlated with improved OS, however, the rest of molecules didn't correlate with OS (HIF-1α p=0.529, PDHK1 p=0.804,

GLUT1+HIF-1α p=0.466, HIF-1α+PDHK1 p=0.438, GLUT1+PDHK1 p=0.098, GLUT1+ HIF-1α+PDHK1 p=0.932). Moreover, there was no statistical significance for each metabolic molecule and their combinations in tumor stromal area of PC primary tumor on DFS (GLUT1 p=0.537, HIF-1α p=0.244, PDHK1 p=0.788, GLUT1+HIF-1α p=0.648, HIF-1α+PDHK1 p=0.436, GLUT1+PDHK1 p=0.163, GLUT1+HIF-1α+PDHK1 p=0.943) (**Figure 28**).

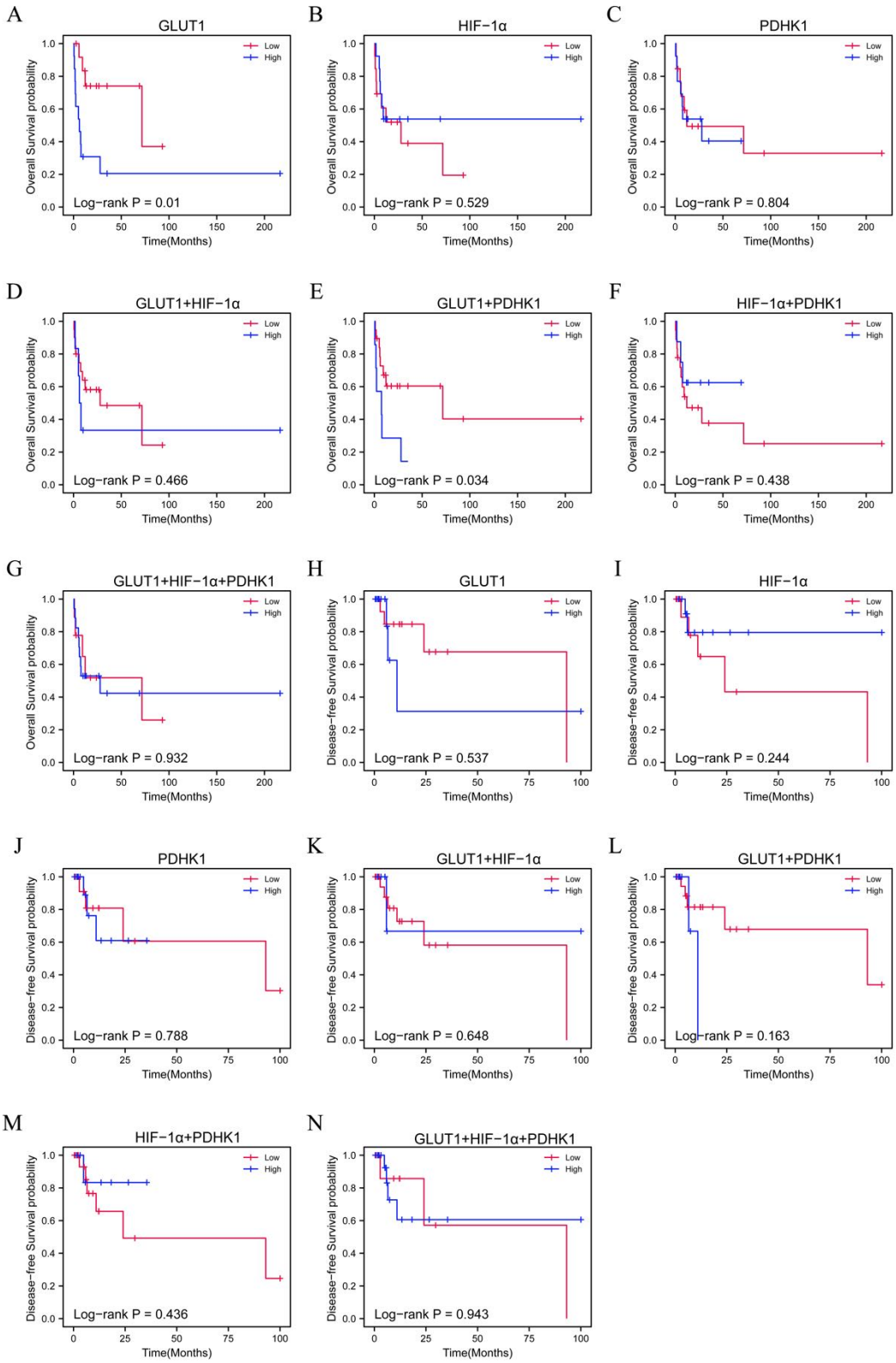

Figure 28. The prognostic value of MCMs in the tumor stromal areas of PC metastatic tumors on OS (A, B, C, D, E, F, G) and DFS (H, I, J, K, L, M, N).

3.10.4 Time-dependent ROC curve of MCMs in tumor stromal area of metastatic tumor of PC on OS (1 year) and DFS (1 year)

GLUT1 (AUC=0.865) in tumor stromal area of PC metastatic tumors showed significant ability to predict the OS, while PDHK1 (AUC=0.479) and HIF-1α (AUC=0.558) did not. Furthermore, GLUT1 (AUC=0.736), HIF-1α (AUC=0.448), and PDHK1 (AUC=0.588) in tumor stromal area of PC metastatic tumor showed no significant ability to predict the DFS (**Figure 29**).

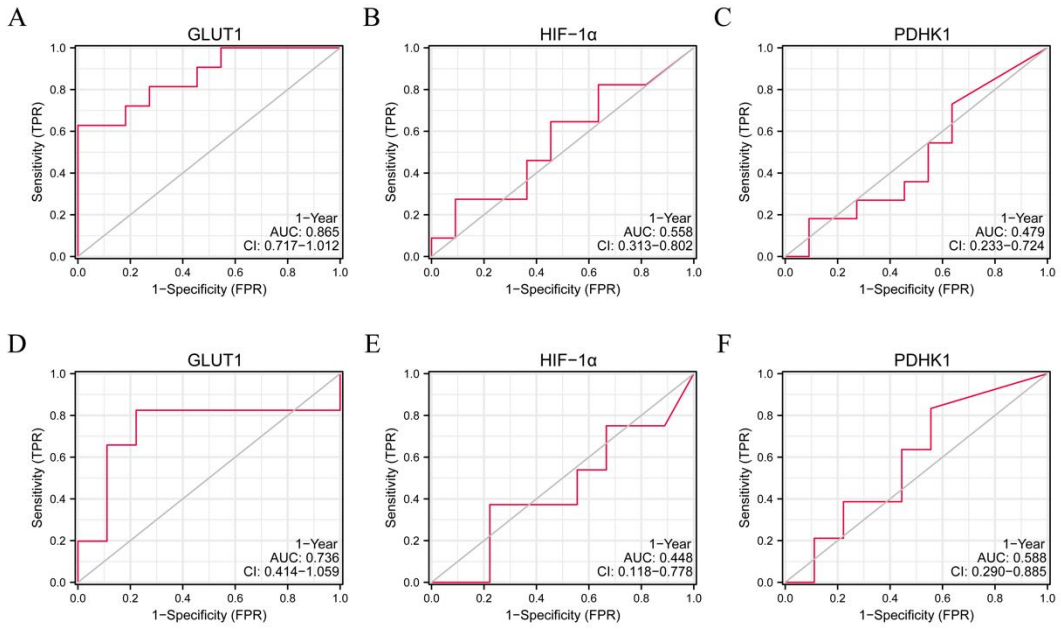

Figure 29. Time-dependent ROC curves were drawn to predict the OS (A, B, C) and DFS (D, E, F) in the tumor stromal areas of PC metastatic tumors.

3.11 Differences in density of MCMs between tumor cell areas and tumor stromal areas

A comparison on metabolic molecules between tumor cell area and tumor stromal area was made and the result showed that the density of HIF-1α ($p<0.001$) and PDHK1 ($p<0.001$) in tumor cell area were higher than in the

tumor stroma area in both PC primary and metastatic tumors, while GLUT1 did not (**Figure 30**).

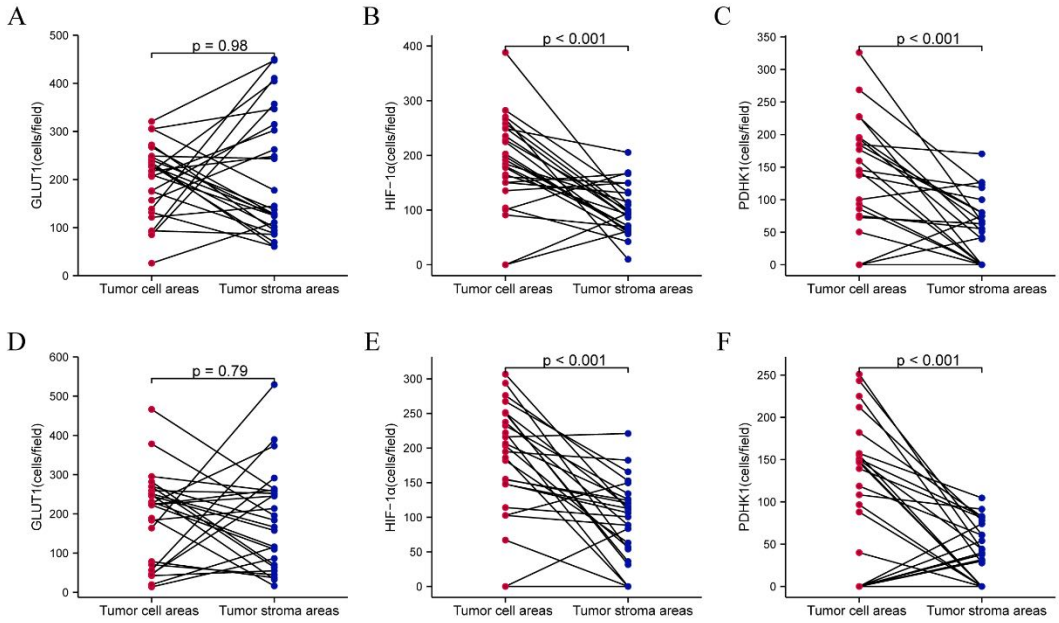

Figure 30. Differential analysis of MCMs between the tumor cell areas and the tumor stromal areas in primary (A, B, C,) and metastasis group (D, E, F).

3.12 Prognostic value of preoperational laboratory values on patient's survival

3.12.1 Prognostic value of preoperational laboratory values on OS and DFS

Low level of platelets (p=0.014) showed significant ability to predict the OS. However, the rest of the laboratory values did not correlate with OS (CEA p=0.74, CA 19-9 p=0.944, Leukocytes p=0.391, INR p=0.903, Bilirubin p=0.999). Moreover, there was no prognostic value of preoperational laboratory values on DFS (CEA p=0.157, CA 19-9 p=0.605, Leukocytes p=0.35, platelets p=0.853, INR p=0.147, Bilirubin p=0.92) (**Figure 31**).

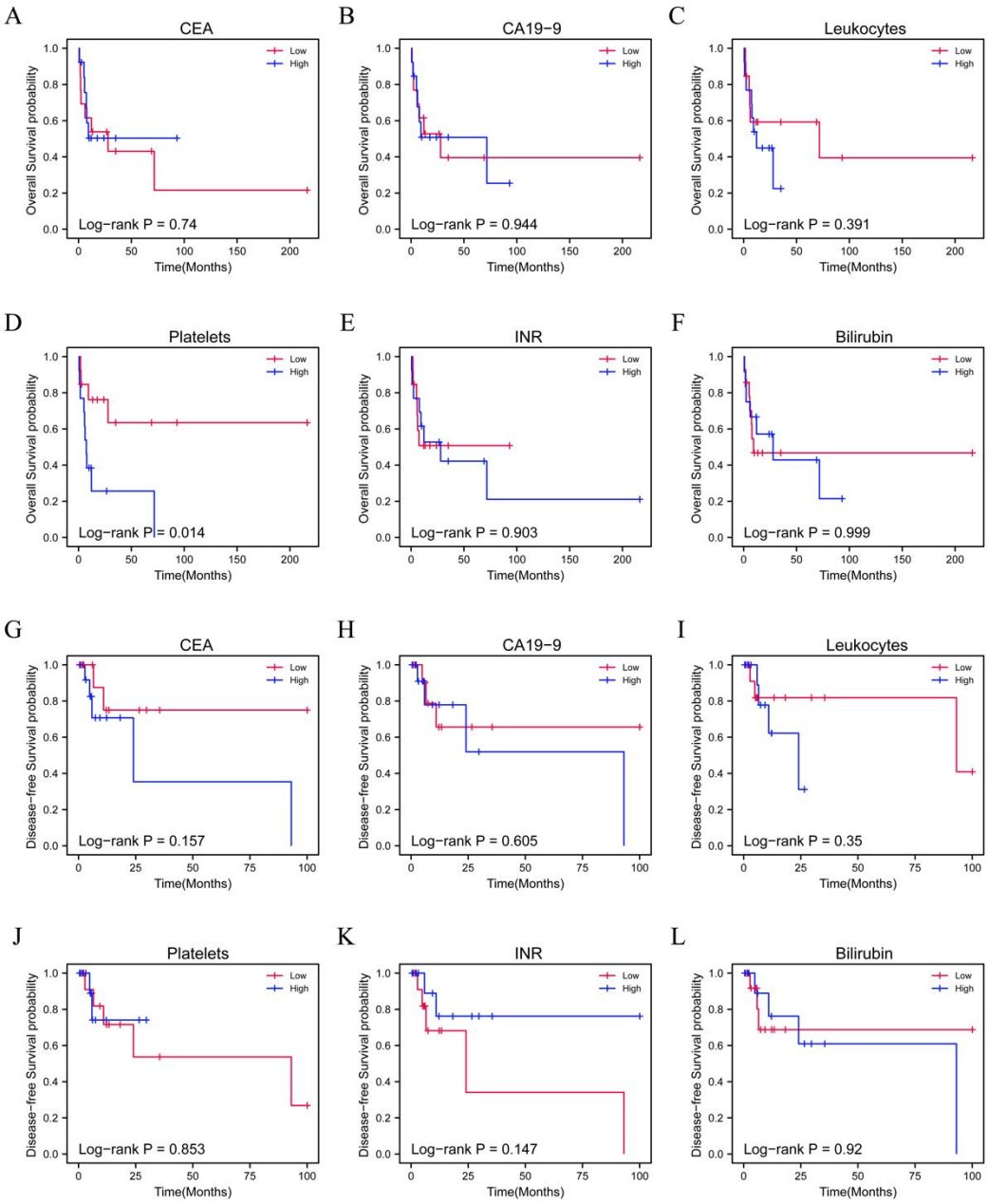

Figure 31. The prognostic value of preoperational laboratory values on OS (A, B, C, D, E, F) and DFS (G, H, I, J, K, L).

3.12.2 Time-dependent ROC curve of preoperational laboratory values on OS (1 year) and DFS (1 year)

The Time-dependent ROC curves for preoperational laboratory values on survival prognosis were analyzed and platelets (AUC=0.836) were found to

show significant ability to predict OS, while the rest of laboratory values did not (CEA AUC=0.57, CA 19-9 AUC=0.596, Leukocytes AUC=0.703, INR AUC=0.535, Bilirubin AUC=0.408). Furthermore, Leukocytes (AUC=0.782) showed significant ability to predict DFS, while the rest of the laboratory values did not (CEA AUC=0.427, CA 19-9 AUC=0.516, platelets AUC=0.714, INR AUC=0.604, Bilirubin AUC=0.528) (**Figure 32**).

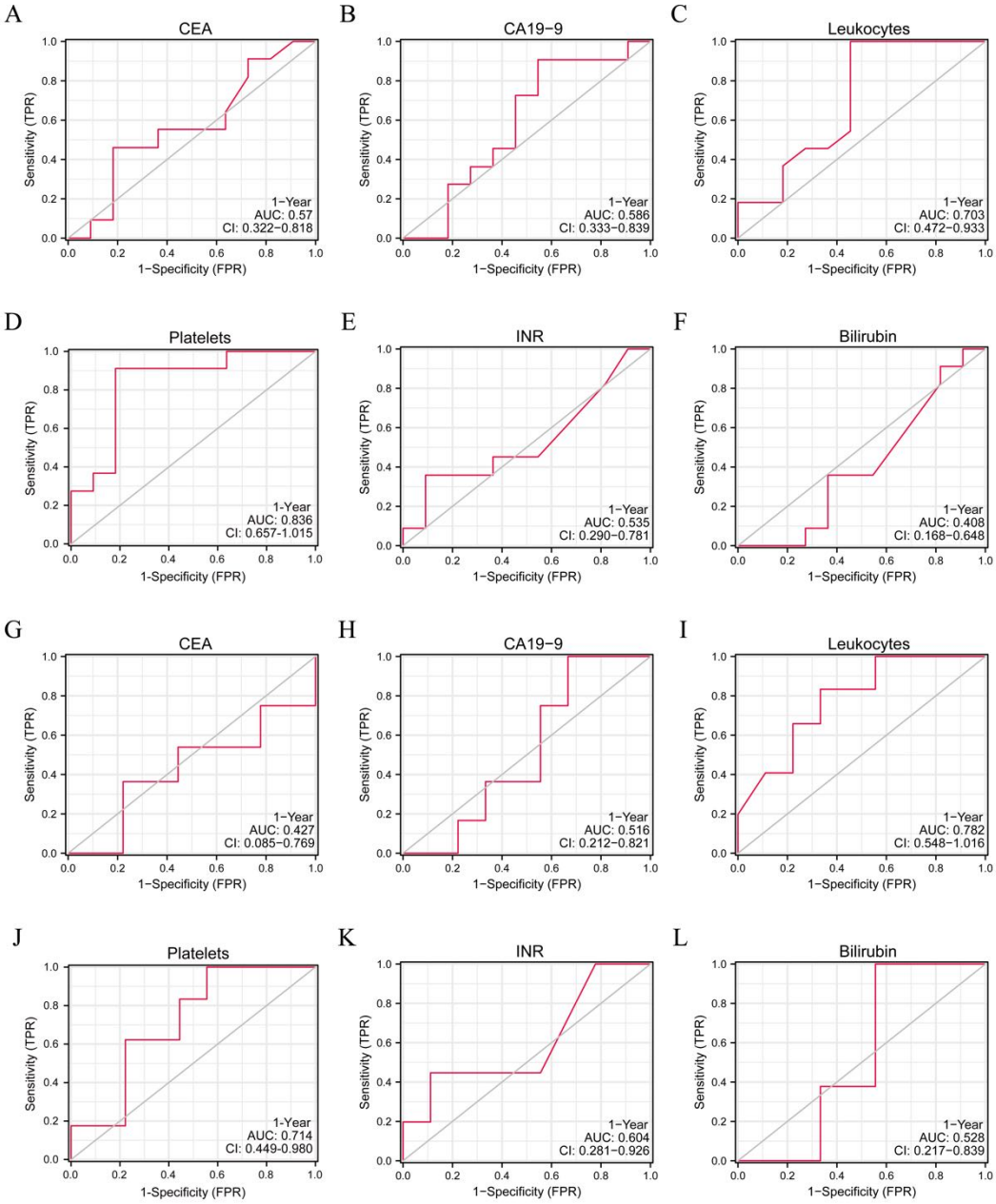

Figure 32. The predictive values of Time-dependent ROC curves for preoperational laboratory values on OS (A, B, C, D, E, F) and DFS (G, H, I, J, K, L).

3.13 Correlation between IHC staining markers and laboratory values

All IHC staining markers and laboratory values were examined as a continuous variable by Spearman correlation. The correlation coefficients ranged from -1 to 1, as shown in **Figure 27**, with Positive relationships in red, whereas negative correlations are presented in blue. For example, positive correlation between $CD3^+$ P and $CD20P^+$, and T GLUT1 M, and Amylase, were positively correlated, while $CD3^+$ P and S PDHK1 M were negatively correlated (**Figure 33**).

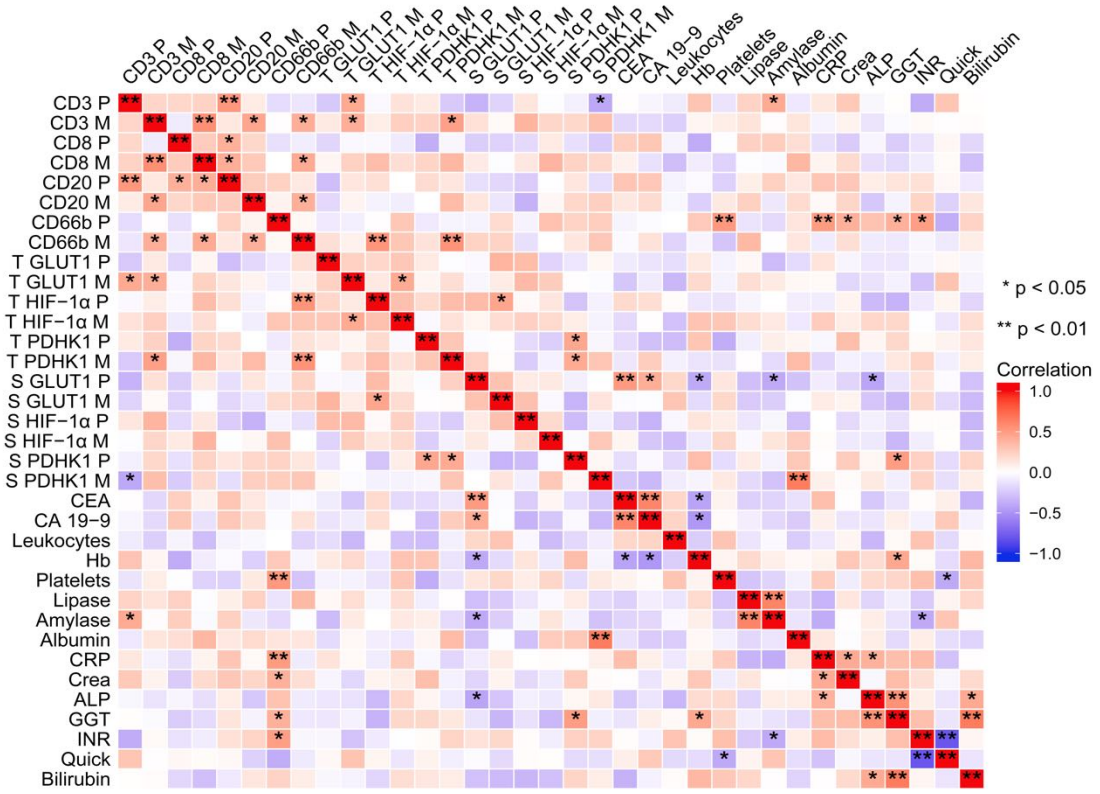

Figure 33. Correlation between IHC staining markers and laboratory values. (Abbreviations: CEA: Carcinoma Embryonic Antigen; CA19-9: Carbohydrate antigen 19-9; Hb: Hemoglobin; CRP: C-reactive protein; Crea: Creatinine; ALP: alkaline phosphatase; GGT: Gamma-glutamyl transpeptidase; INR: international normalized ratio. **T** stands for Tumor cell areas, **S** stands for Tumor stromal areas; **P** stands for Primary tumor, **M** stands for metastasis tumor)

3.14 Cox regression for IHC staining markers and clinical parameters

Cox regression was performed for IHC staining markers and clinical Parameters. Univariate cox regression analysis was performed on seven staining markers and clinical parameters with OS and DFS as dependent variables (Due to the potential statistical consequences of double-use, combination groups of different immune cell types and metabolic checkpoint molecules was excluded). As shown in **Table 6**, in the case of univariate cox regression analysis, high infiltration of $CD20^+$ (p=0.021) in PC primary tumors and high infiltration of $CD8^+$ (P=0.033) in metastatic tumors correlated with improved OS; low density of GLUT1 (P=0.015, P=0.018) in tumor stromal areas of PC correlated with improved OS; low level of platelets (P=0.022) correlated with improved OS in PC. However, no variables were associated with DFS. P-values <0.050 in univariate analysis were included in multivariate for analysis, and statistical significance was considered as a P-value of less than 0.050. In the case of multivariate cox regression analysis (**table 7**), CD8+ was found in metastatic tumors, and GLUT1 in tumor stromal areas of primary and metastatic tumors was independent variables to predict survival prognosis.

Table 6. Univariate Cox regression analysis of all independent variables with OS and DFS as dependent variables.

Variables	Overall survival				Disease-free Survival			
	HR	95% CI		P-value	HR	95% CI		P-value
Gender: Male vs. Female	0.490	0.160	1.470	0.201	0.900	0.190	4.200	0.894
Age: >65 vs <=65 years	0.870	0.300	2.520	0.795	0.830	0.180	3.780	0.805
T3+T4 vs T2	0.373	0.081	1.720	0.206	0.436	0.049	3.884	0.457
N+(N1+N2) vs N0	1.260	0.430	3.710	0.669	2.350	0.450	12.170	0.308
R0 vs R+(R1+R2)	0.850	0.290	2.480	0.764	1.300	0.290	5.810	0.733
Chemotherapy: No vs Yes	2.070	0.680	6.290	0.201	3.020	0.630	14.500	0.167
Metastasis sites: liver vs non-liver	0.610	0.170	2.180	0.447	1.870	0.370	9.420	0.449
Synchronous vs Metachronous	4.020	0.850	19.040	0.079	2.100	0.390	11.360	0.389
CD3 **P**	0.420	0.140	1.270	0.126	0.930	0.200	4.330	0.931
CD8 **P**	0.880	0.310	2.520	0.809	0.620	0.140	2.780	0.532
CD20 **P**	0.250	0.080	0.810	**0.021**	1.850	0.360	9.610	0.464
CD66b **P**	1.320	0.450	3.830	0.610	0.440	0.090	2.270	0.326
CD3 **M**	0.750	0.250	2.250	0.611	2.200	0.390	12.230	0.369
CD8 **M**	0.270	0.080	0.900	**0.033**	0.600	0.120	3.000	0.535

CD20 **M**	0.810	0.280	2.360	0.706	5.680	0.660	49.090	0.115
CD66b **M**	1.100	0.380	3.170	0.863	1.560	0.350	7.030	0.564
S GLUT1 **P**	4.687	1.347	16.306	**0.015**	4.684	0.704	31.151	0.110
S HIF-1α **P**	1.927	0.623	5.967	0.255	3.453	0.591	19.986	0.170
S PDHK1 **P**	0.767	0.268	2.194	0.621	0.233	0.043	1.263	0.091
S GLUT1 **M**	4.137	1.281	13.357	**0.018**	1.621	0.345	7.619	0.541
S HIF-1α M	0.710	0.244	2.067	0.530	0.389	0.075	2.018	0.261
S PDHK1 **M**	1.149	0.385	3.422	0.804	1.246	0.249	6.235	0.789
T GLUT1 **P**	0.870	0.300	2.500	0.794	1.250	0.280	5.610	0.768
T HIF-1α **P**	2.020	0.690	5.880	0.197	2.540	0.550	11.770	0.233
T PDHK1 **P**	0.490	0.160	1.520	0.218	0.460	0.070	2.830	0.401
T GLUT1 **M**	1.210	0.420	3.480	0.721	1.590	0.320	7.920	0.574
T HIF-1α **M**	2.250	0.750	6.770	0.149	1.080	0.240	4.900	0.922
T PDHK1 **M**	0.810	0.280	2.330	0.698	1.210	0.270	5.410	0.807
CEA	0.834	0.285	2.438	0.74	3.124	0.595	16.391	0.178
CA 19-9	1.039	0.362	2.981	0.944	1.482	0.331	6.643	0.607
Leukocytes	1.632	0.528	5.052	0.395	2.223	0.399	12.391	0.362
Hb	1.574	0.525	4.717	0.418	0.313	0.060	1.637	0.169
Platelets	4.038	1.225	13.313	**0.022**	0.850	0.152	4.749	0.853
Lipase	0.917	0.32	2.628	0.872	1.029	0.207	5.107	0.972
Amylase	0.647	0.233	1.873	0.422	0.725	0.138	3.807	0.704
Albumin	0.817	0.284	2.353	0.708	0.130	0.016	1.089	0.060
CRP	0.901	0.311	2.609	0.848	0.582	0.106	3.184	0.533
Creatinine	0.579	0.192	1.741	0.33	0.365	0.061	2.171	0.268
ALP	0.422	0.135	1.316	0.137	0.236	0.040	1.397	0.111
GGT	0.707	0.243	2.02	0.51	0.820	0.175	3.841	0.801
INR	1.069	0.366	3.117	0,903	0.313	0.060	1.637	0.169
Quick	0.574	0.191	1.721	0.322	2.976	0.571	15.507	0.195
Bilirubin	1.001	0.348	2.878	0.999	1.083	0.230	5.090	0.920

p-values under 0.050 appear in bold (n = 26). Median values described Tumor-infiltrating leukocytes and metabolic checkpoint molecules for the high infiltration group (high-density group) or low infiltration group (low-density group). **P** stands for Primary lesion of PC, **M** stands for metastatic tumors of PC, **S** stands for tumor stroma areas, **T** stands for tumor cell areas. Significant p-values were bolded.

Table 7. P-values <0.050 in univariate analysis were included in multivariate analysis. Significant p-value was bolded (n = 26).

Variables	Overall survival			
	HR	95% CI		P-value
CD20 **P**	0.272	0.066	1.124	0.072
CD8 **M**	0.196	0.044	0.872	**0.032**
S GLUT1 **P**	5.816	1.006	33.624	**0.049**
S GLUT1 **M**	5.056	1.258	20.324	**0.022**
Platelets	3.706	0.769	17.851	0.102

P stands for Primary lesion of PC, **M** stands for metastatic tumors of PC, **S** stands for tumor stroma areas, **T** stands for tumor cell areas. Significant *p*-values were bolded.

3.15 Binary logistic regression for IHC staining markers and clinical Parameters

Regarding the relationship between IHC staining markers and clinical parameters with metastatic patterns (synchronous vs. metachronous metastasis), and metastasis sites (liver vs. non-liver metastasis), Binary logistic regression was conducted with metastatic patterns and metastasis sites as dependent variables. P-values <0.050 in univariate analysis were included in multivariate analysis. It was found that males are more likely to develop synchronous metastasis than females, and N+(N1+N2) is more likely to develop metachronous metastasis than N0 in univariate and multivariable logistic regression. However, there is no connection between HC staining markers, clinical parameters, and metastasis sites (liver vs. non-liver metastasis) **(table 8 and 9**)

Table 8. Binary logistic regression analysis was conducted with synchronous vs. metachronous metastasis as dependent variables. P-values <0.050 in univariate analysis were included in multivariate analysis.

Variables	Univariate Logistic regression				Multivariate Logistic regression			
	OR	95% CI		P value	OR	95% CI		P value
Gender: Male vs Female	0.086	0.008	0.899	**0.040**	0.042	0.002	0.783	**0.034**
Age: >65 vs <=65years	0.500	0.074	3.378	0.477				
T3+T4 vs T2	0.436	0.049	3.884	0.457				
N+(N1+N2) vs N0	11.667	1.112	122.381	**0.040**	23.793	1.276	443.546	**0.034**
R0 vs R+(R1+R2)	3.000	0.440	20.436	0.262				
CD3 **P**	2.444	0.361	16.547	0.360				
CD8 **P**	0.409	0.060	2.769	0.360				
CD20 **P**	0.133	0.013	1.365	0.090				
CD66b **P**	1.000	0.161	6.200	1.000				
S GLUT1 **P**	1.000	0.161	6.200	1.000				
S HIF-1α **P**	7.500	0.733	76.773	0.090				
S PDHK1 **P**	0.133	0.013	1.365	0.090				
T GLUT1 **P**	7.500	0.733	76.773	0.090				
T HIF-1α **P**	2.444	0.361	16.547	0.360				
T PDHK1 **P**	0.409	0.060	2.769	0.360				
CEA	2.444	0.361	16.547	0.360				
CA 19-9	1.000	0.161	6.200	1.000				
Leukocytes	2.444	0.361	16.547	0.360				
Hb	1.000	0.161	6.200	1.000				
Platelets	7.500	0.733	76.773	0.090				
Lipase	1.000	0.161	6.200	1.000				
Amylase	1.000	0.161	6.200	1.000				
Albumin	0.409	0.060	2.769	0.360				
CRP	0.818	0.132	5.084	0.830				
Creatinine	0.333	0.049	2.271	0.262				
ALP	0.409	0.060	2.769	0.360				
GGT	0.133	0.013	1.365	0.090				
INR	0.133	0.013	1.365	0.090				
Quick	2.444	0.361	16.547	0.360				
Bilirubin	0.333	0.049	2.271	0.262				

P stands for Primary lesion of PC. **S** for tumor stroma areas, **T** for tumor cell areas. Significant *p*-values were bolded.
(Abbreviations: HR: Hazard ratio; CI: confidence interval)

Table 9. Binary logistic regression analysis was conducted with liver vs. non-liver metastasis as dependent variables. Only univariate logistic analyses were conducted due to no variable had a p-value under 0.05.

Variables	Univariate Logistic regression			
	OR	95% CI		P-value
Gender: Male vs Female	3.333	0.588	18.891	0.174
Age: >65 vs <=65years	0.800	0.151	4.245	0.793
Chemotherapy: No vs Yes	1.500	0.230	9.796	0.672
T3+T4 vs T2	0.875	0.068	11.313	0.919
N+(N1+N2) vs N0	1.333	0.242	7.348	0.741
Synchronous vs Metachronous	3.000	0.452	19.928	0.255
R0 vs R+(R1+R2)	3.750	0.589	23.867	0.162
CD3 **P**	1.000	0.189	5.289	1.000
CD8 **P**	2.083	0.378	11.482	0.399
CD20 **P**	2.083	0.378	11.482	0.399
CD66b **P**	1.000	0.189	5.289	1.000
S GLUT1 **P**	0.480	0.087	2.645	0.399
S HIF-1α **P**	1.000	0.189	5.289	1.000
S PDHK1 **P**	2.083	0.378	11.482	0.399
S GLUT1 **P**	2.083	0.378	11.482	0.399
S HIF-1α **P**	0.480	0.087	2.645	0.399
S PDHK1 P	1.000	0.189	5289	1.000
CEA	4.714	0.734	30.278	0.102
CA 19-9	4.714	0.734	30.278	0.102
Leukocytes	1.000	0.189	5.289	1.000
Hb	0.212	0.033	1.362	0.102
Platelets	2.083	0.378	11.482	0.399
Lipase	0.212	0.033	1.362	0.102
Amylase	0.480	0.087	2.645	0.399
Albumin	1.000	0.189	5.289	1.000
CRP	2.619	0.471	14.577	0.272
Creatinine	1.250	0.236	6.633	0.793
ALP	0.212	0.033	1.362	0.102
GGT	1.000	0.189	5.289	1.000
INR	2.083	0.378	11.482	0.399
Quick	1.000	0.189	5.289	1.000
Bilirubin	0.600	0.109	3.296	0.557

P stands for Primary lesion of PC. **S** for tumor stroma areas, **T** for tumor cell areas. Significant *p*-values were bolded.
(Abbreviations: HR: Hazard ratio; CI: confidence interval)

4. Discussion

Up to now, PC remains a fatal disease with a poor prognosis, and the incidence and health burden of PC is increasing every year [5, 145]. Clinically, only about 10% of patients with PC could achieve 5-year survival through curative resection due to advanced-stage disease at the time of diagnosis [16, 17]. However, metastatic PC has a five-year survival rate of approximately 2.9% [18]. The TME of PC contains immune cells, cytokines, stromal fibroblasts, and extracellular matrix (ECM), forming a complex structure involved in pancreatic cancer proliferation, metastasis, and drug resistance [133, 146, 147], which may be responsible for the failure of multiple treatment modalities, including chemotherapy, radiotherapy, and immunotherapy. Therefore, understanding TME, such as TILs and MCMs, may help find an effective therapy for PC [146, 148].

4.1 Tumor-infiltrating leukocytes (TILs and TINs) in PC

Previous studies revealed that high infiltrated $CD3^+$ T lymphocytes or $CD8^+$ T lymphocytes in the TME had been used as a favorable prognostic indicator of PC [3, 77, 143, 149-151]. Compared to other solid tumors, $CD3^+$ or $CD8^+$ cells also have the prognostic value for hepatocellular cancer [142], colorectal cancer [152-154], breast cancer [155-157], and ovarian cancer [158, 159]. As described above, high infiltration of CD3+ T lymphocytes is associated with improved OS in PC. CD8+ cytotoxic T lymphocytes are essential antitumor immune cells that act by secreting perforin and granzyme and expressing Fas ligand [160]. As mentioned previously, many studies have demonstrated the prognostic value of high infiltrating of CD8+ for long-term survival of PC patients. So far as we know, this is the first study to elucidate the function of stromal

tumor-infiltrating leukocytes in metastatic PC. In this study, I found high infiltrated $CD8^+$ T lymphocytes in metastatic lesions of PC correlated with improved overall survival; more importantly, high infiltration of CD8+ cells in metastatic lesions of PC was an independent factor of favorable overall survival. The reason for the above results may be that cytotoxic CD8+ T cells have the function of tumor-killing in the tumor microenvironment, as well as the presence of being immunosuppressed features [161]. Unfortunately, $CD3^+$ T lymphocytes did not affect OS and DFS in metastatic PC, probably due to the individualized differential expression of $CD3^+$ T lymphocytes, which are also a marker of T-regulatory cell (Treg). In addition, the effect of pre-surgical neoadjuvant chemotherapy on the host's immune function, as well as the insufficient number of cases, may also contribute to this outcome.

The B cell is an essential component of humoral immunity, identified as a critical player in the fight against tumors [162]. Tumor infiltrated B lymphocytes may directly kill tumor cells via an antibody-independent approach and promote cell-mediated immunity [163]. On the other hand, regulatory T cells may inhibit B cell activation, proliferation, and antibody production [164]. There were some favorable effects of high infiltration of $CD20^+$ B-lymphocyte on survival in PC [3, 77, 165]. Furthermore, Patients only with highly infiltrated $CD8^+$ T lymphocytes or $CD20^+$ T lymphocytes had lower survival compared to patients with both highly infiltrated $CD8^+$ T lymphocytes and $CD20^+$T lymphocytes in ovarian cancer [166]. This may indicate a collaborative activity between T lymphocytes and B lymphocytes in cancer immunity. The present study showed that high infiltration of $CD20^+$ B cells in primary lesions of metastatic PC in univariate analysis was associated with the improved OS but not with DFS. This is consistent with the finding of our institute finding in Upfront Resection of Pancreatic Cancer [3] and our assumptions in the designing of the project. One

possible reason for this is that CD20+ is also expressed on the regulatory B cell (B reg).

One study suggests that innate immunity may play an important role in the progression of chronic pancreatitis to PC [167]. The $CD66b^+$ neutrophils are considered the body's first line of defense against infection and respond to inflammatory conditions, including cancer [168]. Among all tumor types, tumor-infiltrating neutrophils were significantly correlated with worse outcomes in renal cell carcinoma [169], testicular germ cell tumors [170], cervical cancer [171], and pancreatic cancer [172]. However, it did correlate significantly with better survival in gastric cancer [173]. Two studies of colorectal cancer also showed conflicting prognostic effects reported separately [174, 175]. Our findings revealed no significant prognostic value regarding the infiltration of CD66b+ cells. This could be explained by antibody heterogeneity or by the use of different methods of analysis. In peripheral blood, NLR reflects the link between innate (neutrophils) and adaptive immune responses (lymphocytes) in diseases and various pathological conditions, which are influenced by many factors such as age, medications, and disease state [176]. A low neutrophil-to-lymphocyte ratio (NLR) reflects low-density neutrophils and/or high-density lymphocytes in pathological tissues. Takakura, K. et al. reported NLR ($CD66b^+/CD20^+$) both in peripheral blood and pathological and demonstrated the prognostic value of NLR in PC [90]. I found that lower NLR in the tissue of primary lesions was associated with more favorable outcomes in metastatic PC. This may also explain that the high infiltration of CD20+ B cells in the primary lesion correlates with improved OS.

Our study demonstrated the differential distribution of TILs between PC primary and metastatic tumors, with a higher density of TILs in primary tumors than in

metastatic tumors. This data was consistent with prior research, indicating that immune escape plays a role in tumor progression [177-180].

In the present study, a single infiltrating white leukocyte inside the tumor was observed instead of a hot spot, which may be a result of the immune escape function of pancreatic cancer cells [181, 182]. Therefore, we choose to quantify the infiltrating leukocyte in the stroma.

4.2 Glucose metabolism in PC

Several studies have revealed that the tumor microenvironment (TME) is rich in components that influence tumor progression [146, 183, 184]. Hypoxia is a hallmark of the TME feature in solid tumors due to the imbalance between increased oxygen utilization and inadequate oxygen supply [185-187]. Furthermore, hypoxia is a complex factor in tumor invasion and metastasis in the tumor microenvironment [188, 189]. As described before, hypoxic condition contributes to the expression of HIF and then induces the expression of GLUT1 and increases glucose uptake; HIF can also induce the expression of PDHK1 [125]. Previous studies described the prognostic value of HIF-1α [127, 190-192] and GLUT1[138, 139, 193-195] in patients with PC and PDHK1 in non-small cell lung cancer [196]. This study quantified GLUT1, HIF-1α, and PDHK1 in tumor cell areas by the QTS algorithm and found that those molecules had no prognostic value for metastatic pancreatic cancer. Then I quantified those molecules in tumor stromal areas and found low-density of GLUT1 both in primary and metastatic lesions correlated with improved OS. Notably, GLUT1 in the tumor stroma of primary and metastatic lesions, like CD8 in the metastatic lesion, is an independent factor for metastatic PC. This study has not observed the prognostic significance of HIF-1α and PDHK1, probably because of the heterogeneity of metastatic pancreatic cancer and the small sample size. In actual work, I found the QTS algorithm is suitable for counting GLUT1 in tumor

stromal areas because GLUT1 staining in stromal areas is visually clearer and easier to discriminate than staining on tumor cells.

Glucose can not only provide energy for cell growth, but also more importantly, serve as an essential carbon source for cells to synthesize lipids and non-essential amino acids [197]. In the TME, tumor cells and stromal cells appear to compete for glucose consumption [198]. Cancer cells preferentially undergo glycolysis to accumulate lactate in the TME through the Warburg effect [111, 112]. In this way, high levels of lactate acidify the tumor microenvironment and promote tumor development, drug resistance, metastasis, and, more importantly, immune escape [102, 199]. For instance, lactate promotes the overexpression of IL-23, and the presence of IL-23 promotes the expression of IL17, and matrix metalloproteinase 9 (MMP-9), with the consequence of increased angiogenesis and reduced CD8 penetration in tumors, and promoted immunosuppression and tumor growth [200]. Therefore, an understanding of this will help find potential therapeutic approaches against tumors.

4.3 Preoperative laboratory values for PC

Preoperative laboratory values can help physicians assess the status of PC patients before surgery. CEA and CA19-9 are two tumor markers for pancreatic cancer. A meta-analysis suggested that CEA and CA19-9 may be poor prognostic predictors of PC [201]. However, their prognostic effect was not found in the present study. Lipase and amylase are two enzymes secreted by the pancreas and are associated with pancreatic inflammation. Albumin, bilirubin, INR, GGT, ALP, and Quick were used to assess liver function, which is necessary before surgery. Creatinine is a test to assess kidney function. Typically, leukocytes and CRP are markers of the body's inflammatory status.

Moreover, hemoglobin (Hb) is a marker of anemia and reflects the body's nutritional status. Regarding the blood platelet test, previous studies demonstrated that high platelet counts and decreased mean platelet volume (MPV) predict poor prognosis in patients with pancreatic cancer [202, 203]. MPV value is the total mass of platelets divided by the total number of platelets in the blood sample [204]. The same results were exhibited in colorectal cancer [205], head and neck squamous cell carcinoma [206]. In this study, low-level platelets (cut-off value 240.923/mm^3) correlated with improved OS.

4.4 Correlation between staining markers and laboratory data

Spearman correlation was implied to reveal the correlation between staining markers and laboratory data. Several studies have revealed the positive correlation between $CD20^+$ B lymphocytes and $CD8^+$ T lymphocytes, such as colorectal cancer [207], breast cancer [208], ovarian cancer [209]. The correlation between $CD20^+$ B cells and $CD8^+$ T cells in metastatic PC was also found in this study. In non-small cell lung cancer, the relationship between inflammatory markers CRP and CD66b+ cells (neutrophils) has been demonstrated [210], and the same result was found in this study. As mentioned before, HIF induces the expression of GLUT1. A positive correlation between HIF-1α and GLUT1 was found and confirmed in gastric cancer [211], and renal cell carcinoma [212]. In esophageal squamous carcinoma, the expression of HIF-1α and TILs was positively correlated, but patients with high expression of them had a terrible prognosis [213]. The present study did not find a positive correlation between tumor-infiltrating leukocytes and metabolic molecules.

Traditional clinicopathological prognostic factors for PC, including CA19-9, TNM classification system, have been proven ineffective in prognosis [214-216]. In the current study, these two variables were not significant for OS or DFS. This might be due to the heterogeneity in metastatic pancreatic cancer and the

limited sample size. The continuous improvement of techniques in and basic research, such as genotype-phenotype [217], DNA-based molecular techniques[218], and single-cell RNA sequencing[219], it has led to a deeper understanding of pancreatic cancer, providing potentially effective treatments for the treatment of pancreatic cancer[220].

4.5 Limitations of the study

It was not easy to obtain cancer specimens from 26 cases of metastatic pancreatic cancer by surgical resection. We are so lucky to analyze those seven markers in metastatic pancreatic cancer by Immunohistochemistry. So far as we know, this is the first time to elucidate the differences in tumor-infiltrating leukocytes and metabolic molecules between primary and metastatic lesions of metastatic pancreatic cancer and the correlation of seven staining markers with clinical data, including OS and DFS. However, this study has limitations: First, lung and peritoneal metastasis could not be analyzed separately due to the sample size, but rather as a non-liver metastasis group versus the liver metastasis group. Second, chemotherapy and radiotherapy may affect the immune status, which is not involved in this study.

5. Conclusions

In this study, the QTS algorithm was used to quantify the density of four types of leukocytes ($CD3^+$ TILs, $CD8^+$ TILs, $CD20^+$ TILs, and $CD66b^+$ TINs) and three types of metabolic molecules (HIF-1α, GLUT1, PDHK1) both in tumor cell area and stroma area. High infiltrated $CD8^+$ T lymphocytes in metastatic tumor of PC correlated with improved OS; high stromal infiltration of $CD20^+$ in primary tumors correlated with improved OS; low density of GLUT1 in tumor stroma areas of primary PC and metastatic tumors correlated with improved OS; low level of platelets in blood circulation system associated with improved OS. Notably, it was found that $CD8^+$ TILs in metastatic tumors, and GLUT1 in tumor stromal areas in both primary and metastatic tumors were independent factors for OS.

6. References

1. Christenson, E., E. Jaffee, and N. Azad, *Current and emerging therapies for patients with advanced pancreatic ductal adenocarcinoma: a bright future.* The Lancet. Oncology, 2020. **21**(3): p. e135-e145.
2. Kabacaoglu, D., et al., *Immune Checkpoint Inhibition for Pancreatic Ductal Adenocarcinoma: Current Limitations and Future Options.* Front Immunol, 2018. **9**: p. 1878.
3. Miksch, R.C., et al., *Prognostic Impact of Tumor-Infiltrating Lymphocytes and Neutrophils on Survival of Patients with Upfront Resection of Pancreatic Cancer.* Cancers (Basel), 2019. **11**(1): p. 39.
4. Haeberle, L. and I. Esposito, *Pathology of pancreatic cancer.* Translational Gastroenterology and Hepatology, 2019. **4**: p. 50-50.
5. Sung, H., et al., *Global Cancer Statistics 2020: GLOBOCAN Estimates of Incidence and Mortality Worldwide for 36 Cancers in 185 Countries.* CA Cancer J Clin, 2021. **71**(3): p. 209-249.
6. Mizrahi, J.D., et al., *Pancreatic cancer.* The Lancet, 2020. **395**(10242): p. 2008-2020.
7. Pourshams, A., et al., *The global, regional, and national burden of pancreatic cancer and its attributable risk factors in 195 countries and territories, 1990–2017: a systematic analysis for the Global Burden of Disease Study 2017.* The Lancet Gastroenterology & Hepatology, 2019. **4**(12): p. 934-947.
8. Rawla, P., T. Sunkara, and V. Gaduputi, *Epidemiology of Pancreatic Cancer: Global Trends, Etiology and Risk Factors.* World J Oncol, 2019. **10**(1): p. 10-27.
9. Bender, E., *The pancreas problem.* 2020.
10. Midha, S., S. Chawla, and P.K. Garg, *Modifiable and non-modifiable risk factors for pancreatic cancer: A review.* Cancer Lett, 2016. **381**(1): p. 269-77.
11. Eibl, A.S.a.G., *PANCREATIC DUCTAL ADENOCARCINOMA.* 2015.
12. Hruban, R.H., et al., *Progression Model for Pancreatic Cancer.* Clinical Cancer Research 2000. **6**: p. 2968-2972.
13. Peters, M.L.B., et al., *Progression to pancreatic ductal adenocarcinoma from pancreatic intraepithelial neoplasia: Results of a simulation model.* Pancreatology, 2018. **18**(8): p. 928-934.
14. Le Large, T.Y.S., et al., *Key biological processes driving metastatic spread of pancreatic cancer as identified by multi-omics studies.* Seminars in Cancer Biology, 2017. **44**: p. 153-169.
15. Shin, D.W. and J. Kim, *The American Joint Committee on Cancer 8th edition staging system for the pancreatic ductal adenocarcinoma: is it better than the 7th edition?* Hepatobiliary Surgery and Nutrition, 2020. **9**(1): p. 98-100.
16. Werner, J., et al., *Advanced-stage pancreatic cancer: therapy options.* Nature reviews. Clinical oncology, 2013. **10**(6): p. 323-33.
17. Danai, L.V., et al., *Altered exocrine function can drive adipose wasting in early pancreatic cancer.* Nature, 2018. **558**(7711): p. 600-604.

18. Davendra P.S. Sohal, M., et al., *Metastatic Pancreatic Cancer- ASCO Guideline Update 2020.* Journal of Clinical Oncology, 2020. **38**(27): p. 3217-3230.
19. Li, D., et al., *Pancreatic cancer.* The Lancet, 2004. **363**(9414): p. 1049-1057.
20. Luu, A., et al., *Long-term survival after pancreaticoduodenectomy in patients with ductal adenocarcinoma of the pancreatic head.* Hepatobiliary & pancreatic diseases international : HBPD INT, 2021. **20**(3): p. 271-278.
21. Okasha, H., et al., *Real time endoscopic ultrasound elastography and strain ratio in the diagnosis of solid pancreatic lesions.* World journal of gastroenterology, 2017. **23**(32): p. 5962-5968.
22. Conroy, T., et al., *FOLFIRINOX or Gemcitabine as Adjuvant Therapy for Pancreatic Cancer.* The New England journal of medicine, 2018. **379**(25): p. 2395-2406.
23. Chawla, A., et al., *Neoadjuvant Therapy is Associated with Improved Survival in Borderline-Resectable Pancreatic Cancer.* Annals of surgical oncology, 2020. **27**(4): p. 1191-1200.
24. Versteijne, E., et al., *Preoperative Chemoradiotherapy Versus Immediate Surgery for Resectable and Borderline Resectable Pancreatic Cancer: Results of the Dutch Randomized Phase III PREOPANC Trial.* Journal of clinical oncology : official journal of the American Society of Clinical Oncology, 2020. **38**(16): p. 1763-1773.
25. Marthey, L., et al., *FOLFIRINOX for locally advanced pancreatic adenocarcinoma: results of an AGEO multicenter prospective observational cohort.* Annals of surgical oncology, 2015. **22**(1): p. 295-301.
26. Philip, P., et al., *Nab-paclitaxel plus gemcitabine in patients with locally advanced pancreatic cancer (LAPACT): a multicentre, open-label phase 2 study.* The lancet. Gastroenterology & hepatology, 2020. **5**(3): p. 285-294.
27. Heinrich, S., et al., *Opinions and use of neoadjuvant therapy for resectable, borderline resectable, and locally advanced pancreatic cancer: international survey and case-vignette study.* BMC cancer, 2019. **19**(1): p. 675.
28. Lambert, A., et al., *An update on treatment options for pancreatic adenocarcinoma.* Therapeutic advances in medical oncology, 2019. **11**: p. 1758835919875568.
29. De Dosso, S., et al., *Treatment landscape of metastatic pancreatic cancer.* Cancer treatment reviews, 2021. **96**: p. 102180.
30. Chan, K., et al., *Real-world outcomes of FOLFIRINOX vs gemcitabine and nab-paclitaxel in advanced pancreatic cancer: A population-based propensity score-weighted analysis.* Cancer medicine, 2020. **9**(1): p. 160-169.
31. Wang, Y., P. Camateros, and W. Cheung, *A Real-World Comparison of FOLFIRINOX, Gemcitabine Plus nab-Paclitaxel, and Gemcitabine in Advanced Pancreatic Cancers.* Journal of gastrointestinal cancer, 2019. **50**(1): p. 62-68.
32. Lahoud, M., et al., *Road map for pain management in pancreatic cancer: A review.* World journal of gastrointestinal oncology, 2016. **8**(8): p. 599-606.
33. Yachida, S. and C. Iacobuzio-Donahue, *Evolution and dynamics of pancreatic cancer progression.* Oncogene, 2013. **32**(45): p. 5253-60.
34. Nevala-Plagemann, C., M. Hidalgo, and I. Garrido-Laguna, *From state-of-the-art treatments to novel therapies for advanced-stage pancreatic cancer.* Nature reviews. Clinical oncology, 2020. **17**(2): p. 108-123.

35. Van Cutsem, E., et al., *Phase I/II trial of pimasertib plus gemcitabine in patients with metastatic pancreatic cancer.* International journal of cancer, 2018. **143**(8): p. 2053-2064.
36. Chung, V., et al., *Effect of Selumetinib and MK-2206 vs Oxaliplatin and Fluorouracil in Patients With Metastatic Pancreatic Cancer After Prior Therapy: SWOG S1115 Study Randomized Clinical Trial.* JAMA oncology, 2017. **3**(4): p. 516-522.
37. Moore, M., et al., *Erlotinib plus gemcitabine compared with gemcitabine alone in patients with advanced pancreatic cancer: a phase III trial of the National Cancer Institute of Canada Clinical Trials Group.* Journal of clinical oncology : official journal of the American Society of Clinical Oncology, 2007. **25**(15): p. 1960-6.
38. Schultheis, B., et al., *Gemcitabine combined with the monoclonal antibody nimotuzumab is an active first-line regimen in KRAS wildtype patients with locally advanced or metastatic pancreatic cancer: a multicenter, randomized phase IIb study.* Annals of oncology : official journal of the European Society for Medical Oncology, 2017. **28**(10): p. 2429-2435.
39. Rougier, P., et al., *Randomised, placebo-controlled, double-blind, parallel-group phase III study evaluating aflibercept in patients receiving first-line treatment with gemcitabine for metastatic pancreatic cancer.* European journal of cancer (Oxford, England : 1990), 2013. **49**(12): p. 2633-42.
40. Golan, T., et al., *BRCAMaintenance Olaparib for Germline -Mutated Metastatic Pancreatic Cancer.* The New England journal of medicine, 2019. **381**(4): p. 317-327.
41. Alistar, A., et al., *Safety and tolerability of the first-in-class agent CPI-613 in combination with modified FOLFIRINOX in patients with metastatic pancreatic cancer: a single-centre, open-label, dose-escalation, phase 1 trial.* The Lancet. Oncology, 2017. **18**(6): p. 770-778.
42. Ramanathan, R., et al., *Phase IB/II Randomized Study of FOLFIRINOX Plus Pegylated Recombinant Human Hyaluronidase Versus FOLFIRINOX Alone in Patients With Metastatic Pancreatic Adenocarcinoma: SWOG S1313.* Journal of clinical oncology : official journal of the American Society of Clinical Oncology, 2019. **37**(13): p. 1062-1069.
43. De Jesus-Acosta, A., et al., *Phase 2 study of vismodegib, a hedgehog inhibitor, combined with gemcitabine and nab-paclitaxel in patients with untreated metastatic pancreatic adenocarcinoma.* British journal of cancer, 2020. **122**(4): p. 498-505.
44. Kamath, S., et al., *Ipilimumab and Gemcitabine for Advanced Pancreatic Cancer: A Phase Ib Study.* The oncologist, 2020. **25**(5): p. e808-e815.
45. Elsayed, M. and M. Abdelrahim, *The Latest Advancement in Pancreatic Ductal Adenocarcinoma Therapy: A Review Article for the Latest Guidelines and Novel Therapies.* Biomedicines, 2021. **9**(4).
46. Kato, T., et al., *Cancer-Associated Fibroblasts Affect Intratumoral CD8 and FoxP3 T Cells Via IL6 in the Tumor Microenvironment.* Clinical cancer research : an official journal of the American Association for Cancer Research, 2018. **24**(19): p. 4820-4833.
47. Sukumar, M., R. Roychoudhuri, and N. Restifo, *Nutrient Competition: A New Axis of Tumor Immunosuppression.* Cell, 2015. **162**(6): p. 1206-8.
48. Farhood, B., M. Najafi, and K. Mortezaee, *CD8(+) cytotoxic T lymphocytes in cancer immunotherapy: A review.* J Cell Physiol, 2019. **234**(6): p. 8509-8521.

49. Kaneda, M., et al., *PI3Kγ is a molecular switch that controls immune suppression.* Nature, 2016. **539**(7629): p. 437-442.
50. De Henau, O., et al., *Overcoming resistance to checkpoint blockade therapy by targeting PI3Kγ in myeloid cells.* Nature, 2016. **539**(7629): p. 443-447.
51. Gunderson, A., et al., *Bruton Tyrosine Kinase-Dependent Immune Cell Cross-talk Drives Pancreas Cancer.* Cancer discovery, 2016. **6**(3): p. 270-85.
52. Weiss, G., et al., *Phase Ib/II study of gemcitabine, nab-paclitaxel, and pembrolizumab in metastatic pancreatic adenocarcinoma.* Investigational new drugs, 2018. **36**(1): p. 96-102.
53. Vonderheide, R., et al., *CD40 immunotherapy for pancreatic cancer.* Cancer immunology, immunotherapy : CII, 2013. **62**(5): p. 949-54.
54. Vonderheide, R., *CD40 Agonist Antibodies in Cancer Immunotherapy.* Annual review of medicine, 2020. **71**: p. 47-58.
55. Yan, Y., et al., *Combining Immune Checkpoint Inhibitors With Conventional Cancer Therapy.* Frontiers in immunology, 2018. **9**: p. 1739.
56. Leroux, C. and G. Konstantinidou, *Targeted Therapies for Pancreatic Cancer: Overview of Current Treatments and New Opportunities for Personalized Oncology.* Cancers (Basel), 2021. **13**(4).
57. Encarnación-Rosado, J. and A. Kimmelman, *Harnessing metabolic dependencies in pancreatic cancers.* Nature reviews. Gastroenterology & hepatology, 2021. **18**(7): p. 482-492.
58. Rojas, L. and V. Balachandran, *Scaling the immune incline in PDAC.* Nature reviews. Gastroenterology & hepatology, 2021. **18**(7): p. 453-454.
59. Ghesquiere, B., et al., *Metabolism of stromal and immune cells in health and disease.* Nature, 2014. **511**(7508): p. 167-76.
60. Hato, T. and P.C. Dagher, *How the Innate Immune System Senses Trouble and Causes Trouble.* Clin J Am Soc Nephrol, 2015. **10**(8): p. 1459-1469.
61. Inman, K.S., A.A. Francis, and N.R. Murray, *Complex role for the immune system in initiation and progression of pancreatic cancer.* World J Gastroenterol, 2014. **20**(32): p. 11160-11181.
62. Schlee, M. and G. Hartmann, *Discriminating self from non-self in nucleic acid sensing.* Nature Reviews Immunology, 2016. **16**(9): p. 566-580.
63. Corthay, A., *How do Regulatory T Cells Work?* Scandinavian Journal of Immunology, 2009. **70**(4): p. 326-336.
64. Mallett, G., A. Laurence, and S. Amarnath, *Programmed Cell Death-1 Receptor (PD-1)-Mediated Regulation of Innate Lymphoid Cells.* Int J Mol Sci, 2019. **20**(11): p. 2836.
65. William Vernau and P.F. Moore, *An immunophenotypic study of canine leukemias and preliminary assessment of clonality by polymerase chain reaction.* Veterinary Immunology and Immunopathology, 1999. **69**: p. 145 -164.
66. Orhan, A., et al., *The prognostic value of tumour-infiltrating lymphocytes in pancreatic cancer: a systematic review and meta-analysis.* Eur J Cancer, 2020. **132**: p. 71-84.
67. Carstens, J.L., et al., *Spatial computation of intratumoral T cells correlates with survival of patients with pancreatic cancer.* Nat Commun, 2017. **8**: p. 15095.

68. Tahkola, K., et al., *Immune cell score in pancreatic cancer-comparison of hotspot and whole-section techniques.* Virchows Arch, 2019. **474**(6): p. 691-699.
69. Karakhanova, S., et al., *Prognostic and predictive value of immunological parameters for chemoradioimmunotherapy in patients with pancreatic adenocarcinoma.* Br J Cancer, 2015. **112**(6): p. 1027-36.
70. Helm, O., et al., *Comparative characterization of stroma cells and ductal epithelium in chronic pancreatitis and pancreatic ductal adenocarcinoma.* PLoS One, 2014. **9**(5): p. e94357.
71. Bayne, L.J., et al., *Tumor-derived granulocyte-macrophage colony-stimulating factor regulates myeloid inflammation and T cell immunity in pancreatic cancer.* Cancer Cell, 2012. **21**(6): p. 822-35.
72. Pylayeva-Gupta, Y., et al., *Oncogenic Kras-induced GM-CSF production promotes the development of pancreatic neoplasia.* Cancer Cell, 2012. **21**(6): p. 836-47.
73. Galon, J. and D. Bruni, *Approaches to treat immune hot, altered and cold tumours with combination immunotherapies.* Nat Rev Drug Discov, 2019. **18**(3): p. 197-218.
74. van der Woude, L.L., et al., *Migrating into the Tumor: a Roadmap for T Cells.* Trends Cancer, 2017. **3**(11): p. 797-808.
75. Dunkelberger, J.R. and W.-C. Song, *Complement and its role in innate and adaptive immune responses.* Cell Research, 2010. **20**(1): p. 34-50.
76. Rodriguez-Pinto, D., *B cells as antigen presenting cells.* Cell Immunol, 2005. **238**(2): p. 67-75.
77. Tewari, N., et al., *The presence of tumour-associated lymphocytes confers a good prognosis in pancreatic ductal adenocarcinoma- an immunohistochemical study of tissue microarrays.* BMC Cancer, 2013. **13**: p. 436.
78. Li, Y., et al., *The regulatory roles of neutrophils in adaptive immunity.* Cell Communication and Signaling, 2019. **17**(1).
79. Wu, Y., et al., *Neutrophils promote motility of cancer cells via a hyaluronan-mediated TLR4/PI3K activation loop.* J Pathol, 2011. **225**(3): p. 438-47.
80. Cong, X., et al., *CD66b(+) neutrophils and alpha-SMA(+) fibroblasts predict clinical outcomes and benefits from postoperative chemotherapy in gastric adenocarcinoma.* Cancer Med, 2020. **9**(8): p. 2761-2773.
81. Galdiero, M.R., et al., *Occurrence and significance of tumor-associated neutrophils in patients with colorectal cancer.* Int J Cancer, 2016. **139**(2): p. 446-456.
82. Li, Y.-W., et al., *Intratumoral neutrophils: a poor prognostic factor for hepatocellular carcinoma following resection.* J Hepatol, 2011. **54**(3): p. 497-505.
83. Jensen, H.K., et al., *Presence of intratumoral neutrophils is an independent prognostic factor in localized renal cell carcinoma.* J Clin Oncol, 2009. **27**(28): p. 4709-4017.
84. Mahajan, U.M., et al., *Immune cell and stromal signature associated with progression-free survival of patients with resected pancreatic ductal adenocarcinoma.* Gastroenterology, 2018. **155**(5): p. 1625–1639.e2.
85. Ishizuka, M., et al., *Combination of platelet count and neutrophil to lymphocyte ratio is a useful predictor of postoperative survival in patients undergoing surgery for gastric cancer.* Journal of surgical oncology, 2014. **110**(8): p. 935-41.

86. Kim, I., S. You, and Y. Kim, *Neutrophil-lymphocyte ratio predicts pathologic tumor response and survival after preoperative chemoradiation for rectal cancer.* BMC surgery, 2014. **14**: p. 94.
87. Azab, B., et al., *The Usefulness of the Pretreatment Neutrophil/Lymphocyte Ratio as a Predictor of the 5-Year Survival in Stage 1-3 Triple Negative Breast Cancer Patients.* Breast care (Basel, Switzerland), 2021. **16**(1): p. 43-49.
88. Hasegawa, T., et al., *Neutrophil-lymphocyte ratio associated with poor prognosis in oral cancer: a retrospective study.* BMC cancer, 2020. **20**(1): p. 568.
89. Iwai, N., et al., *Neutrophil to lymphocyte ratio predicts prognosis in unresectable pancreatic cancer.* Scientific reports, 2020. **10**(1): p. 18758.
90. Takakura, K., et al., *Comprehensive assessment of the prognosis of pancreatic cancer: peripheral blood neutrophil-lymphocyte ratio and immunohistochemical analyses of the tumour site.* Scandinavian journal of gastroenterology, 2016. **51**(5): p. 610-7.
91. Guo, Q., et al., *Prognostic value of neutrophil-to-lymphocyte ratio in peripheral blood and pathological tissue in patients with esophageal squamous cell carcinoma.* Medicine, 2020. **99**(29): p. e21306.
92. Wang, J., et al., *The clinical significance of tumor-infiltrating neutrophils and neutrophil-to-CD8+ lymphocyte ratio in patients with resectable esophageal squamous cell carcinoma.* Journal of translational medicine, 2014. **12**: p. 7.
93. Candeias, S. and U. Gaipl, *The Immune System in Cancer Prevention, Development and Therapy.* Anti-cancer agents in medicinal chemistry, 2016. **16**(1): p. 101-7.
94. Kolb, D., et al., *Metabolic Modulation of the Tumor Microenvironment Leads to Multiple Checkpoint Inhibition and Immune Cell Infiltration.* ACS nano, 2020. **14**(9): p. 11055-11066.
95. Palmer, C.S., et al., *Glucose metabolism regulates T cell activation, differentiation, and functions.* Front Immunol, 2015. **6**: p. 1.
96. Kareva, I., *Metabolism and Gut Microbiota in Cancer Immunoediting, CD8/Treg Ratios, Immune Cell Homeostasis, and Cancer (Immuno)Therapy: Concise Review.* Stem cells (Dayton, Ohio), 2019. **37**(10): p. 1273-1280.
97. Dang, C.V., *Links between metabolism and cancer.* Genes & Development, 2012. **26**(9): p. 877-890.
98. Rodriguez, C., et al., *Regulation of cancer cell glucose metabolism is determinant for cancer cell fate after melatonin administration.* J Cell Physiol, 2021. **236**(1): p. 27-40.
99. Wang, G., et al., *New strategies for targeting glucose metabolism-mediated acidosis for colorectal cancer therapy.* Journal of cellular physiology, 2018. **234**(1): p. 348-368.
100. Ocana, M.C., et al., *Metabolism within the tumor microenvironment and its implication on cancer progression: An ongoing therapeutic target.* Med Res Rev, 2019. **39**(1): p. 70-113.
101. Pearce, E., et al., *Fueling immunity: insights into metabolism and lymphocyte function.* Science (New York, N.Y.), 2013. **342**(6155): p. 1242454.
102. Xia, L., et al., *The cancer metabolic reprogramming and immune response.* Molecular Cancer, 2021. **20**(1).
103. Mowat, A. and J. Baum, *Chemotaxis of polymorphonuclear leukocytes from patients with diabetes mellitus.* The New England journal of medicine, 1971. **284**(12): p. 621-7.

104. Donnelly, R.P. and D.K. Finlay, *Glucose, glycolysis and lymphocyte responses.* Mol Immunol, 2015. **68**(2 Pt C): p. 513-9.
105. Caro-Maldonado, A., et al., *Metabolic Reprogramming Is Required for Antibody Production That Is Suppressed in Anergic but Exaggerated in Chronically BAFF-Exposed B Cells.* The Journal of Immunology, 2014. **192**(8): p. 3626-3636.
106. O' Neill, L.A.J., R.J. Kishton, and J. Rathmell, *A guide to immunometabolism for immunologists.* Nat Rev Immunol, 2016. **16**(9): p. 553-565.
107. Kennedy, K.M., et al., *Catabolism of exogenous lactate reveals it as a legitimate metabolic substrate in breast cancer.* PLoS One, 2013. **8**(9): p. e75154.
108. Feron, O., *Pyruvate into lactate and back: from the Warburg effect to symbiotic energy fuel exchange in cancer cells.* Radiother Oncol, 2009. **92**(3): p. 329-33.
109. Hensley, C.T., et al., *Metabolic Heterogeneity in Human Lung Tumors.* Cell, 2016. **164**(4): p. 681-94.
110. Elebo, N., et al., *Role of different immune cells and metabolic pathways in modulating the immune response in pancreatic cancer (Review).* Mol Med Rep, 2020. **22**(6): p. 4981-4991.
111. Vander Heiden, M.G., L.C. Cantley, and C.B. Thompson, *Understanding the Warburg effect: the metabolic requirements of cell proliferation.* Science, 2009. **324**(5930): p. 1029-1033.
112. Otto Warburg, Franz Wind, and E. Negelein, *The metabolism of tumors in the body.* The Journal of General Physiology, 1927. **8**: p. 519-530.
113. Colegio, O.R., et al., *Functional polarization of tumour-associated macrophages by tumour-derived lactic acid.* Nature, 2014. **513**(7519): p. 559-63.
114. Cao, L., et al., *Glycometabolic rearrangements--aerobic glycolysis in pancreatic cancer: causes, characteristics and clinical applications.* J Exp Clin Cancer Res, 2020. **39**(1): p. 267.
115. von Ahrens, D., et al., *The role of stromal cancer-associated fibroblasts in pancreatic cancer.* J Hematol Oncol, 2017. **10**(1): p. 76.
116. Ying, H., et al., *Oncogenic Kras maintains pancreatic tumors through regulation of anabolic glucose metabolism.* Cell, 2012. **149**(3): p. 656-70.
117. Liang, C., et al., *Energy sources identify metabolic phenotypes in pancreatic cancer.* Acta Biochim Biophys Sin (Shanghai), 2016. **48**(11): p. 969-979.
118. Wang, G.L. and G.L. Semenza, *Purification and characterization of hypoxia-inducible factor 1.* The Journal of Biological Chemistry, 1995. **70**: p. 1230-1237.
119. Narayan V. Iyer, et al., *Cellular and developmental control of O2 homeostasis by hypoxia-inducible factor 1 alpha.* Genes & development, 1998. **12**(2): p. 149-162.
120. Semenza, G.L., *Regulation of mammalian O2 homeostasis by hypoxia-inducible factor 1.* Annu Rev Cell Dev Biol, 1999. **15**: p. 551-578.
121. Bing Hua Jiang, et al., *Hypoxia-inducible factor 1 levels vary exponentially relevant range of O 2tension.* American Journal of Physiology - Cell Physiology, 1996. **271**: p. C1172-C1180.
122. Unruh, A., et al., *The hypoxia-inducible factor-1 alpha is a negative factor for tumor therapy.* Oncogene, 2003. **22**(21): p. 3213-20.

123. Sun, H.-c., et al., *Expression of hypoxia-inducible factor-1α and associated proteins in pancreatic ductal adenocarcinoma and their impact on prognosis.* International Journal of Oncology, 2007. **30**: p. 1359-1367.
124. Semenza, G.L., *Targeting HIF-1 for cancer therapy.* Nat Rev Cancer, 2003. **3**(10): p. 721-32.
125. He, G., et al., *The effect of HIF-1alpha on glucose metabolism, growth and apoptosis of pancreatic cancerous cells.* Asia Pac J Clin Nutr, 2014. **23**(1): p. 174-80.
126. Huang, C., et al., *Interleukin 35 expression correlates with microvessel density in pancreatic ductal adenocarcinoma, recruits monocytes, and promotes growth and angiogenesis of xenograft tumors in mice.* Gastroenterology, 2018. **154**(3): p. 675-688.
127. T Kitada, et al., *Clinicopathological significance of hypoxia-inducible factor-1a expression in human pancreatic carcinoma.* Histopathology, 2003. **43**: p. 550–555.
128. Wang, J., et al., *STIM1 overexpression in hypoxia microenvironment contributes to pancreatic carcinoma progression.* Cancer Biol Med, 2019. **16**(1): p. 100-108.
129. Matsuo, Y., et al., *Hypoxia inducible factor-1 alpha plays a pivotal role in hepatic metastasis of pancreatic cancer: an immunohistochemical study.* J Hepatobiliary Pancreat Sci, 2014. **21**(2): p. 105-12.
130. Holness, M.J. and M.C. Sugden, *Regulation of pyruvate dehydrogenase complex activity by reversible phosphorylation.* Biochemical Society Transactions, 2003. **31**: p. 1143–1151.
131. Papandreou, I., et al., *HIF-1 mediates adaptation to hypoxia by actively downregulating mitochondrial oxygen consumption.* Cell Metab, 2006. **3**(3): p. 187-97.
132. Kim, J.W., et al., *HIF-1-mediated expression of pyruvate dehydrogenase kinase: a metabolic switch required for cellular adaptation to hypoxia.* Cell Metab, 2006. **3**(3): p. 177-85.
133. Weniger, M., K.C. Honselmann, and A.S. Liss, *The Extracellular Matrix and Pancreatic Cancer: A Complex Relationship.* Cancers (Basel), 2018. **10**(9): p. 316.
134. Horvat, N., et al., *Imaging for pancreatic ductal adenocarcinoma.* Chin Clin Oncol, 2017. **6**(6): p. 62.
135. Lau, A.N. and M.G. Vander Heiden, *Metabolism in the Tumor Microenvironment.* Annual Review of Cancer Biology, 2020. **4**(1): p. 17-40.
136. J S Flier, et al., *Elevated levels of glucose transport and transporter messenger RNA are induced by ras or src oncogenes*. Science, 1987. **235**: p. 1492–1495.
137. Davis-Yadley, A.H., et al., *Increased Expression of the Glucose Transporter Type 1 Gene Is Associated With Worse Overall Survival in Resected Pancreatic Adenocarcinoma.* Pancreas, 2016. **45**(7): p. 974-9.
138. Lu, K.A.I., et al., *Expression and clinical significance of glucose transporter-1 in pancreatic cancer.* Oncology Letters, 2016. **12**(1): p. 243-249.
139. Achalandabaso Boira, M., et al., *GLUT-1 as a predictor of worse prognosis in pancreatic adenocarcinoma: immunohistochemistry study showing the correlation between expression and survival.* BMC Cancer, 2020. **20**(1): p. 909.
140. Golias, T., et al., *Microenvironmental control of glucose metabolism in tumors by regulation of pyruvate dehydrogenase*. Int J Cancer, 2019. **144**(4): p. 674-686.

141. Rainer Christoph Miksch, J.H., et al., *Development of a reliable and accurate algorithm to quantify the tumor immune stroma (QTiS) across tumor types.* Oncotarget, 2017. **8**: p. 114935-114944.
142. Schoenberg, M.B., et al., *Perivascular Tumor-Infiltrating Leukocyte Scoring for Prognosis of Resected Hepatocellular Carcinoma Patients.* Cancers (Basel), 2018. **10**(10).
143. Ino, Y., et al., *Immune cell infiltration as an indicator of the immune microenvironment of pancreatic cancer.* Br J Cancer, 2013. **108**(4): p. 914-23.
144. Reid, M., et al., *Calculation of the Ki67 index in pancreatic neuroendocrine tumors: a comparative analysis of four counting methodologies.* Modern pathology : an official journal of the United States and Canadian Academy of Pathology, Inc, 2016. **29**(1): p. 93.
145. Moore, A. and T. Donahue, *Pancreatic Cancer.* JAMA, 2019. **322**(14): p. 1426.
146. Karamitopoulou, E., *The Tumor Microenvironment of Pancreatic Cancer.* Cancers (Basel), 2020. **12**(10).
147. Stephanie K. Dougan, P., *The Pancreatic Cancer Microenvironment.* The Cancer Journal, 2017. **23**: p. 321-325.
148. Ho, W.J., E.M. Jaffee, and L. Zheng, *The tumour microenvironment in pancreatic cancer - clinical challenges and opportunities.* Nat Rev Clin Oncol, 2020. **17**(9): p. 527-540.
149. Tang, Y., et al., *An increased abundance of tumor-infiltrating regulatory T cells is correlated with the progression and prognosis of pancreatic ductal adenocarcinoma.* PLoS One, 2014. **9**(3): p. e91551.
150. Jamieson, N., et al., *The relationship between tumor inflammatory cell infiltrate and outcome in patients with pancreatic ductal adenocarcinoma.* Annals of surgical oncology, 2012. **19**(11): p. 3581-90.
151. Balachandran, V.P., et al., *Identification of unique neoantigen qualities in long-term survivors of pancreatic cancer.* Nature, 2017. **551**(7681): p. 512-516.
152. Galon, J., et al., *Type, density, and location of immune cells within human colorectal tumors predict clinical outcome.* Science (New York, N.Y.), 2006. **313**(5795): p. 1960-4.
153. Pagès, F., et al., *Effector memory T cells, early metastasis, and survival in colorectal cancer.* The New England journal of medicine, 2005. **353**(25): p. 2654-66.
154. Guo, L., et al., *Colorectal Cancer Immune Infiltrates: Significance in Patient Prognosis and Immunotherapeutic Efficacy.* Frontiers in immunology, 2020. **11**: p. 1052.
155. He, J., et al., *Prognostic value of tumour-infiltrating lymphocytes based on the evaluation of frequency in patients with oestrogen receptor-positive breast cancer.* European journal of cancer (Oxford, England : 1990), 2021. **154**: p. 217-226.
156. Denkert, C., et al., *Tumour-infiltrating lymphocytes and prognosis in different subtypes of breast cancer: a pooled analysis of 3771 patients treated with neoadjuvant therapy.* The Lancet. Oncology, 2018. **19**(1): p. 40-50.
157. Van Bockstal, M., et al., *Interobserver variability in the assessment of stromal tumor-infiltrating lymphocytes (sTILs) in triple-negative invasive breast carcinoma influences the association with pathological complete response: the IVITA study.* Modern pathology : an official journal of the United States and Canadian Academy of Pathology, Inc, 2021.

158. Stumpf, M., et al., *Intraepithelial CD8-positive T lymphocytes predict survival for patients with serous stage III ovarian carcinomas: relevance of clonal selection of T lymphocytes.* British journal of cancer, 2009. **101**(9): p. 1513-21.
159. Hermans, C., et al., *Analysis of FoxP3+ T-regulatory cells and CD8+ T-cells in ovarian carcinoma: location and tumor infiltration patterns are key prognostic markers.* PloS one, 2014. **9**(11): p. e111757.
160. Martinez-Lostao, L., A. Anel, and J. Pardo, *How Do Cytotoxic Lymphocytes Kill Cancer Cells?* Clin Cancer Res, 2015. **21**(22): p. 5047-56.
161. Maimela, N., S. Liu, and Y. Zhang, *Fates of CD8+ T cells in Tumor Microenvironment.* Computational and structural biotechnology journal, 2019. **17**: p. 1-13.
162. Reuschenbach, M., M. Von Knebel Doeberitz, and N. Wentzensen, *A systematic review of humoral immune responses against tumor antigens.* Cancer Immunology, Immunotherapy, 2009. **58**(10): p. 1535-1544.
163. Largeot, A., et al., *The B-Side of Cancer Immunity: The Underrated Tune.* Cells, 2019. **8**(5): p. 449.
164. Nelson, B.H., *CD20+ B cells: the other tumor-infiltrating lymphocytes.* J Immunol, 2010. **185**(9): p. 4977-82.
165. Brunner, M., et al., *Upregulation of CD20 Positive B-Cells and B-Cell Aggregates in the Tumor Infiltration Zone is Associated with Better Survival of Patients with Pancreatic Ductal Adenocarcinoma.* Int J Mol Sci, 2020. **21**(5).
166. Milne, K., et al., *Systematic Analysis of Immune Infiltrates in High-Grade Serous Ovarian Cancer Reveals CD20, FoxP3 and TIA-1 as Positive Prognostic Factors.* PLoS ONE, 2009. **4**(7): p. e6412.
167. Kirkegård, J., F.V. Mortensen, and D. Cronin-Fenton, *Chronic Pancreatitis and Pancreatic Cancer Risk: A Systematic Review and Meta-analysis.* American Journal of Gastroenterology, 2017. **112**(9): p. 1366-1372.
168. Coussens, L. and Z. Werb, *Inflammation and cancer.* Nature, 2002. **420**(6917): p. 860-7.
169. Jensen, H., et al., *Presence of intratumoral neutrophils is an independent prognostic factor in localized renal cell carcinoma.* Journal of clinical oncology : official journal of the American Society of Clinical Oncology, 2009. **27**(28): p. 4709-17.
170. Yamada, Y., et al., *Prognostic value of CD66b positive tumor-infiltrating neutrophils in testicular germ cell tumor.* BMC Cancer, 2016. **16**(1): p. 898.
171. Carus, A., et al., *Tumour-associated CD66b+ neutrophil count is an independent prognostic factor for recurrence in localised cervical cancer.* Br J Cancer, 2013. **108**(10): p. 2116-22.
172. Ino, Y., et al., *Immune cell infiltration as an indicator of the immune microenvironment of pancreatic cancer.* British journal of cancer, 2013. **108**(4): p. 914-23.
173. Caruso, R., et al., *Prognostic value of intratumoral neutrophils in advanced gastric carcinoma in a high-risk area in northern Italy.* Modern pathology : an official journal of the United States and Canadian Academy of Pathology, Inc, 2002. **15**(8): p. 831-7.
174. Rao, H.-L., et al., *Increased Intratumoral Neutrophil in Colorectal Carcinomas Correlates Closely with Malignant Phenotype and Predicts Patients' Adverse Prognosis.* PLoS ONE, 2012. **7**(1): p. e30806.

175. Governa, V., et al., *The Interplay Between Neutrophils and CD8+ T Cells Improves Survival in Human Colorectal Cancer.* Clinical Cancer Research, 2017. **23**(14): p. 3847-3858.
176. Zahorec, R., *Neutrophil-to-lymphocyte ratio, past, present and future perspectives.* Bratislava Medical Journal, 2021. **122**(07): p. 474-488.
177. Ogiya, R., et al., *Comparison of tumor-infiltrating lymphocytes between primary and metastatic tumors in breast cancer patients.* Cancer Science, 2016. **107**(12): p. 1730-1735.
178. Cimino-Mathews, A., et al., *Metastatic triple-negative breast cancers at first relapse have fewer tumor-infiltrating lymphocytes than their matched primary breast tumors: a pilot study.* Human pathology, 2013. **44**(10): p. 2055-63.
179. Sobottka, B., et al., *Similar lymphocytic infiltration pattern in primary breast cancer and their corresponding distant metastases.* OncoImmunology, 2016. **5**(6): p. e1153208.
180. Shibutani, M., et al., *A comparison of the local immune status between the primary and metastatic tumor in colorectal cancer: a retrospective study.* BMC Cancer, 2018. **18**(1): p. 371.
181. Ansari, D., et al., *The role of quantitative mass spectrometry in the discovery of pancreatic cancer biomarkers for translational science.* Journal of Translational Medicine, 2014. **12**(1): p. 87.
182. Ansari, D., et al., *Pancreatic cancer: disease dynamics, tumor biology and the role of the microenvironment.* Oncotarget, 2018. **9**(5): p. 6644-6651.
183. Anderson, N.M. and M.C. Simon, *The tumor microenvironment.* Curr Biol, 2020. **30**(16): p. R921-R925.
184. Petrova, V., et al., *The hypoxic tumour microenvironment.* Oncogenesis, 2018. **7**(1): p. 10.
185. Pouysségur, J., F. Dayan, and N. Mazure, *Hypoxia signalling in cancer and approaches to enforce tumour regression.* Nature, 2006. **441**(7092): p. 437-43.
186. Shao, C., et al., *Role of hypoxia-induced exosomes in tumor biology.* Mol Cancer, 2018. **17**(1): p. 120.
187. Jing, X., et al., *Role of hypoxia in cancer therapy by regulating the tumor microenvironment.* Mol Cancer, 2019. **18**(1): p. 157.
188. Brahimi-Horn, M., J. Chiche, and J. Pouysségur, *Hypoxia and cancer.* Journal of molecular medicine (Berlin, Germany), 2007. **85**(12): p. 1301-7.
189. Harris, A., *Hypoxia--a key regulatory factor in tumour growth.* Nature reviews. Cancer, 2002. **2**(1): p. 38-47.
190. Jin, X., et al., *Implications of HIF-1alpha in the tumorigenesis and progression of pancreatic cancer.* Cancer Cell Int, 2020. **20**: p. 273.
191. Leppanen, J., et al., *Weak HIF-1alpha expression indicates poor prognosis in resectable pancreatic ductal adenocarcinoma.* World J Surg Oncol, 2018. **16**(1): p. 127.
192. Yuen, A. and B. Diaz, *The impact of hypoxia in pancreatic cancer invasion and metastasis.* Hypoxia (Auckl), 2014. **2**: p. 91-106.
193. ITO, H., et al., *GLUT-1 Expression as an Independent Predictor of Outcome in Patients with R1 Pancreatic Ductal Adenocarcinoma.* The Showa University Journal of Medical Sciences, 2016. **28**(3): p. 249-260.

194. Pizzi, S., et al., *Glucose transporter1 expression and prognostic significance in pancreatic carcinogenesis.* Histology and histopathology, 2009. **24**(2): p. 175-185.
195. Sharen, G., et al., *Prognostic value of GLUT-1 expression in pancreatic cancer- results from 538 patients.* Oncotarget, 2017. **8**(12): p. 19760-19767.
196. Koukourakis, M.I., et al., *Pyruvate dehydrogenase and pyruvate dehydrogenase kinase expression in non small cell lung cancer and tumor-associated stroma.* Neoplasia, 2005. **7**(1): p. 1-6.
197. Zhu, J. and C. Thompson, *Metabolic regulation of cell growth and proliferation.* Nature reviews. Molecular cell biology, 2019. **20**(7): p. 436-450.
198. Li, F. and M.C. Simon, *Cancer Cells Don't Live Alone: Metabolic Communication within Tumor Microenvironments.* Dev Cell, 2020. **54**(2): p. 183-195.
199. Pérez-Tomás, R. and I. Pérez-Guillén, *Lactate in the Tumor Microenvironment: An Essential Molecule in Cancer Progression and Treatment.* Cancers, 2020. **12**(11): p. 3244.
200. Shime, H., et al., *Tumor-secreted lactic acid promotes IL-23/IL-17 proinflammatory pathway.* J Immunol, 2008. **180**(11): p. 7175-83.
201. Meng, Q., et al., *Diagnostic and prognostic value of carcinoembryonic antigen in pancreatic cancer: a systematic review and meta-analysis.* OncoTargets and Therapy, 2017. **Volume 10**: p. 4591-4598.
202. Yagyu, T., et al., *Decreased mean platelet volume predicts poor prognosis in patients with pancreatic cancer.* BMC surgery, 2021. **21**(1): p. 8.
203. Suzuki, K., et al., *Platelets counts closely correlate with the disease-free survival interval of pancreatic cancer patients.* Hepato-gastroenterology, 2004. **51**(57): p. 847-53.
204. Korniluk, A., et al., *Mean Platelet Volume (MPV): New Perspectives for an Old Marker in the Course and Prognosis of Inflammatory Conditions.* Mediators of inflammation, 2019. **2019**: p. 9213074.
205. Wallace, K., et al., *Platelet and hemoglobin count at diagnosis are associated with survival in African American and Caucasian patients with colorectal cancer.* Cancer epidemiology, 2020. **67**: p. 101746.
206. Rachidi, S., et al., *Lower circulating platelet counts and antiplatelet therapy independently predict better outcomes in patients with head and neck squamous cell carcinoma.* Journal of hematology & oncology, 2014. **7**: p. 65.
207. Edin, S., et al., *The Prognostic Importance of CD20+ B lymphocytes in Colorectal Cancer and the Relation to Other Immune Cell subsets.* Scientific Reports, 2019. **9**(1).
208. Kuroda, H., et al., *Tumor-infiltrating B cells and T cells correlate with postoperative prognosis in triple-negative carcinoma of the breast.* BMC Cancer, 2021. **21**(1).
209. Nielsen, J.S., et al., *CD20+ Tumor-Infiltrating Lymphocytes Have an Atypical CD27− Memory Phenotype and Together with CD8+ T Cells Promote Favorable Prognosis in Ovarian Cancer.* Clinical Cancer Research, 2012. **18**(12): p. 3281-3292.
210. Carus, A., et al., *Tumor-associated neutrophils and macrophages in non-small cell lung cancer: no immediate impact on patient outcome.* Lung cancer (Amsterdam, Netherlands), 2013. **81**(1): p. 130-7.
211. Hao, L.S., et al., *Correlation and expression analysis of hypoxia-inducible factor 1α, glucose transporter 1 and lactate dehydrogenase 5 in human gastric cancer.* Oncology Letters, 2019.

212. Lidgren, A., et al., *Glucose transporter-1 expression in renal cell carcinoma and its correlation with hypoxia inducible factor-1 alpha*. BJU international, 2008. **101**(4): p. 480-4.
213. Zhang, L., et al., *Increased HIF-1alpha expression in tumor cells and lymphocytes of tumor microenvironments predicts unfavorable survival in esophageal squamous cell carcinoma patients*. International journal of clinical and experimental pathology, 2014. **7**(7): p. 3887-97.
214. Pandiaraja, J., et al., *The Role of CA19-9 in Predicting Tumour Resectability in Carcinoma Head of Pancreas.* Journal of clinical and diagnostic research : JCDR, 2016. **10**(3): p. PC06-9.
215. Ansari, D., et al., *Relationship between tumour size and outcome in pancreatic ductal adenocarcinoma.* The British journal of surgery, 2017. **104**(5): p. 600-607.
216. Tahkola, K., et al., *High immune cell score predicts improved survival in pancreatic cancer.* Virchows Arch, 2018. **472**(4): p. 653-665.
217. Hayashi, A., J. Hong, and C. Iacobuzio-Donahue, *The pancreatic cancer genome revisited.* Nature reviews. Gastroenterology & hepatology, 2021. **18**(7): p. 469-481.
218. Singhi, A. and L. Wood, *Early detection of pancreatic cancer using DNA-based molecular approaches.* Nature reviews. Gastroenterology & hepatology, 2021. **18**(7): p. 457-468.
219. Han, J., R. DePinho, and A. Maitra, *Single-cell RNA sequencing in pancreatic cancer.* Nature reviews. Gastroenterology & hepatology, 2021. **18**(7): p. 451-452.
220. *Advancing on pancreatic cancer.* Nat Rev Gastroenterol Hepatol, 2021. **18**(7): p. 447.

7. Acknowledgment

Pursuing an M.D. is a challenge, especially when someone has to quit a stable job and drag the family abroad for study. After 20 years of study, I obtained my master's degree in surgery in 2011 and stayed in Beijing to work. I was very lucky to continue clinical study alongside my tutor, Prof. Zhou, a prestigious professor and expert of HPB surgery in China and president of CRSA (Clinical Robotic Surgery Association) in China. However, he left us five years ago due to pancreatic cancer. His death shook my life and work ultimately. Fortunately, I met Professor Werner, a world-renowned expert on pancreatic cancer, in 2018. With his help, I took my wife and 2-year-old daughter to Munich to learn about advanced research, diagnosis, and treatment concepts for pancreatic cancer. Over the past two years, I have witnessed my daughter's unpleasant adjustment to the new environment. It is lucky that we keep healthy during the COVID-19 pandemic. But unfortunately, my wife was diagnosed with rheumatoid arthritis this March.

I am very excited to complete my dissertation and present it to you. This dissertation would not have finished without the guidance and help from many individuals. My greatest honor is to convey my appreciation to my generous and selfless mentors, kind and friendly colleagues, and dear friends that I luckily met during my doctoral study at Ludwig-Maximillian University Munich, Germany.

First and foremost, I would like to thank my supervisors and my thesis advisory committee, Prof. Dr. med. Jens Werner, Prof. Alexandr V. Bazhin, and Prof. Jens Neumann. They offered me the opportunity to accomplish my doctoral study and consistently supported my project and related research. In addition,

Prof. Dr. med. Jens Werner and Prof. Alexandr V. Bazhin gave financial support during my research. So, I would like to express my gratitude again.

I am grateful to thank my scientific advisor Rainer Christoph Miksch for his patience and valuable efforts which help me to overcome numerous challenges throughout my study.

I would like to thank Steffen Ormanns, Jan D'Haese, and Tobias S. Schiergens for their cooperation in this project. I would also like to thank Nadine Gesse for her excellent technical support. Furthermore, thank all my colleagues in Experimental Surgery Division in the Department of General, Visceral, and Transplantation Surgery of Ludwig Maximilian-University.

I would like to express my deep gratitude to my parents, Qiusheng Zhang and Ying Huang from China, and my parents-in-law Zhao Jiming and Hong Yilian, for providing me with firm support and continuous encouragement throughout my doctoral study.

Finally, my deepest thankfulness goes to my dear wife Daoyuan Chen and my lovely daughter Yichen Zhang for their unselfish love and warm company, which enabled me to accomplish my doctoral study.

This dissertation would not have been completed without them.

LMU LUDWIG-MAXIMILIANS-UNIVERSITÄT MÜNCHEN

Dean's Office
Faculty of Medicine

MMRS

Affidavit

Zhang Tao

Surname, first name

Street

Zip code, town

Country

I hereby declare, that the submitted thesis entitled

Quantification of the Tumor immune Stroma (QTiS) and the Metabolic Checkpoint Molecules in Pancreatic Cancer: Comparison between Primary and Metastatic Tumor

is my own work. I have only used the sources indicated and have not made unauthorised use of services of a third party. Where the work of others has been quoted or reproduced, the source is always given.

I further declare that the submitted thesis or parts thereof have not been presented as part of an examination degree to any other university.

Beijing 11.02.2022

Place, date

Tao Zhang

Signature doctoral candidate